JOINT PATTERN AND TRACE ELEMENT DISTRIBUTION IN THE IGNEOUS ROCKS OF THE JARILLA MOUNTAINS, NEW MEXICO

By

Raymond L. Morley

A REPORT

Submitted in Partial Fulfillment of the Requirements
for the Degree of Master of Science in Geology

New Mexico Institute of Mining and
Technology, Socorro, New Mexico

1977

Outline of independent study

Joint Pattern and Metal Distribution in the Jarilla Mt. Intrusiv Rocks.

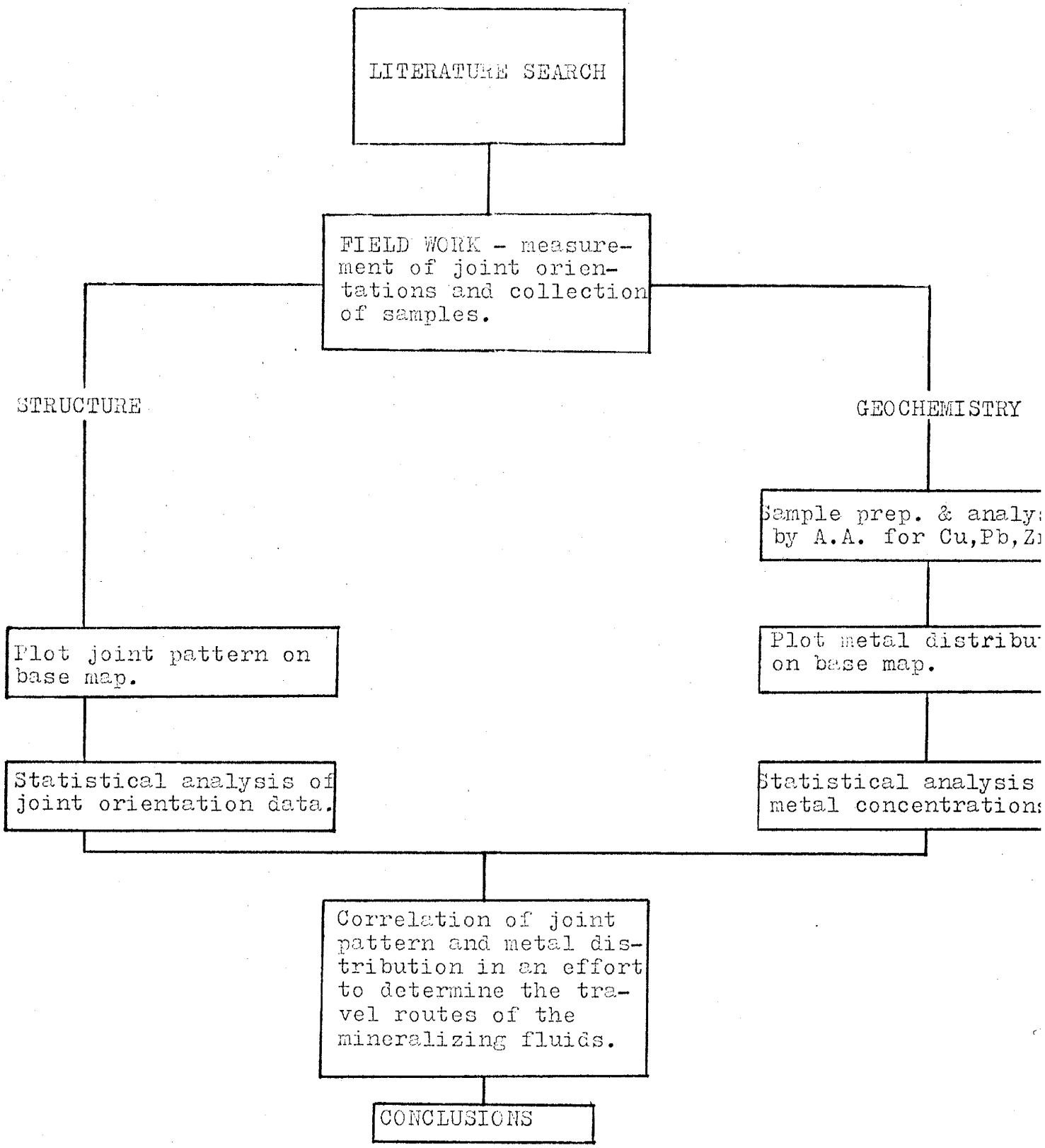

TABLE OF CONTENTS

TABLE OF CONTENTS

CONTINUED

ABSTRACT

The joint pattern in the Jarilla Mountains igenous rocks does not have a strong preferred orientation. Statistically the orientation is shown to be nearly random. The range has two large areas of strong to moderate fracture intensity. The rock geochemistry studies show anomalous values for barium, copper and lead. The copper and lead concentrations are bimodally distributed as determined from log probability plots. The distributions containing the higher Cu and Pb values are interpreted to be related to hydrothermal mineralization. There are no strong preferred orientations to the geochemical anomalies. But a strong correlation does exist between the areas of strong to moderate fracture intensity and the anomalous copper and lead values. Geochemical values obtained in this study are compared to the concentrations obtained in the orientation study at Kalamazoo, San Manuel District, Arizona.

ACKNOWLEDGEMENTS

Acknowledgement is made to Dr. R. E. Beane of the University of Arizona for originally suggesting this study. Gerald Eshbaugh, District Geologist for Pioneer Nuclear, Incorporated, provided a field vehicle and some facilities for the study. David Schwab, with Albuquerque Assay Laboratories, provided much helpful advice regarding the analytical procedures. Special thanks are extended to Dr. Clay Smith, of the New Mexico Institute of Mining and Technology, for assuming the responsibility of advisor to this project.

SCOPE OF THE STUDY

Purpose of the Research

The intrusive igneous rocks of the Jarilla Mountains were studied with respect to their content of copper, lead, zinc, iron and other elements, and their joint pattern and intensity of fracture. The purpose of the study was to determine the relationship of the metal distribution in the igneous rocks to the orientation and intensity of fracturing and to the areas of known or possible mineralization. Detailed geology and mineralogy of the ore bodies has already been published and is not the purpose of this study. The Jarilla Mountains have produced copper, lead, iron, gold, and silver (Schmidt and Craddock, 1964). Most of the production was from replacement bodies in limestones that lie adjacent to the intrusive rocks and from a few small placers.

This study indicates that the metal concentrations in the intrusive rocks are related to the areas of known mineralization and to the intensity of fracturing in the intrusive rocks. This relationship may prove helpful in determining the origin and travel routes of the mineralizing fluids. Also the copper, lead and zinc concentrations may be used as background values with which more detailed surface or drill samples can be compared.

Location of the Study

The area investigated is the Jarilla Mountains located in the Tularosa Basin, south-central New Mexico. The range is in the south-west quadrant of Otero County near the town of Orogrande lying in Townships 21 and 22 South, Range 8 East, west of U. S. Highway 54 (See Figure 1).

PHYSICAL CHARACTERISTICS OF THE JARILLA MOUNTAINS

Physiography, Climate, and Vegetation

The physiography, climate and vegetation of the Jarilla Mountains have been described in some detail by Seager (1961) and by Schmidt and Craddock (1964). For the purpose of this report the area may be described as a low range of mountains (1200 feet maximum relief) with steep, rugged slopes, a hot, dry climate and very little vegetation. These factors dictate the type of material available for geochemical sampling, essentially rock or colluvium in this case. They also effect the type of metallic dispersion patterns around mineral deposits, in this case secondary dispersion is severly limited and requires that geochemical prospecting focus on the primary patterns.

METHODOLOGY

Field Sampling Procedure

The rock samples were collected and joint orientation measurements were made at the same predetermined locations. These locations were occasionally adjusted in the field. The total area of igneous outcrop was determined from the geologic map of Schmidt & Craddock (1964), with a planimeter, to be 6.9

square miles. The monzonite adamellite (Tim) crops out over an area of 5.3 square miles (including interior metamorphic rocks). The monzonite adamellite area represents 76% of the igneous outcrop. In this area, mapped as Tim, 71 locations were sampled and at 66 of these locations joint orientations were measured. Syenodiorite crops out over an area of 0.8 square miles representing 12% of the igneous outcrop - 14 locations were occupied in the area mapped as Tis. Orthoclase adamellite corps out over 0.6 square miles or 9% of the area and 11 locations mapped as Tio were occupied. The leucorhyolite covers 0.2 square miles or 3% of the area and 3 locations were occupied in the area mapped as Til. The outcrop area of the undifferentiated dikes was not measured, but 16 areas were samples and joint orientations measured. Table 1 summarizes the sample locations.

In each of the four major rock types, the sample locations were spaced as evenly as possible. The greatest distortion from a uniform distribution occurs in the south end of the area mapped as Tim (Figure 2). In this area, numerous unmapped outcrops of metamorphic rocks, prospect pits and mine dumps caused the distortion in uniform sampling distribution. Each sample area represents approximately 0.07 square miles of igneous outcrop. The sample areas are about 1500 feet apart on the average and never closer than 500 feet. Each location was predetermined, in the office, based on uniform distribution, and adjusted in the field, based on megascopic observation, to be the same as, or representative of, approximately 0.07 square miles (1400 x 1400 feet) of igneous outcrop surrounding the sample area. The rocks were collected and joint orientations measured from an area

TABLE 1 : SAMPLE LOCATIONS

	Igneous Outcrop in sq. mi.	Percentage of Total Igneous Outcrop	Number of Locations Sampled for Geochem.	Number of Locations Joints Measured
(Tim) Monzonite Adamellite	5.3	76	71	66
(Tis) Syenodiorite	0.8	12	14	14
(Tio) Orthoclase Adamellite	0.6	9	11	11
(Til) Leucorhyolite	0.2	3	3	3
(Tid) Undifferentiated Dikes			16	16
TOTALS	6.9	100	115	110

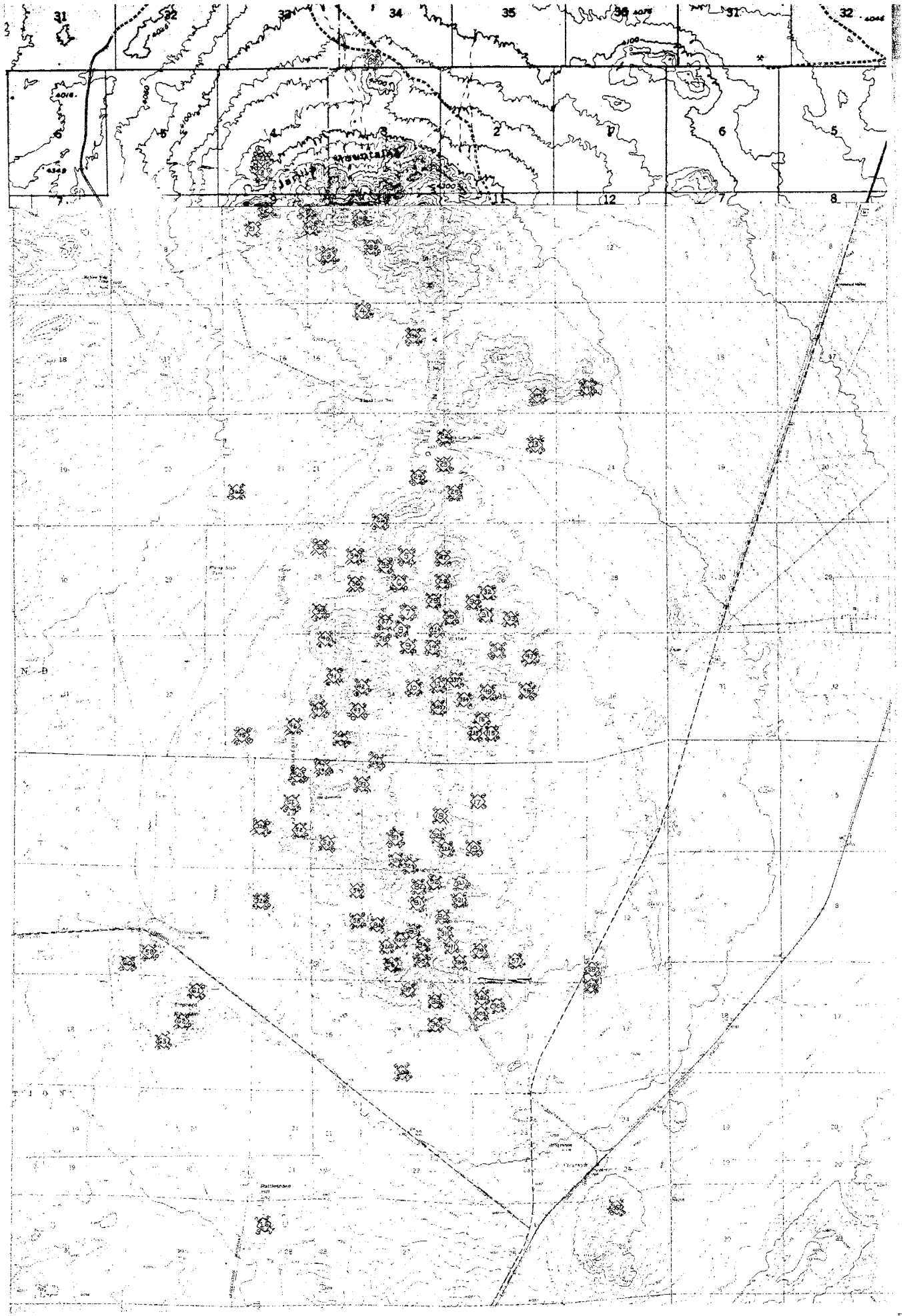
SCALE 1:24000
CONTOUR INTERVAL 20 FEET
SAMPLE NUMBER

FIGURE 2

FRACTURE PATTERN IN THE IGNEOUS ROCKS OF THE JARILLA MOUNTAINS

Tic — Tic-C

SCALE 1:24000

1 MILE

FRACTURE INTENSITY

- STRONG
- MODERATE
- WEAK

at least 10 yards in diameter at each location. Locally mineralized veins or prospects were avoided. One area of pyritized monzonite adamellite was sampled because the sulfides were distributed over a wide area.

REVIEW OF THE LITERATURE

Previous Research in the Jarilla Mountains

The geology of the Jarilla Mountains has been described by Hidden (1893), Lindgren, Graton and Gordon (1910), Meinzer and Hare (1915), Darton (1921, 1928), Lasky and Wooton (1933), Needham (1937), Kelley (1949), Reynolds and Craddock (1959), Seager (1961), Schmidt (1962), Schmidt and Craddock (1964), Jaramillo (1973), Beane, Jaramillo and Bloom (1975), and Bloom (1977). Most of these contributions are concerned with some aspect of the metallic mineralization in the range. The bulletin by Schmidt and Craddock (1964) has the most recent geologic map of the entire range and was therefore used as a base in this report. Samples collected for this report are cross-referenced with Plate 2 in Schmidt and Craddock (1964) (See Table 14).

Joint Pattern and Fracture Intensity

Rehrig and Heidrick (1972) related regional fracturing to porphyry copper mineralization in a number of Laramide stocks in Arizona. Mackin (1954) and others showed how tensional joints in the Granite Mountain laccolith formed travel routes for mineralizing fluids that fed magnetite/hematite replacement bodies in limestones adjacent to the intrusive.

RESULTS OF THE STUDY

Data Analysis

In this study, the orientation of steeply dipping joints and the intensity of fracturing was measured at 110 locations as described in the section on Sampling Procedures (see page 4). The data, which is presented in Map 1 and Figure 2, was then subjected to statistical analysis. The joints were measured at a number of locations in each sample area and then a single average was recorded. The strikes and dips refer to joint sets rather than individual joints. An arbitrary field classification was devised for categorizing the fracture intensity into three groups: strong, moderate, and weak. The strong group consisted of numerous joints per set, spaced at intervals from a fraction of an inch to three inches apart. In most of the areas classified as strong fracture intensity, the rock could not be broken to a fresh surface. Moderate fracture intensity had a fair number of joints per set, with the fractures greater than three inches apart. The areas classified as weak had only a few widely spaced joints per set. Sheeting, as produced by exfoliation, was not recorded since this type of jointing was found to be near surface phenomenon and invariably oriented parallel to existing topography. The histogram labelled Tim in Figure 3, shows the joint orientation for monzonite adamellite (Tim), which is the most abundant rock type in the range. The fractures appear to have two preferred orientations, one at N-50°-E and the other at N-60°-W with the N-50°-E set slightly more prominent. Vistelius (1966) has described a statistical technique for determining the probability that the observed

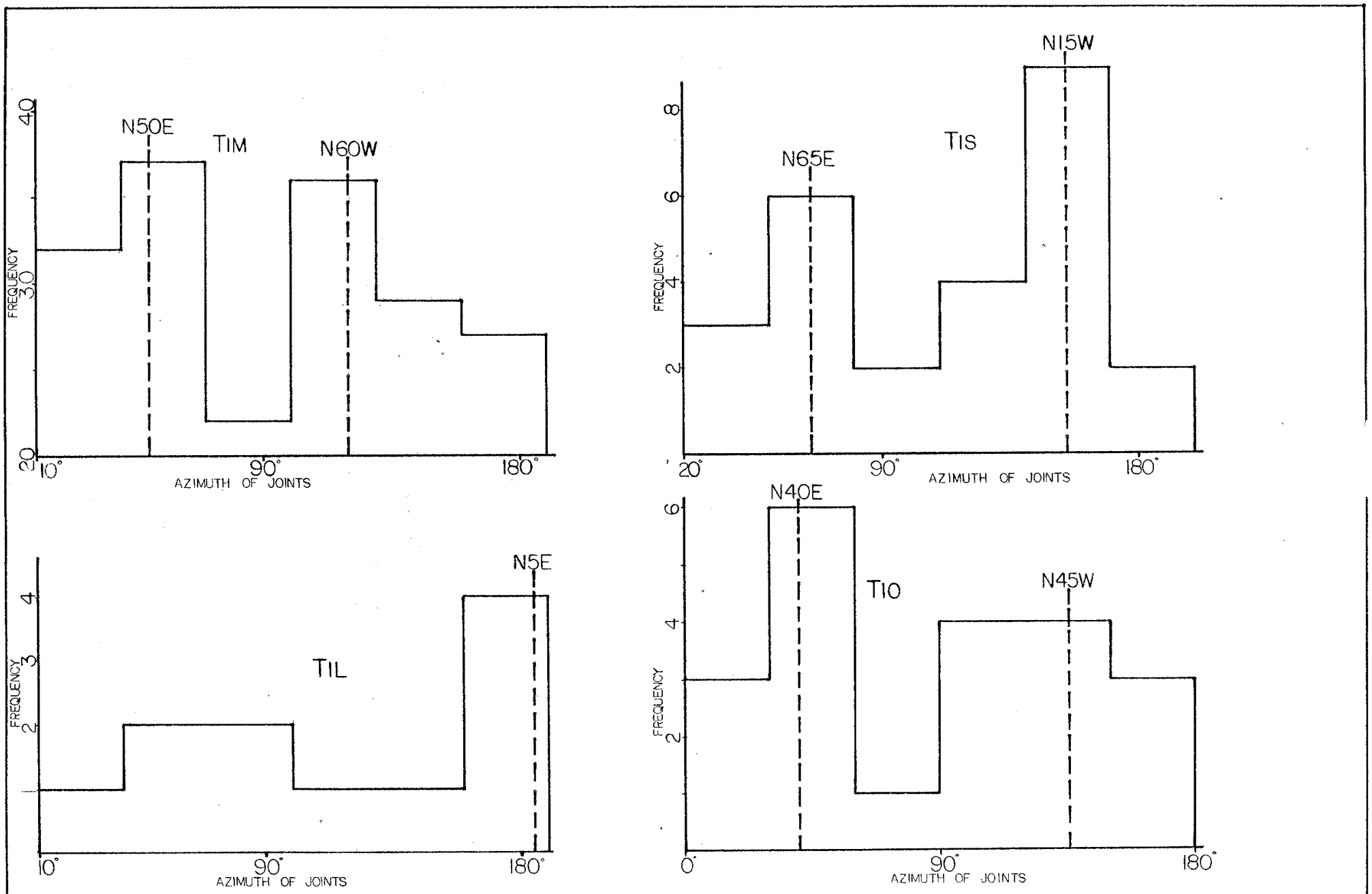

FIG. 3 STRIKE HISTOGRAMS FOR STEEPLY DIPPING JOINTS IN THE MAJOR ROCK TYPES IN THE JARILLA MOUNTAINS

distribution (histogram Tim) is the result of random deviations from a uniform distribution, or that a preferred orientation exists. The data from the joint measurements in monzonite adamellite will be used to describe the details of the technique.

The sampling distribution of χ^2 (Chi Square) is given by the expression:

$$\chi^2 = \sum_{i=1}^{r} \frac{(m_i - n\alpha_i)^2}{n\alpha_i}$$

where m_i is the number of observations in the i^{th} class corresponding to the probability α_i, and n is the overall number of observations. The degrees of freedom listed for Chi Square is equal to the number of independent sums generating χ^2, that is the degrees of freedom $\nu = r-1$. In applying this distribution to the data observed in the field, $n\alpha_i$ becomes m'_i, which is the expected value if the distribution is uniform. This is, $m'_i = \sum m_i \div$ number of intervals used in the histogram, giving the formula:

$$\chi^2 = \sum_{i=1}^{r} \frac{(m_i - m_i')^2}{m'_i}$$

The problem is then stated as follows:

> The joints in the monzonite adamellite (Tim) have different orientations as shown in the histogram of Figure 3 and the Table in Figure 4.

The null hypothesis (H_o) consists of the supposition of a uniform distribution of the orientations of the joints. In accordance with the H_o, in each interval there will be an identical frequency of orientations

FIGURE 4 - AZIMUTH INTERVAL

	10°-40°	40°-70°	70°-100°	100°-130°	130°-160°	160°-10°	TOTALS
m_i (observed frequency of joints oriented in each 30° interval)	32	37	22	36	29	27	183 observ.
$\frac{(m_i - m_i')^2}{m_i'}$	.07	1.39	2.37	.99	.07	.40	5.29

$m_i' = 183/6 = 30.5$ (the frequency of observations in each interval if the distribution was uniform.)

interval 10°-$40^{0} = \frac{(32-30.5)^2}{30.5} = .07$

$\chi^2 = \sum_{i=1}^{r} \frac{(m_i - m_i')^2}{m_i} = 5.29$ Degree of freedom = 6-1=5

equal to the total number (183) divided by the number of sections (6). The expected value in theory is equal to 30.5 The critical value, which would allow rejection of this distribution under the null hypothesis, in favor of an alternative distribution, is equal to 5.29, with 5 degrees of freedom, and $\alpha = .05$ (Burington, 1965). This value lies in the interval $0.50 < \alpha_5(5.29) < 0.25$ ($\alpha_5(5.29) \approx$ .40 from interpolation) suggesting a probability of about 40% that the distribution in histogram Tim is due to random fluctuations of a uniform distribution. Geologically this indicates that the fracture pattern is complicated and may be radial, concentric or haphazard, as is found in a shattered stockwork. The statistical treatment provides additional information on how many observations might be required to determine a statistically significant preferred orientation. In this case, if the number of observations were doubled and the distribution stayed exactly the same, the probability that the observed histogram was due to random fluctuations in a uniform distribution would be less than 10%. If the joint pattern were to be used to determine the stress environment, then at least double, and possibly three or four times as many observations would be required to distinguish a clear signal from the high background noise. This indicates another potential type of misinterpretation. That is, if the number of observations is high enough there will almost surely be a statistically significant preferred orientation. This is where geologic judgement becomes critical and it becomes necessary to define the problem being solved very specifically and it is mandatory that the number of observations per unit area be taken into account, if two or

more areas are being compared. In this case, the data shows the joint pattern approaching a stock work configuration for Tim, which is corroborated by the radial dike patterns shown on the geologic maps of Schmidt and Craddock (1964) and Seager (1961), and a weak preferred orientation. The joint histogram for Syenodiorite (Tis), labelled Tis in Figure 3, displays the major preferred orientation of N-15°-W and a smaller peak at N-65°-E. Using the same statistical technique as described above, $0.25 < \chi^2_5 < 8.63 < 0.10$ indicates that there is a 13% probability that the distribution in the Tis histogram is due to the random fluctuations of a uniform distribution. The preferred orientation in this case is much more assured than in the Monzonite Adamellite. If the number of measurements with this distribution were doubled the probability of a preferred orientation would exceed 99.5%. The Syenodiorite has obviously undergone a different stress history than the Monzonite Adamellite.

Figure 3 labels the joint histogram for the Leucorhyolite, Til. Although there is only one significant peak at N-5°-E, statistically the Til histogram has a high probability of being due to random fluctuations of a uniform distribution ($0.75 < \chi^2_5 < 3.74 < 0.50$). At least three times as many measurements would be required to give a statistically significant preferred orientation.

The strike histogram of the Orthoclase Adamellite (Tio) is labelled Tio on Figure 3. The fractures strike N-40°-E and N-45°-W but the statistical significance of the preferred orientation is low ($0.75 < \chi^2_5 < 3.86 < 0.50$), and the number of measurements should be increased by at least a factor of three to obtain statistical significance.

The joint orientation and fracture intensity data is summarized in Table 2.

The areas of intense fracturing are outlined on Figure 2 (see page 8). In the northwest corner of the map, an isolated outcrop of Monzonite Adamellite is moderately fractured. The center of the map contains a "T" shaped area, trending east-northeast-south-southwest and north-northwest-south-southeast, of moderate and strong fracture intensity. The rock types in this area are Syendiorite, Monzonite Adamellite and Orthoclase Adamellite. The largest area of moderate and strong fracturing occurs at the south end of the range in an elliptical shaped area that trends northwest-southeast. The rock type in this area is predominantly Monzonite Adamellite with a small area of Leucorhyolite. Fracture intensity is compared to the metal distribution in the rock geochemistry section (pate 19 et al).

Rehrig and Heidrick (1972) in their study of regional fracturing concluded that "the crucial structural difference which best contrasts ore-grade prophyries from the barren stocks is the intensity and complexity of the fine fractures and the resulting interlaced network of ore-bearing micro-veinlets and micro-joints which were available to the mineralizing fluids". In the Jarilla Mountains, the Syenodiorite (Tis) appears to fall quite clearly into a non-productive stock classification. It has a system of orthogonal fractures striking east-northeast and north-northwest and the intensity of fracturing is weak. Monzonite Adamellite (Tim), on the other hand, appears to be closely similar to productive stocks in regard to fracture intensity. Since the fracture intensity scale used in this study is

TABLE 2 - FRACTURE PATTERN SUMMARY

ROCK TYPE	BEARING OF STRIKE - 1	BEARING OF STRIKE - 2	PROBABILITY THAT INDICATED PREFERRED ORIENTATION IS REAL	PERCENTAGE OF ROCK WITH STRONG/MODERATE FRACTURE INTENSITY
Tim	N-50-E	N-60-W	60%	46%
Tis	N-15-W	N-65-E	87%	14%
Tio	N-40-E	N-45-W	40%	44%
Til	N- 5-E		40%	100%

relative fracture intensity of the rocks in the Jarilla Mountains, the correlation with other non-productive and productive Laramide stocks in the southwest is tenative at best.

The fracture pattern in the Jarilla Mountains intrusive rocks do not appear to be comparable to the tensional joints described in the study by Mackin and others (1954). In general, the fracture sets in the Jarilla's are much more hapazard then those described in the Granite Mountain study. However, there may be an interior depletion of iron in the Jarilla's that is similar to that described by Mackin (1954).

Beane and others (1975) note that two distinct fracture orientations are exhibited by the intrusive rocks of the Jarilla Mountains. In the granodiorite and latite (Syenodiorite and leucorhyolite in this study) they found fractures trending N-5°-E and N-50° to 55°-E compared to N-15°-W, N-65°-E, and N-5°-E for the respective rock types in this study. In the monzonite (monzonite adamellite in this study) they report joint sets have N-34°-E and N-85°-W trends compared to N-50°-E, N-60°-W in this study. Beane and others (1975) use the fracture orientation data to corroborate petrological data that indicates that the granodiorite and latite (syenodiorite, leucorhyolite; this report) are genetically related and that the monzonite (monzinite adamellite; this report) post dates both. The data presented here would support the conclusion that the syenodiorite and monzonite adamellite were subjected

to quite different stress regimes. Although the syenodiorite appears to have similar fracture orientations to the leucorhyolite their respective fracture intensities are different, so without additional joint orientation measurements this study cannot support a structural relationship between the syenodiorite and leucorhyolite.

LITHOLOGY

The base geologic map used in this study was from Schmidt and Craddock (1964), as were the igneous rock names. Sedimentary and metamorphic units were not sampled in this study and are not described. (For details see Schmidt and Craddock (1964), Seager (1961), Beane et al (1975), and Bloom (1977).) The igneous rocks consist of: extrusive basalt of Recent age, and Tertiary intrusive biotite syenodiorite, monzonite adamellite, orthoclase adamellite, leucorhyolite, and undifferentiated dikes. Talbe 3 summarizes the mineralogy and nomenclature used by workers in the Jarillas for the major igneous rock types.

ROCK GEOCHEMISTRY

Application of Rock Geochemistry Literature to This Study

Mackin and Ingerson (1960) found that biotite and hornblende phenocrysts were largely destroyed in the interior of the Granite Mountain Laccolith. Tension joints with bleached selvages appear to be the conduits that allowed the iron which was removed from mafic minerals in the center of the igneous body to be transported to their peripheral

TABLE 3 IGNEOUS ROCK TYPES

a. Schmidt and Craddock (1964)
b. Seager (1961)
c. Beane et al (1975)

ROCK TYPE	Basalt (a) Olivine Basalt (b)	Biotite Syenodiorite (a) Biotote Granodiorite (b) Granodiorite (c)	Monzonite Adamellite (a) Hornblend Monzonite Porphyry Phase I(b) Monzonitic Rocks (c)	Leucorhyolite (a) Quartz Latite (b) Leucocratic Quartz Latite (c)	Orthoclase Adamellite (a) Monzonite Porphyry, Phase II (b) Orthoclase Quartz Monzonite (c)	Undifferentiated Dikes Andesite Propylite Diabase All other major rock types
MINEROLOGY	Plagioclase An_{60}-40% Augite - 30% Forsterite - 15% Magnetite - 15%	Plageoclase zoned An_{8-70}-55-65% Orthoclase/Microcline -10-30% Biotite - 5-15% Hornblend/ Actindite - 4-8% Quartz - 5-30% Augite/Diopside-8% Magnetite - 2% Apatite Chlorite Epidote Pyrite Serecite Sphene	Plagioclase An_{10-50}-20-45% Hornblend/ Actinolite-5-15% Quartz - tr-15% Apatite Biotite Calcite Clay Epidote Magnetite Sericite Sphene Sulfides Zircon	Plagioclase An_{23}-10% Quartz - 20% K-Feldspar - 60% Biotite Calcite Pyrite Sericite	Orthoclase - 40% Quartz 10-20% Plagioclase An_{10-50} 20-40% Hornblend/ Actinolite 5-30% Chlorite 6-10% Biotite 0-5% Calcite 0-7% Apatite Clay Epidote Magnetite Sericite Sphene Sulfides Zircon	

limestones. They propose deuteric alteration as a hypothesis for the origin of the ore-forming fluid.

Theobald and Havens (1960) found that the alteration of biotite in a quartz monzonite sill resulted in the loss of iron and other base metals.

Griffitts and Nakagowa (1960) proposed that anamolous copper and zinc values in monzonites were due to leakage from nearby ore deposits during mineralization rather than to an originally high metal content of the parent magma.

The Searchlight, Nevada, quartz monzonite stock was studied by Shrivastava and Proctor (1962) and Proctor and others (1973). They found that the lowest copper values in unaltered rocks were spatially associated with an area that gave the highest copper values in altered rock. They also found that the highest concentration of copper in unaltered rock is in the area nearest the vein system that produced the largest amount of copper. The whole-rock contents of gold, silver, lead, and zinc also revealed well-defined patterns that were related to alteration and spatially associated with mineral deposits. They concluded that "significant losses of trace elements in the altered igneous rock mass suggests a non-productive intrusive body."

Putman and Alfors (1967)(1969) in an extensive study of the Rocky Hill granodiorite stock determined the metal variation patterns within

the stock, estimated the within-pluton variance and compared this data to petrologic facies within the stock and to other similar intrusives in Arizona. They concluded that whole-rock trace element data is better than mineral phase trace element data and sampling should be governed by local variations found in the field and not held to rigid grid intersections.

Mantei and others (1970) suggest that anomalous Au, Ag, Cu, Pb, and Zn values in the Marysville, Montana, granodiorite stock are the result of solutions from mineralized veins penetrating out into the wall rock. The vein material is relatively more enriched in Au and Ag than in base metals and that anomalous values for Au and Ag are stronger and more extensive than those for the base metals.

Govett (1972) in a rock geochemistry orientation survey in Cyprus demonstrated that anomalous dispersion patterns for Cu, Zn, Ni and Co could be reliably measured in pillow lavas for a maximum distance of only 20 meters from the massive sulfide deposit. By the use of a statistical discriminant analysis technique an anomalous zone could be recognized more than 2000 meters from the mineralization.

Coope (1973) lists several important porphyry copper deposits which were discovered, or their potential indicated, by the application of geochemical exploration methods. He describes the various methods used in selected case histories and indicates the direction of on-going research.

Sheraton and Block (1973) studied tin bearing granites in Australia and determined that granites associated with copper or lead/zinc mineralization did not show anomalous abundances of Cu, Pb, or Zn. They concluded that if mineralization is regarded as an independent by-product of magma generation, rather than of differentiation processes, then the lack of correlation is explicable.

Olade and Fletcher (1976) used a selective extraction technique to investigate the sulfide iron distribution in the Highland Valley, B. C. porphyry copper deposit. The results emphasize patterns related to sulfide, versus total metal, and are shown to be consistent with mineralogical zoning within the deposit.

Chaffee (1976) described the zonal distribution of selected elements above the Kalamazoo porphyry copper deposit. The paper presents the best rock-geochemical orientation study published to date in the United States. Core and cuttings from two drill holes were analysed for 60 different elements. Each hole sampled a different major rock unit and penetrated all the existing alteration zones and the ore zone. It was found that Cu, Mo, Ag, Au, Co, Mn, Zn, Tl, Rb, Li, Fe, Na, K, S, Se, Ba, B show some type of zoning relative to the ore zone. Chaffee suggests that trace elements should be valuable in evaluating areas where disseminated pyrite is found, and that elemental zoning should be at least as useful as alteration-mineralization zoning for evaluating rock bodies thought to contain blind deposits similar to the Kalamazoo deposit.

Olade (1977) studied major element halos in granitic wall rocks of porphyry copper deposits in British Columbia. It was found that Na_2O, GaO, MgO, and total Fe decreases from the outer margins of the deposit to the inner zones of intense hydrothermal alteration and metallization, while K_2O and K_2O/Na_2O ratios increase inward. Olade concluded that the use of major element halos is more advantageous and less time-consuming than quantitative mineralogical techniques in delineating anomalies and distance to mineralization.

Laboratory Procedure

The sample areas where joint orientations were measured and rock specimens taken have been previously described in the section on Field Sampling Procedure (see page 4). The effects of weathering on the rock specimens was kept to a minimum by collecting large samples and breaking them down in the field to the freshest rock available. In the laboratory the rock samples for chemical analysis were reduced to a powder by the following procedure:

1. The fist size field samples were broken with a hammer on a stainless steel plate. Only completely fresh chips were retained for mechanical crushing.

2. The chips were then successively reduced in a jaw crusher with ceramic plates, a Bico pulverizer and finally about 50 grams were reduced to minus 200 mesh in a Beuhler pulverizer-mixer.

3. The minus 200 mesh material was analyzed by emmission spectrography and atomic absorption.

Twenty samples were analyzed for 35 elements on the Wadsworth mounted, Jarrell-Ash, 1.5 meter, DC arc emission spectrograph, which is equipped with a water cooled arc stand. The film was read on a 15 X Jarrell-Ash microphotometer comparator. A 10 mg. portion of each sample was completely burned in the arc. This work was done by W. A. Bowes & Associates, Steamboat Springs, Colorado.

One hundred and forty samples were analyzed for 4 elements on a Perkin-Elmer Model 103 atomic absorption spectrophotometer and twenty samples were analyzed for 1 element on a Perkin-Elmer #360. For copper, lead, zinc and iron 2 gm of sample were weighed into a beaker. Then 5 ml. of concentrated nitric acid and 15 ml. of concentrated hydrochloric acid were added. This mixture was heated on a hot plate and leached for about 2 hours until all the liquid was nearly evaporated. Finally, 10 ml. of concentrated hydrochloric acid and 100 ml. of distilled water were added and brought to a boil. The solution was then transfered to a 200 ml. volumetric flask and made up to the volume. For molybdenum 10 gm. of sample were weighed into a beaker, 15 ml. of concentrated nitric acid was added and the mixture was heated on a hot plate until the brown fumes were gone. The beaker was allowed to cool and then 15 ml. of concentrated sulfuric acid was added and the mixture was heated until the brown fumes were gone. When the solution was cool 10 ml of concentrated hydrochloric acid was added and again heated until the brown fumes were gone. Finally, 25 ml. of distilled water was added and the mixture was brought to a boil and then allowed to cool. Calcuim and iron interference was eliminated by adding 5 ml. of aluminum chloride solution. The mixture was then transfered to a 100 ml vol-

unmetric flask and made up to volume. The A. A. instrument parameters are summarized in Table 4.

Analytic Results

The emission spectrograph was used in the first stage of this lith-geochemical project to identify and semi-quantify 35 elements that could provide insight into geochemical and ore depositional processes or patterns. Nineteen of the thirty five elements that were looked for were within the limits of detection and are reported below in Table 5. The sixteen elements not reported here include Si and Al, which were present in all samples in amounts above the upper limit of discrimination, and Au, Mo, W, Sn, As, Bi, Sb, Cd, Rb, Ce, Cs, Li, Ga, Re, which were not detected in any samples. The spectographic results were helpful in determining the standards required for the atomic absorption analysis.

Table 5 presents the emission spectrograph data in four groups according to rock type, and in three element groups according to associations. In the chalcophile group copper, lead, and zinc are discussed in detail later in the paper (see page 52 et al). Silver was detected in three samples and apperas to be associated with higher than average lead content regardless of rock type. There does not appear to by any special relationship of silver values with known mineralization, extensive alteration or geochemical anomalies.

The two siderophile elements nickel and cobalt, although often

TABLE 4 ATOMIC ABSORPTION INSTRUMENT PARAMETERS

ELEMENT	WAVE LENGHT (NM)	CATHODE CURRENT (MA)	INSTRUMENT	SILT (NM)	FUEL	OXIDENT
Cu	324.7	6	P.E. 103	.7	C_2H_2	Air
Zn	213.9	8	P.E. 103	.7	C_2H_2	Air
Pb	283.3	6	P.E. 103	.7	C_2H_2	Air
Fe	373.7	10	P.E. 103	.7	C_2H_2	Air
Mo	313.3	30	P.E. 360	.7	C_2H_2	N_2O

TABLE 5 EMISSION SPECTROGRAPHIC ANALYSIS

K, P Reported in %, Fe in PPT, All Other Elements in PPM

SAMPLE NUMBER	CHALCOPHILE				SIDEROPHILE		LITHOPHILE											ROCK TYPE	COMPARISON OF ATOMIC ABSORPTION ANALYSIS			
	Cu	Pb	Zn	Ag	Ni	Co	Cr	V	Ba	Sr	Zr	B	Be	La	Sc	Nb	Y	K	P		Cu	Pb	Zn	Fe
1	20	20	L	-	5	20	100	50	2000	1000	150	L	5	70	20	10	20	1	.1	Tis	10	22	55	35
2	15	20	-	-	5	-	200	30	2000	1000	200	-	5	-	-	10	10	2	L	Tis	6	11	16	25
3	20	20	-	-	5	30	150	50	2000	1000	200	-	5	20	20	10	10	1	L	Tis	13	12	36	38
11	15	30	-	.5	5	-	150	50	2000	1000	200	-	5	20	10	10	L	2	L	Tis	7	24	25	16
Avg.Tis	18	23	-	-	5	.	150	45	2000	1000	188	-	5	37	17	10	13	1.5	.		9	17	33	29
13	40	30	-	-	5	10	70	50	2000	1000	150	-	5	-	L	10	-	2	.1	Tio	35	36	65	24
16	10	10	-	-	5	-	150	50	100	700	100	-	5	-	-	10	-	L	.1	Tio	2	5	21	9
Avg.Tio	25	20	-	-	5	5	110	50	1050	850	125	-	5	-	.	10	-	.	.1					
17	10	30	-	L	5	-	300	-	1000	500	200	-	5	-	-	20	10	3	-	Til	5	8	13	3
18	10	30	-	-	5	-	300	-	2000	300	100	-	5	-	-	10	L	3	-	Til	5	6	23	6
Avg.Til	10	30	-	.	5	-	300	-	2000	400	150	-	5	-	-	15	.	3	-		5	7	18	5
21	40	30	-	L	5	-	300	30	1000	700	150	-	5	100	-	10	10	1.5	.1	Tim	46	17	21	3
24	10	20	-	-	5	10	150	50	2000	1000	200	10	5	100	10	10	20	1.5	.1	Tim	5	5	26	20
32	10	30	-	-	5	-	200	50	2000	1000	200	10	5	50	15	10	30	2	.1	Tim	3	6	21	7
44	10	50	-	-	5	-	150	50	2000	1000	100	10	5	20	L	10	10	2	.1	Tim	5	21	25	15
53	10	10	-	-	5	-	150	50	2000	1000	150	-	5	20	10	10	20	3	.1	Tim	2	7	15	4
55	10	30	-	-	5	-	150	50	2000	1000	150	-	5	-	-	10	10	2	.1	Tim	6	9	40	19
58	10	10	-	-	5	30	100	50	-	200	100	-	5	50	-	10	-	-	.1	Tim	4	4	24	7
60	10	20	-	-	5	-	200	50	2000	1000	100	-	5	70	L	10	-	2	.1	Tim	3	8	25	17
73	10	10	-	-	5	-	150	50	1000	1000	100	-	5	70	10	10	20	2	.1	Tim	3	5	22	7
80	10	10	-	-	5	-	150	30	100	500	200	-	5	20	-	10	20	L	.1	Tim	2	3	11	4
84	10	20	-	-	5	-	150	50	300	500	100	-	5	20	L	10	-	.5	.1	Tim	2	10	30	7
90	10	30	-	-	5	-	200	50	3000	1000	100	-	5	100	L	10	10	3	.1	Tim	5	8	36	10
Avg.Tim	13	23	-	-	5	.	171	47	1582	825	138	.	5	56	.	10	.	2	.1		7	9	25	10
Lower Limit of Detection	5	10	200	.5	5	10	20	10	10	100	10	10	2	20	5	10	10	.5%	.1%					

(-) Not Detected (L) Detected But Below Limit of Determination

associated, have two distinctly different distributions. The nickel is evenly distributed at 5 ppm throughout all the rock types. Rosler and Lange (1972) indicate that Ni should decrease from over 100 ppm in basin igneous rocks to about 50 ppm in intermediate and 8 ppm in acid rocks. The Jarillas appear to be depleted in Ni and magmatic differentiation appears to have had little effect on this element. Cobalt content in most magma series decreases from 50 ppm in basic rocks to about 5 ppm in the felsic end member and there is some indication thatthe distribution in the Jarilla's follows this decreasing mafic to felsic trends. The Co content displayed in Table 5 and Figure 4 is very erratic and is probably most affected by the fact that the concentration is near or below the lower limit of instrument detection. Chaffee (1976) shows a small Co anomaly in the propylitic zone and then a large increase that peaks at 30 ppm in the ore zone between the phyllic and potassic zones.

The quantities of thirteen lithophile elements were determined by emission spectography and listed in Table 5. Chromium in the intrusive rocks of the Jarilla Mountains was present in anomalously high amounts. Hawkes and Webb(1962) indicate that the Cr content of felsic rock is about 25 ppm and that chromium has a strong association with Ni and Mg. Rosler and Lange (1972) report Cr to decrease from 300 ppm in basic rocks to 50 ppm in intermediate to about 30 ppm in acidic rocks. The trend in the Jarillas (see Figure 5) is from an average of 150 ppm in Syenodiroite to 300 ppm in Leucorhyolite - just the opposite of the trend expected and an order of magnitude higher than the quantities reported in the

FIGURE 4

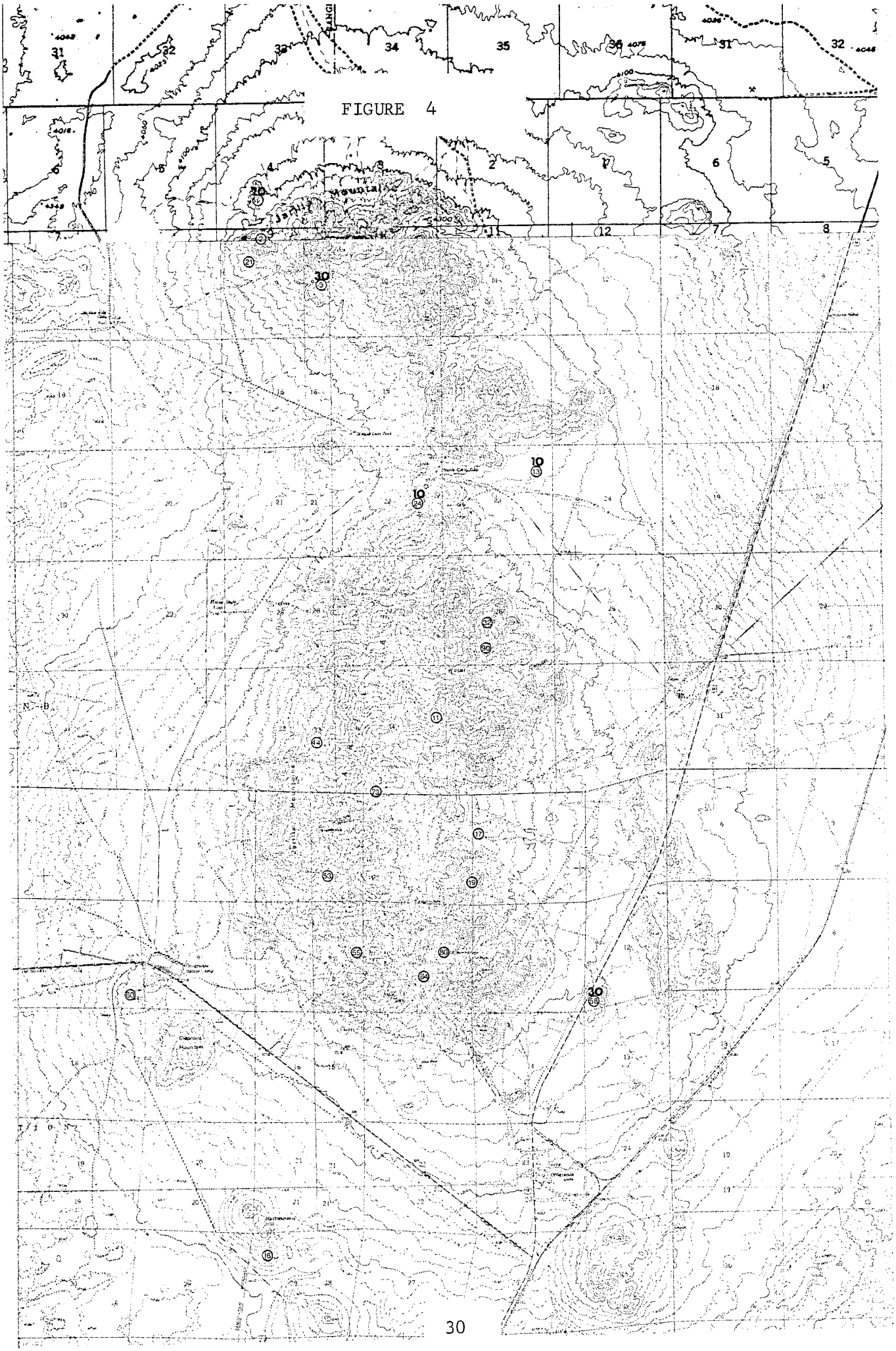

PPM - Co

FIGURE 5

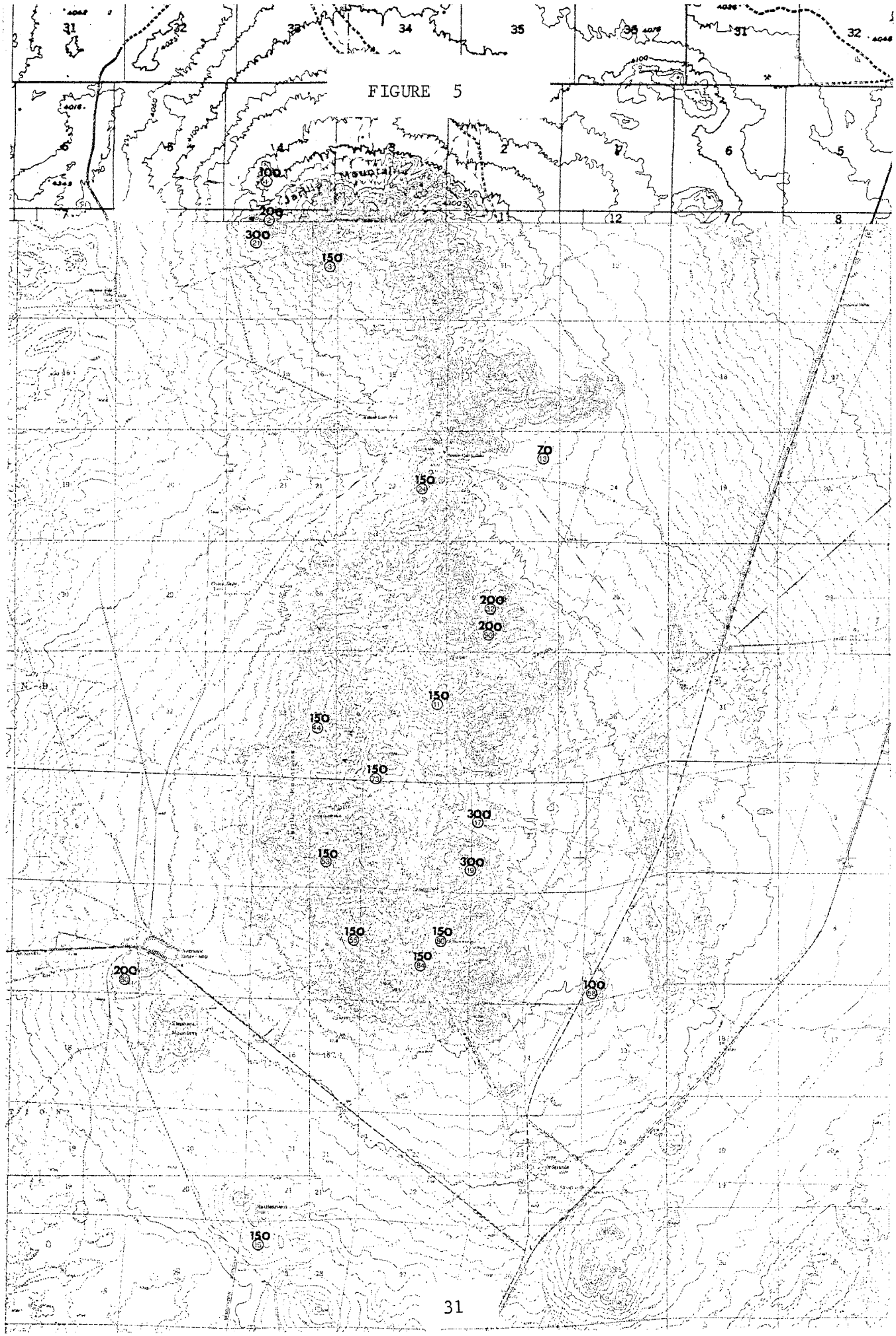
300
150
70
150
200
200
150
150
150
300
150
300
150
150
150
200
100
150
PPM - Cr

literature. The spatial distribution is probably related to rock types since other trends are not apparent. Vanadium is reported in the literature to averate 40 ppm in felsic rocks and about 100 ppm in intermediate types. In the Jarilla's V averages between 40 and 50 ppm and is very evenly distributed throughout the range except in Leucorhyolite where it is apparently absent (see Figure 6). Vanadium is associated with Fe and Ti in magnetite, a mineral which is not found in the Leucorhyolite. The barium content of felsic rocks is reported to average 840 ppm with an increasing trend from basic through intermediate to acidic rocks averaging 300 ppm, 600 ppm, 800 ppm respectively. In the igenous rocks of the Jarilla Mountains, the barium content averages 2000 ppm in biotite syenodiorite and 2000 ppm in leucorhyolite and in the monzonite rocks ranges from less than 10 ppm to 3000 ppm. Chaffee (1976) presents the barium distribution at San Manuel as follows: background - 600 ppm, possible slight anomaly in the propylitic zone - 700 ppm, a strong anomaly in the ore zone that increases below the ore to 1500 ppm, also there may be a negative anomaly above the ore in the phyllic and phyllic-argillic zones. The spatial distribution of barium is shown in Figure 7. In the south east end of the range samples 58, 80, 84, and 16 outline an area of low barium content. Sample 90 is from a pyritized area and has the highest barium concentration found. There are a few barite veins in the north end of the range near samples areas 344 and 27 (see Figure 1). The Ba is probably concentrated in orthoclase and sericite where it substitutes for K in the c crystal lattice. The spatial distribution of Ba (Figure &) and K (Figure 14) are nearly identical. Rosler and Lange (1972) report 400 ppm strontium in absic rocks, 750 ppm

FIGURE 6

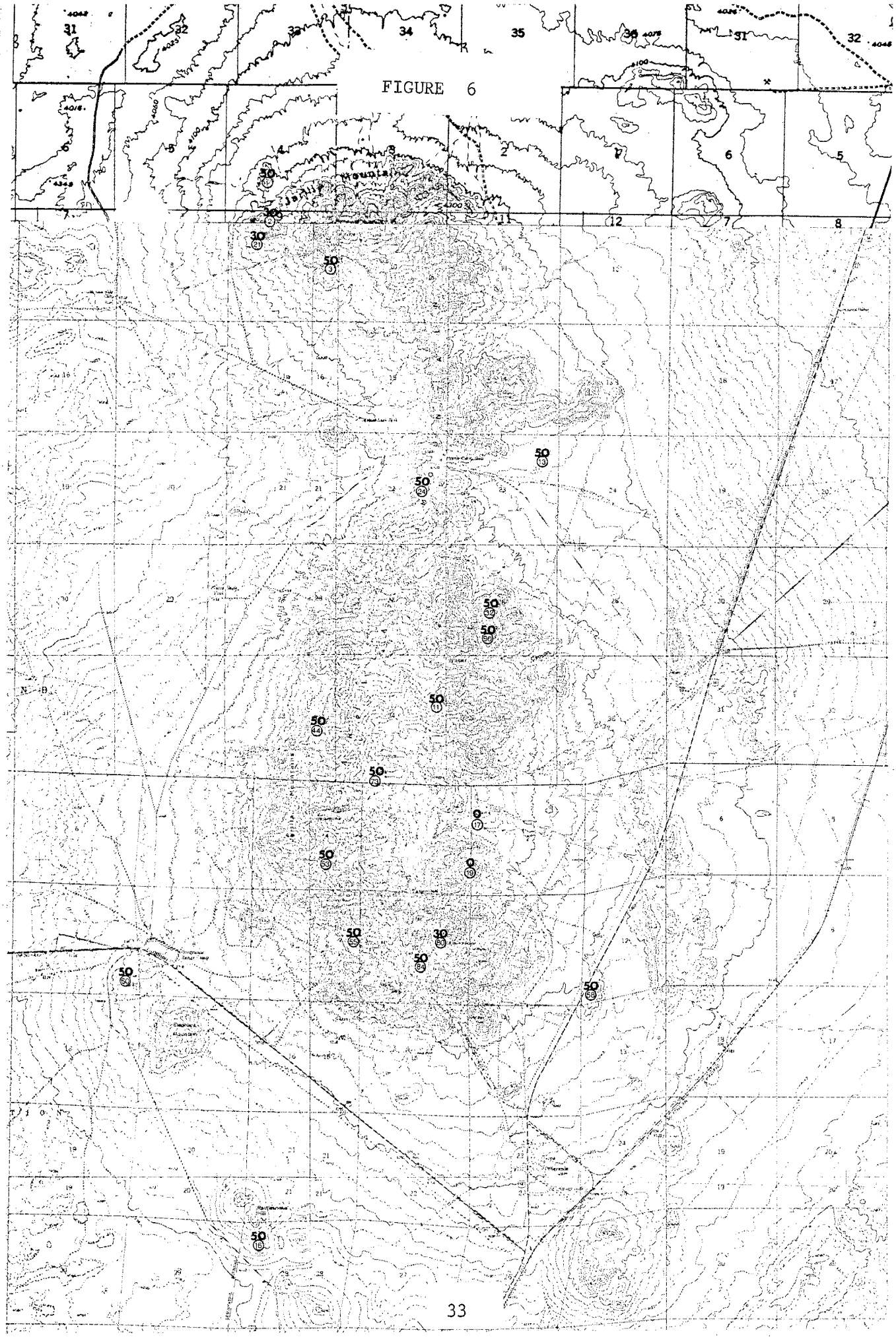

FIGURE 7

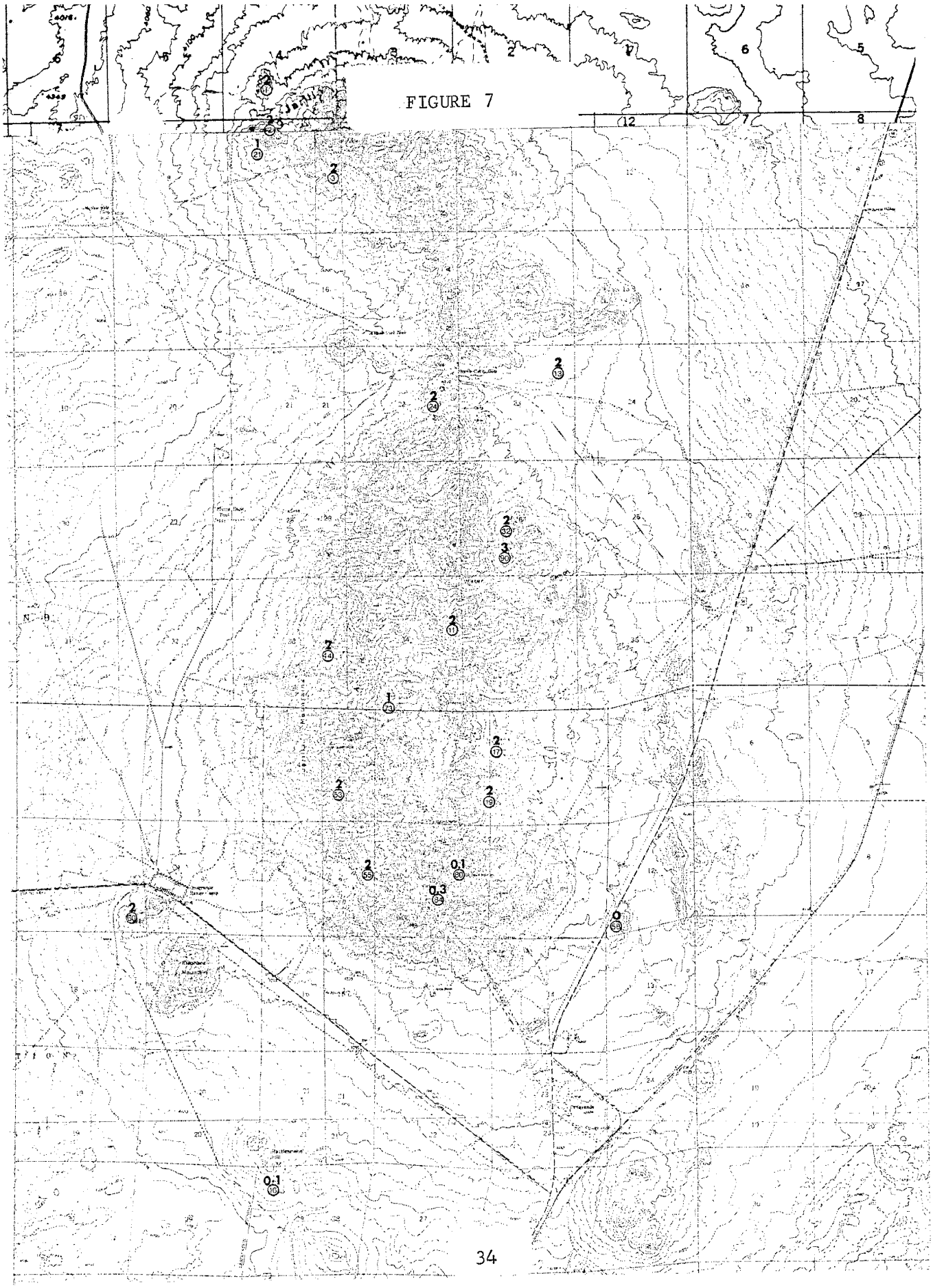

PPT - Ba

in intermediate and 250 ppm in acidic. This study shows 1000 ppm in the biotite syenodiorite and 400 ppm in the leucorhyolite. Figure 8 shows a depletion of Sr in the southeastern part of the range similar to that shown in Figure 7 for barium. The zirconium content, shown in Table 5 and Figure 9 , ranges between 100 and 200 ppm. The literature indicates Zr increases from 100 ppm in basic rocks to 250 ppm in intermediate and decreases slightly to 200 ppm in acid rocks. Essentially all the Zr is found in zircons, which are a common accessory mineral. Boron was found in three samples in the north-central part of the range (Figure 10). The value of 10 ppm or less found in this study agrees with the values reported in the literature, but Chaffee (1975) found a B concentration of up to 35 ppm below the ore zone, which is very similar to the Ba anomalies he found. In the Jarillas, boron and barium are apparently unrelated. Lanthanum concentration ranges from less than 20 ppm to 100 ppm. The literature reports 10 ppm in basic, 60 ppm in intermediate and 40 ppm in acid rocks. La is usually associated with other rare earth elements Sc, Y, Th, Nb, and found in allamite, apatite and monazite. The orthoclase adamellite and leucorhyolite contain no La probably becauee of the absence of apatite in the particular samples analyzed. The spatial distribution (Figure 11) of La does not reveal any association with known mineralization. Scandium was detected in eleven of the twenty samples analyzed, ranging from detectable but less than 5 ppm to 20 ppm. This rare earth is reported to average 20 ppm in basic rocks and about 3 ppm in intermediate and acidic types, so the Jarillas are slightly enriched in this element. Figure 12 shows a depletion of Sc in the southern part of the range, which corresponds to the area of known mineralization. Rösler and Lange

FIGURE 8

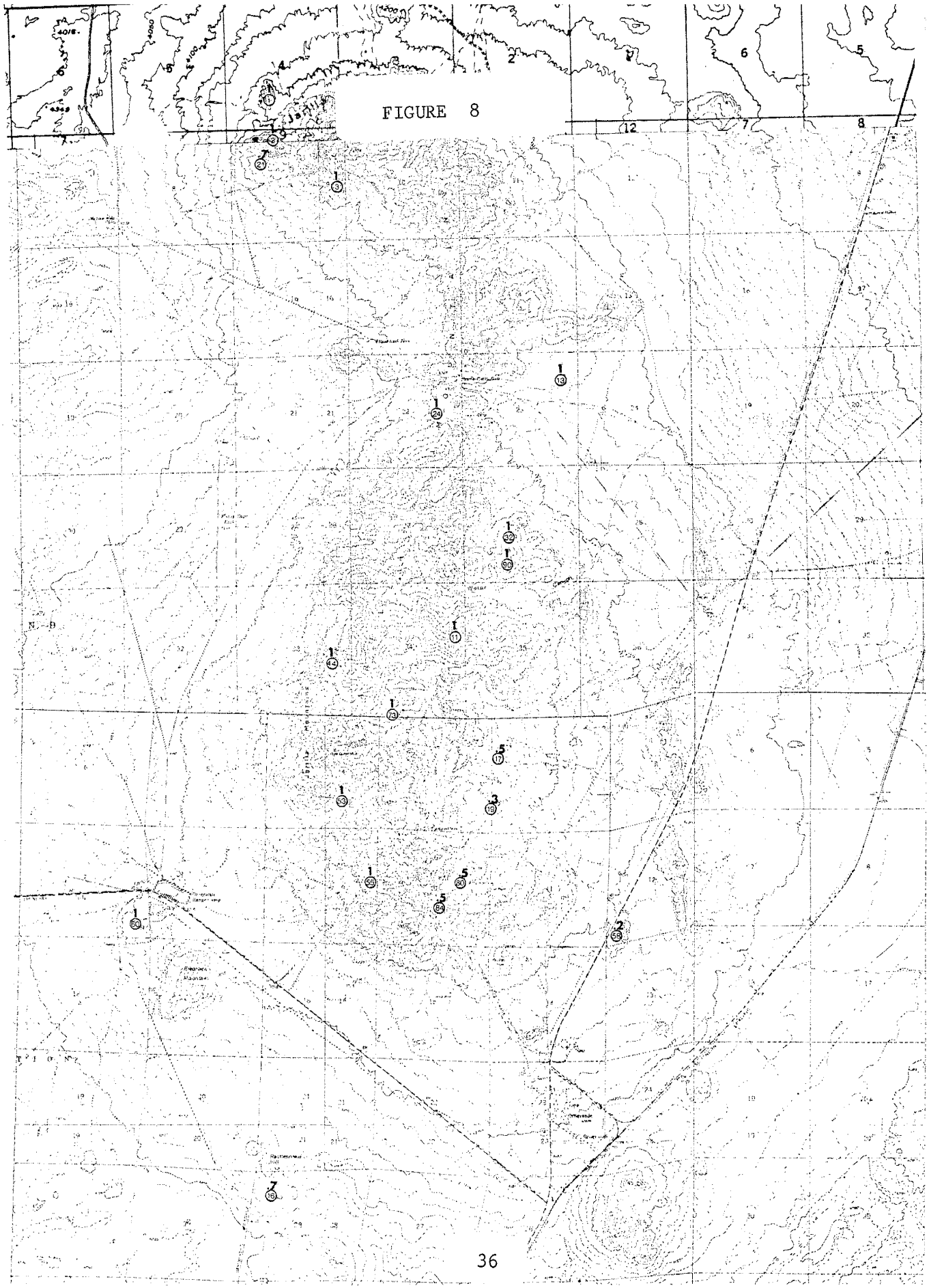

PPT - Sr

FIGURE 9

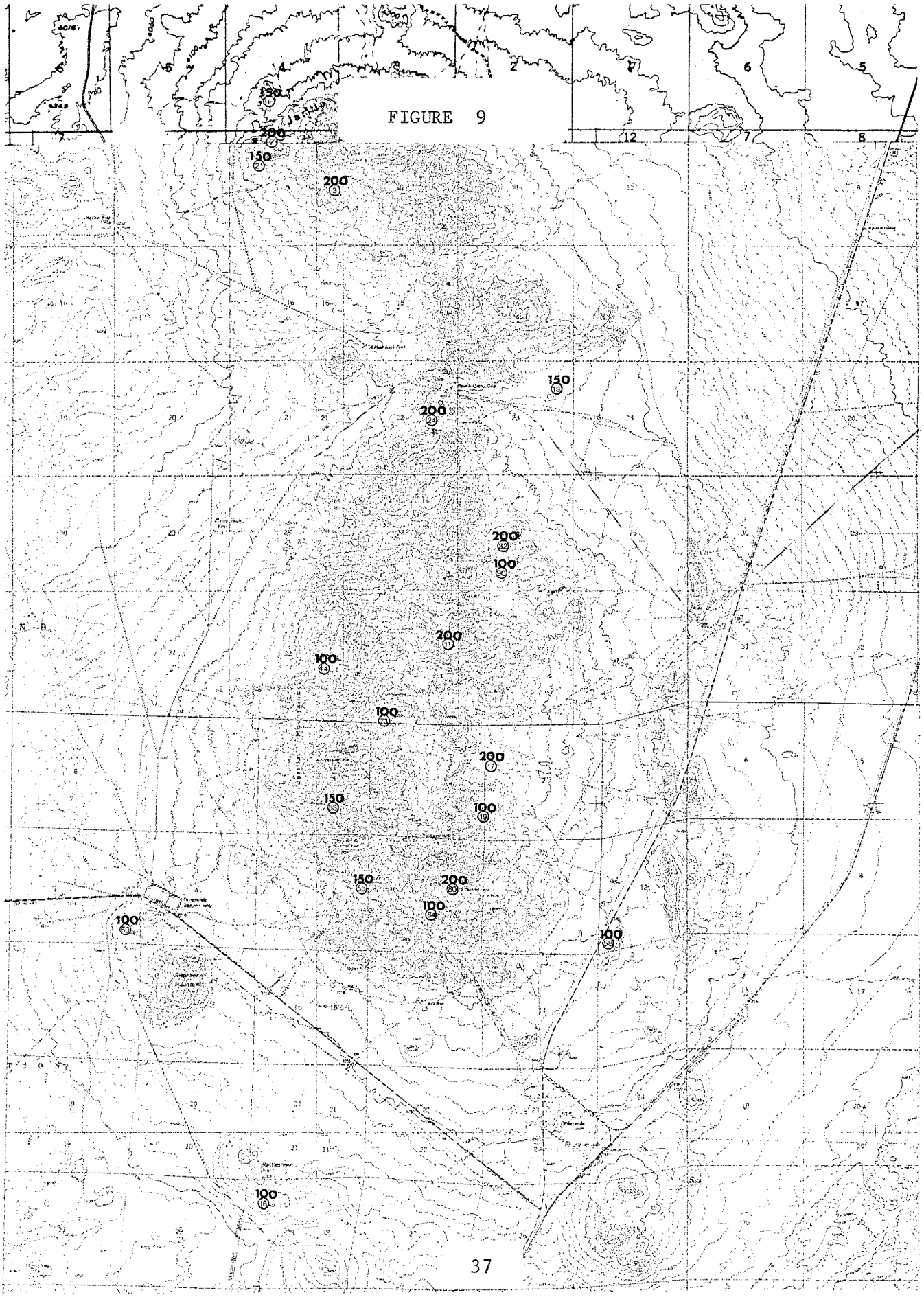

PPM - Zr

FIGURE 10

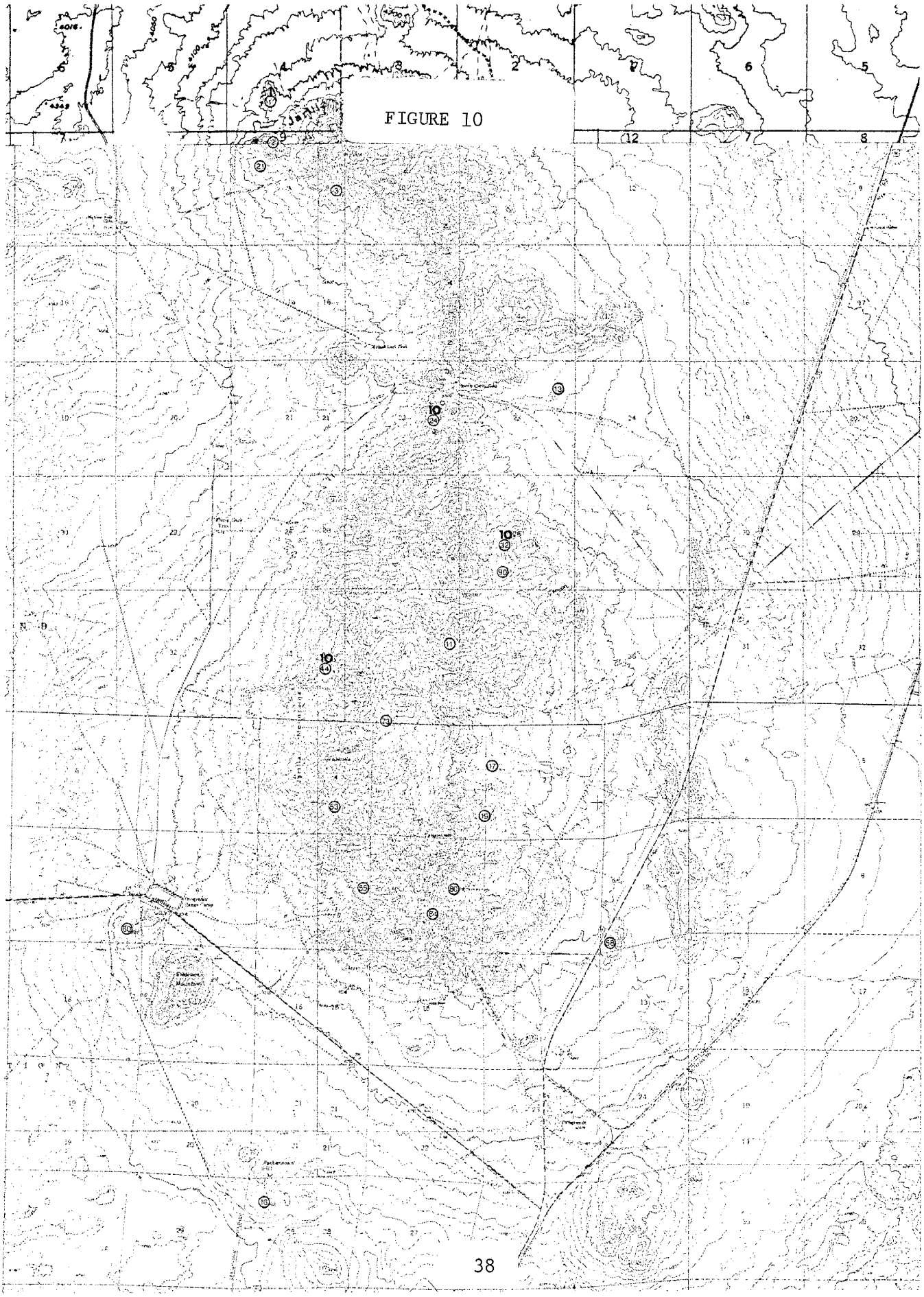

38

PPM-B

FIGURE 11

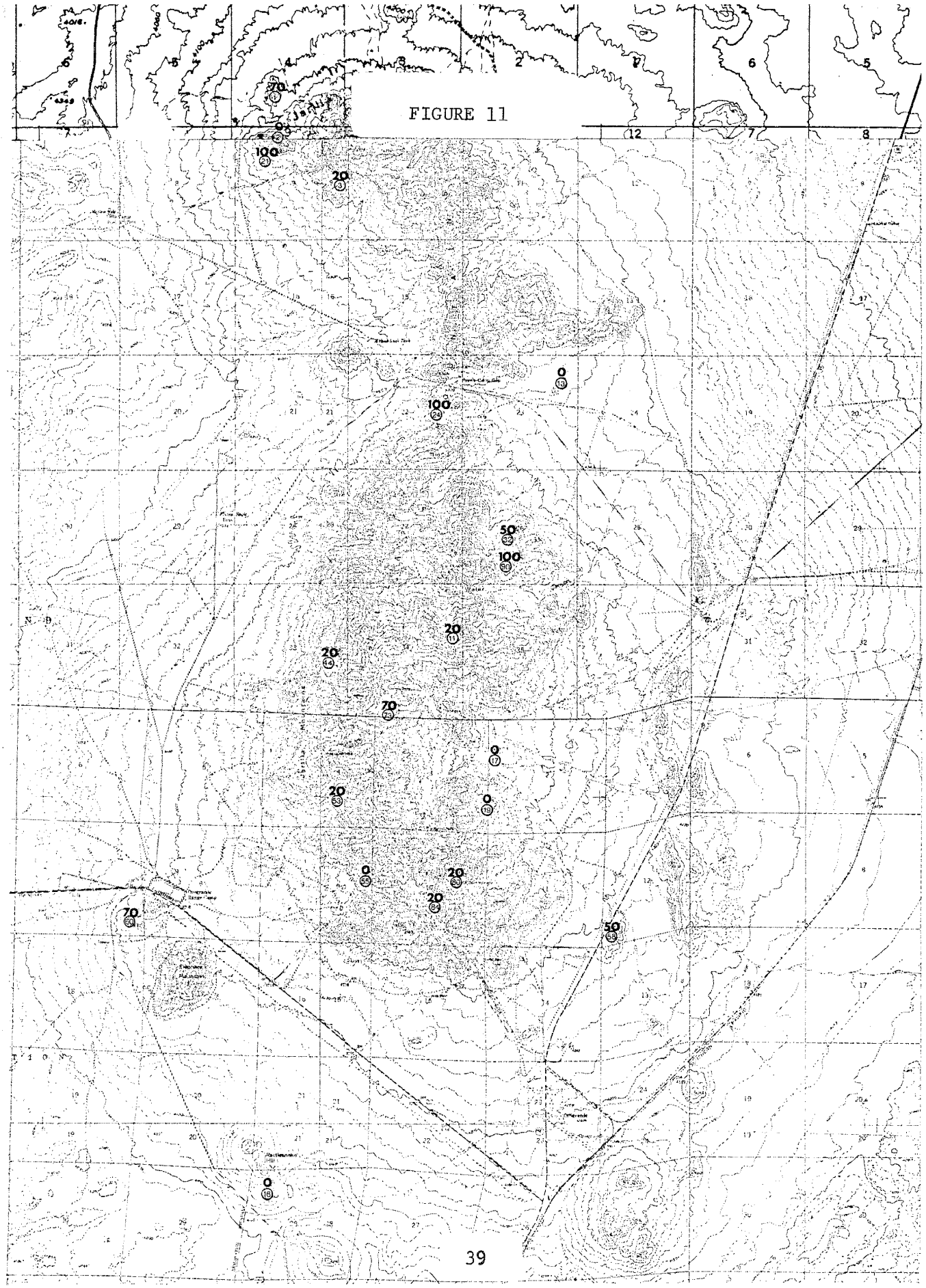

FIGURE 12

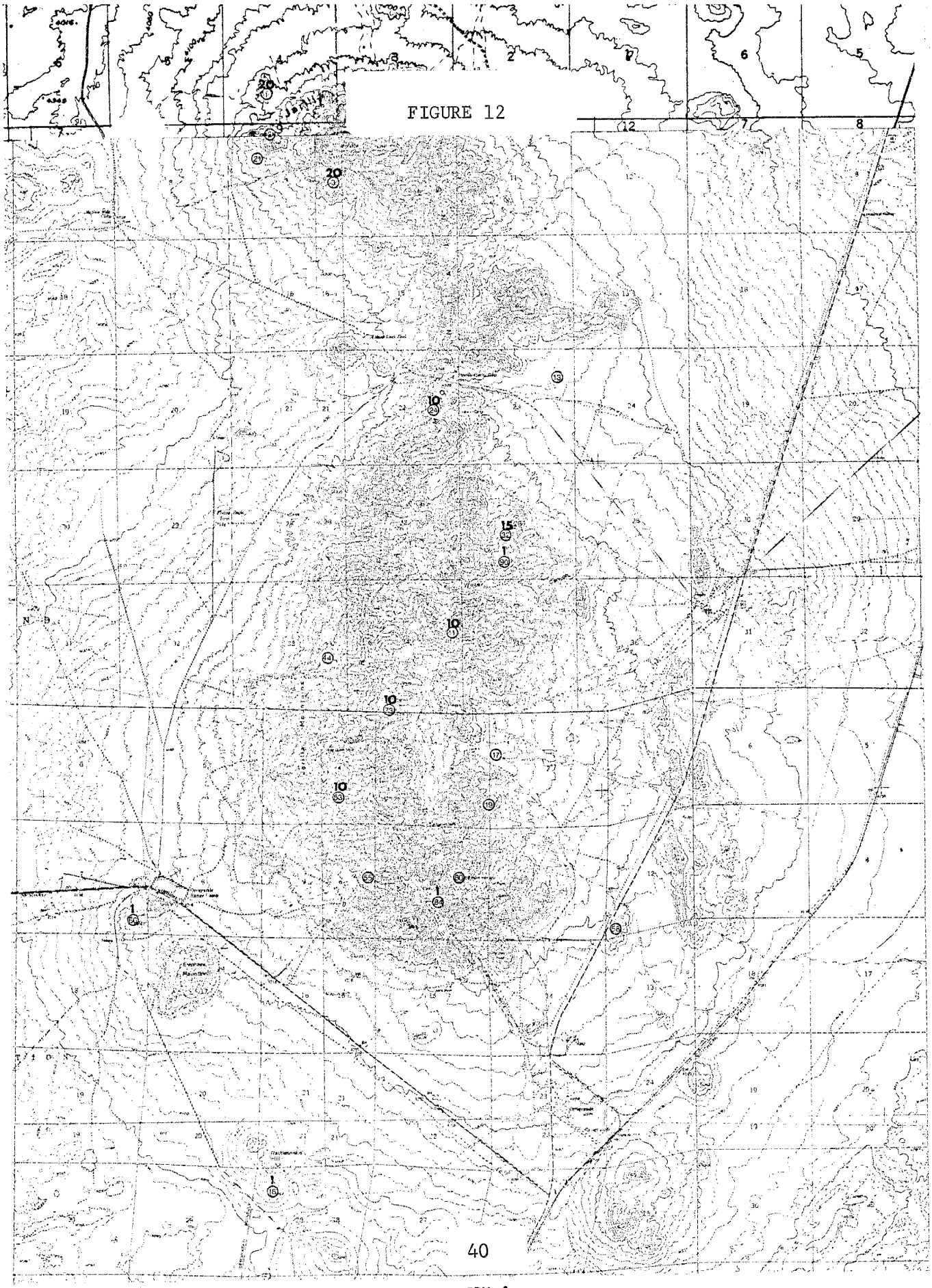

PPM - Sc

(1972) report that yttrium averages 20 ppm in intermediate rocks and 40 ppm in more felsic varities. In the Jarilla Mountains, Y values range from below the limit of detection up to 30 ppm. Unlike the other rare earth elements the leucorhyolite contains detectable amounts of Y. In addition to associating with the other rare earths, Y can substitute for Ca in crystal lattices. The spatial distribution of Y may indicate a depletion in the southern end of the range (Figure 13). Potassium ranges from not detected through detected but below limit of determination up to 3 percent. The literature reports the potassium content of basic rocks average less than 1 percent, intermediate rocks 2 percent, and acid rocks 3-4 percent. The high K values occur in the leucorhyolite and in samples 53 and 90 of monzonite adamellite. Sample area 90 contains abundant pyrite. The spatial distribution of potassium is similar to that of Ba, Sr, and Y, in that the southern end of the range appears to have a lower concentration than the central and northern areas (Figure 14). Phosphorus decreased from 0.1-0.2 percent in basic and intermediate rocks to about 0.07 percent in acidic rocks. In the Jarilla Mountains P is found in all rock types, except leucorhyolite, in a narrow concentration range of detected but below the limit of determination to 0.1 percent, which is the lower limit of determination. The biotite syenodiorite apparently has less P than the monzonitic rocks. All the rock types except leucorhyolite have reported apatite as an accessory mineral.

ATOMIC ABSORPTION INSTRUMENTAL PRECISION

The results of the tests for the precision of the atomic absorption analysis are given in Table 6 (see pages 47,48). Four replicates of two different samples

FIGURE 13

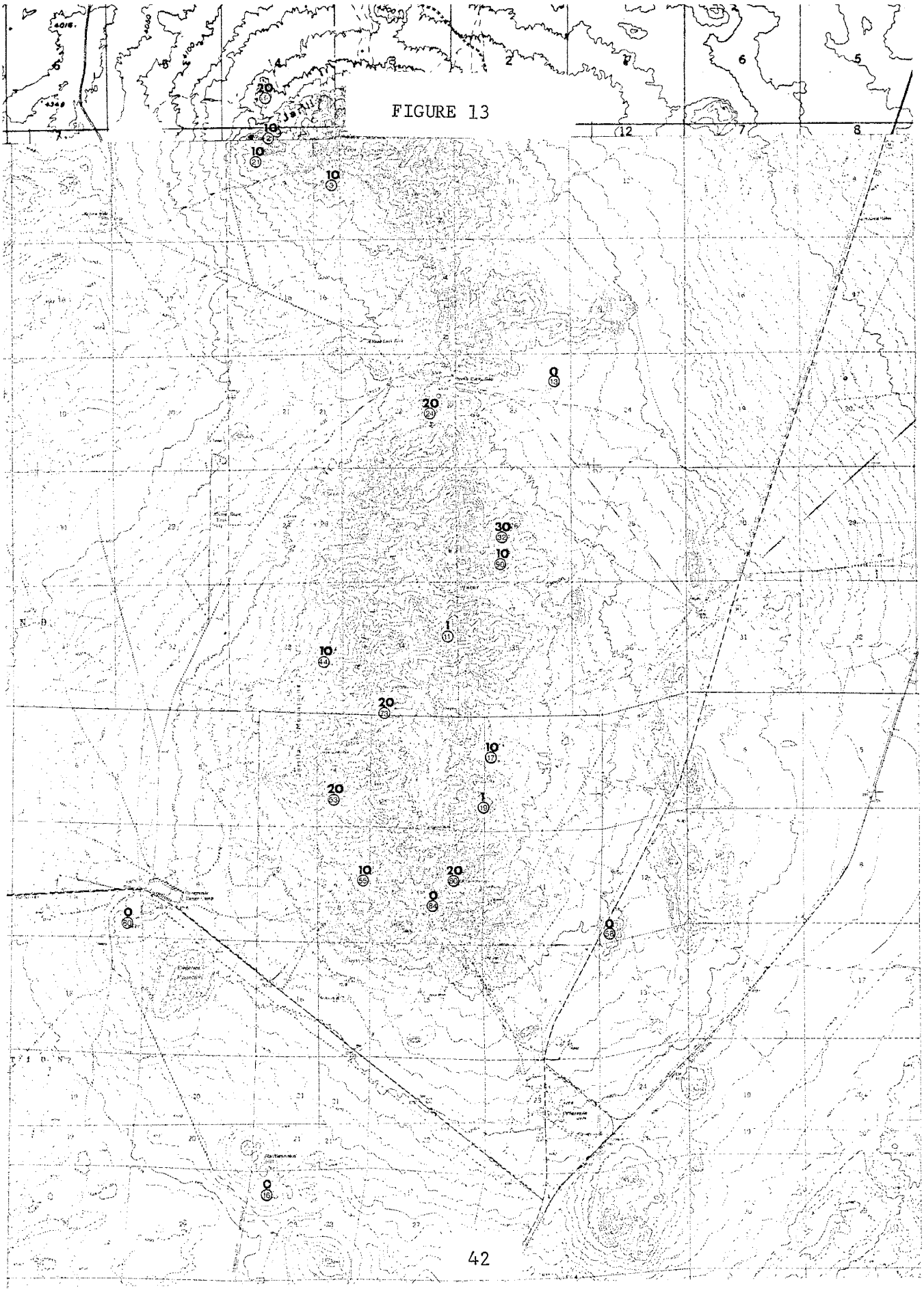

PPM - Y

FIGURE 14

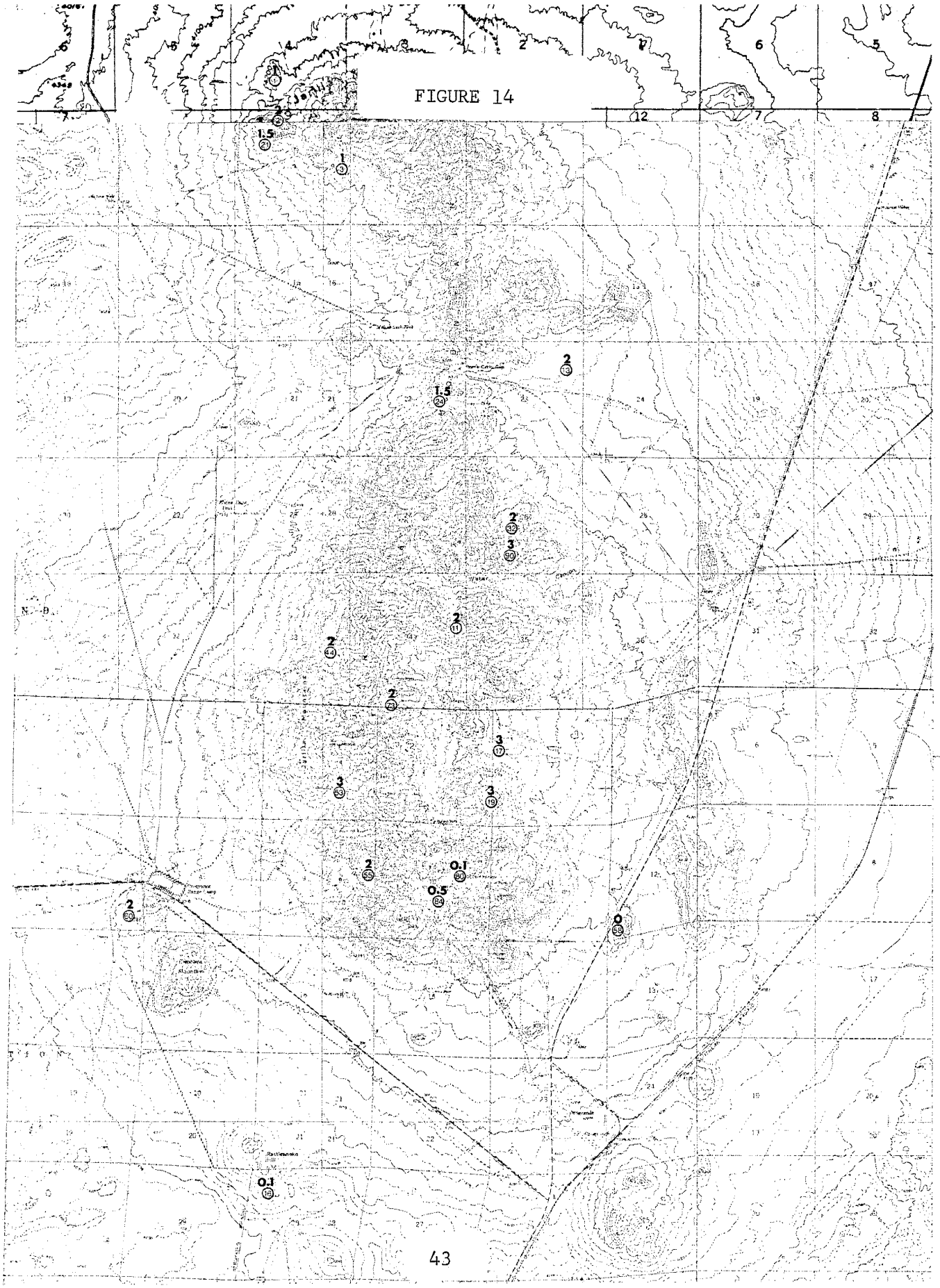

and three replicates of two other samples were used in the test. The values are reported in parts per million for copper, lead and zinc and in parts per thousand for iron.

The statistical terms used in this section are defined as follows: (Koch and Link, 1970; Pawlowicz, 1974; Walpole and Myers, 1972)

Mean - is a measure of central tendency; in a sample of n numbers $X_1, X_2 \ldots\ldots, X_n$ the mean is defined as $\bar{X}$ and $\bar{X} = \sum_{i=1}^{n} X_i / n$

Maximum - is defined as the highest observed value in a set of numbers.

Minimum - is defined as the lowest observed value in a set of numbers.

Range - is defined as the difference between the maximum and minimum observed values.

Variance - is a measure of dispersion about the mean; in a sample of n numbers $X_1, X_2 \ldots\ldots, X_n$ the variance is defined as "S^2" and $S^2 = \sum_{i=1}^{n} \frac{(X_i - \bar{X})^2}{n-1}$

Standard Deviation - (Std.Dev.) is the root-mean-square deviation of a set of observations from their mean. Standard deviation is defined as "S" which is the square root of the variance. $S = \sqrt{S^2}$

Coefficient of Variation - (C.V.%) is defined as the standard deviation expressed as a percentage of the mean.

$C.V.\% = S/\bar{X} \cdot 100\%$

90% Confidence Interval - (90% C.I.) this measurement incorporates three basic attributes of the sample: The mean; The standard deviation; and The sample size. In this case we use a two-sided confidence interval given by the expression 90% C.I. = $\pm t_{5\%} \; S/\sqrt{n}$ where t is student's t statistic
s is the standard deviation, and n is the sample size

Upper Bound - (U.B.) is defined as the mean for a set of observations plus the confidence interval. $U.B. = \bar{X} + t_{5\%} \; S/\sqrt{n}$

Lower Bound - (L.B.) is defined as the mean for a set of observations minus the confidence interval. $L.B. = \bar{X} - t_{5\%} \; S/\sqrt{n}$

NOTE: This use of confidence intervals allows one to say with 90% confidence that the Syenodiorite in sample #3, Table 6 contains not less than 9.2% nor more than 16.2% copper.

Precision - is defined as the closeness of agreement among replicate results obtained under a definite set of conditions. The U.B. and L.B. in Table 6 define the precision of atomic absorption analytical method.

Accuracy - is defined as the nearness of the mean ($\bar{X}$) of a number (n) of results to the "true" result. There is no test of accuracy in this study.

DATA ANALYSIS FOR Cu, Pb, Zn, and Fe

The content of copper, lead, zinc, and iron in the igneous rocks of the Jarilla Mountains is presented in Table 8 - 11. This data is analyzed statistically by a procedure using probability plots and also computer generaged histograms and scatter diagrams are presented (Figures 15 & 16). Tennant and White (1959) describe a method of studying the distribution of geochemical data by plotting the values on logarithmic probability paper. Gutjahr (1973) presents a detailed description of the statistical procedure used to check for normality by plotting the empirical distribution functions of the data on normal probability paper. The data analysis presented in this study combines the techniques described in these two references by first checking for normality of the data according to the method described by Gutjahr and then analyzing the metal distributions geologically using the technique outlined by Tennant and White.

COPPER DISTRIBUTION

Tables 7 through 11 present the copper values and samples locations numbers for Monzonite Adamellite, Leucorhyolite, Syenodiorite, Orthoclase Adamellite and Undifferentiated Dikes respectively. The analysis were separated according to rock type in order to obtain as homogeneous a population as possible. Figure 17 shows the distribution of Cu in Tim,

TABLE 6 - ATOMIC ABSORBTION INSTRUMENTAL PRECISION
SAMPLE NO. 85 MONZONITE ADAMELLITE (Tim)
(Cu, Pb, Zn in PPM; Fe in PPT)

Cu	Pb	Zn	Fe
226.0	42.0	85.0	8.0
203.0	40.0	68.0	9.0
205.0	38.0	81.0	9.0
205.0	39.0	81.0	9.0

Variable	TOTAL	MEAN	MAXIMUM	MINIMUM
Cu	839.0	209.8	226.0	203.0
Pb	159.0	39.8	42.0	38.0
Zn	315.0	78.8	85.0	68.0
Fe	35.0	8.8	9.0	8.0

Variable	RANGE	VARIANCE	STD. DEV.	C.V.%	U.B.	L.B.	90% C.I.
Cu	23.0	118.25	10.874	5.18	222.54	196.96	±12.79 PPM
Pb	4.0	2.91	1.708	4.30	41.76	37.74	± 2.01 PPM
Zn	17.0	54.91	7.411	9.41	87.47	70.03	± 8.72 PPM
Fe	1.0	0.25	0.500	5.71	9.34	8.16	± .59 PPT

SAMPLE NO. 31 MONZONITE ADAMELLITE (Tim)
(Cu, Pb, Zn in PPM; Fe in PPT)

Cu	Pb	Zn	Fe
1.0	5.0	18.0	11.0
2.0	5.0	10.0	12.0
3.0	4.0	18.0	12.0
2.0	5.0	15.0	12.0

Variable	TOTAL	MEAN	MAXIMUM	MINIMUM
Cu	8.0	2.0	3.0	1.0
Pb	19.0	4.8	5.0	4.0
Zn	61.0	15.3	18.0	10.0
Fe	47.0	11.8	12.0	11.0

Variable	RANGE	VARIANCE	STD. DEV.	C.V.%	U.B.	L.B.	90% C.I.
Cu	2.0	.67	.82	40.80	2.96	1.04	± .96 PPM
Pb	1.0	.25	.50	10.53	5.34	4.16	± .59 PPM
Zn	8.0	14.25	3.78	24.75	19.69	10.81	± 4.44 PPM
Fe	1.0	.25	.50	4.26	12.34	11.16	± .59 PPT

SAMPLE NO. 3 SYENODIORITE (Tis)

Cu	Pb	Zn	Fe
15.0	19.0	35.0	42.0
12.0	10.0	40.0	38.0
11.0	7.0	34.0	34.0

Variable	TOTAL	MEAN	MAXIMUM	MINIMUM
Cu	38.0	12.7	15.0	11.0
Pb	36.0	12.0	19.0	7.0
Zn	109.0	36.3	40.0	34.0
Fe	114.0	38.0	42.0	34.0

Variable	RANGE	VARIANCE	STD. DEV.	C.V.%	U.B.	L.B.	90% C.I.
Cu	4.0	4.3	2.08	16.44	16.18	9.16	± 3.51 PPM
Pb	12.0	39.0	6.25	52.04	22.53	1.47	±10.53 PPM
Zn	6.0	10.3	3.22	8.85	41.75	30.91	± 5.42 PPM
Fe	8.0	16.0	4.00	10.53	44.74	31.26	± 6.74 PPT

TABLE 6 CONTINUED

SAMPLE NO. 89 BASALT (Rb)
(Cu, Pb, Zn, Mo in PPM; Fe in PPT)

Cu	Pb	Zn	Fe	Mo
50.0	5.0	70.0	69.0	1.0
42.0	6.0	46.0	46.0	2.0
50.0	7.0	70.0	63.0	4.0

Variable	TOTAL	MEAN	MAXIMUM	MINIMUM
Cu	142.0	47.3	50.0	42.0
Pb	18.0	6.0	7.0	5.0
Zn	186.0	62.0	70.0	46.0
Fe	178.0	59.3	69.0	46.0
Mo	7.0	2.3	4.0	1.0

Variable	RANGE	VARIANCE	STD. DEV.	C.V.%	U.B.	L.B.	90% C.I.
Cu	8.0	21.3	4.6	9.76	55.12	39.55	± 7.79PPM
Pb	2.0	1.0	1.0	16.67	7.68	4.32	± 1.68PPM
Zn	24.0	192.0	13.9	22.35	85.36	38.64	±23.36PPM
Fe	23.0	142.3	11.9	20.11	79.45	39.22	±20.11PPT
Mo	3.0	1.6	1.3	53.5	4.5	0.1	± 2.2 PPM

TABLE 7 - ATOMIC ABSORPTION ANALYSIS OF MONZONITE ADAMELLITE (Tim)
(Cu, Pb, Zn content in PPM; Fe in PPT)

Sample Number	Cu	Pb	Zn	Fe	Mo
24	5.0	5.0	26.0	20.0	
21	46.0	17.0	21.0	3.0	2.0
32	3.0	6.0	21.0	7.0	
44	5.0	21.0	25.0	15.0	0.4
55	6.0	9.0	40.0	19.0	
58	4.0	4.0	24.0	7.0	
60	3.0	8.0	25.0	17.0	
80	2.0	3.0	11.0	4.0	1.0
84	2.0	10.0	30.0	7.0	
90	5.0	8.0	36.0	10.0	
29	3.0	13.0	39.0	5.0	
33	2.0	4.0	37.0	14.0	
51	1.0	1.0	25.0	13.0	
23	11.0	11.0	38.0	17.0	
39	1.0	1.0	30.0	13.0	
20	1.0	8.0	27.0	3.0	
30	2.0	5.0	20.0	19.0	
43	3.0	4.0	10.0	10.0	
57	3.0	10.0	26.0	20.0	
47	1.0	16.0	36.0	23.0	
61	5.0	10.0	23.0	16.0	
48	5.0	23.0	83.0	8.0	1.0
82	6.0	6.0	15.0	19.0	
49	5.0	6.0	42.0	16.0	
36	5.0	5.0	13.0	11.0	
311	4.0	25.0	25.0	4.0	
34	2.0	8.0	22.0	11.0	
28	2.0	9.0	30.0	15.0	
26	6.0	16.0	25.0	15.0	
158	10.0	2.0	19.0	12.0	
62	3.0	7.0	35.0	14.0	
86	6.0	2.0	27.0	8.0	
27	5.0	5.0	19.0	19.0	
45	10.0	6.0	18.0	16.0	
15	20.0	13.0	27.0	8.0	
35	10.0	5.0	17.0	11.0	
37	6.0	2.0	14.0	15.0	
63	7.0	5.0	30.0	17.0	
41	3.0	8.0	14.0	16.0	
50	6.0	12.0	58.0	26.0	
42	9.0	5.0	26.0	19.0	
81	15.0	25.0	65.0	3.0	
54	1.0	5.0	12.0	2.0	
22	6.0	11.0	32.0	28.0	
59	3.0	5.0	20.0	15.0	
25	3.0	8.0	47.0	30.0	
46	1.0	5.0	51.0	17.0	
88	3.0	3.0	39.0	9.0	
40	4.0	4.0	23.0	16.0	
56	2.0	8.0	56.0	9.0	
87	1.0	8.0	15.0	2.0	

TABLE 7 CONTINUED

Sample Number	Cu	Pb	Zn	Fe	Mo
83	4.0	8.0	34.0	9.0	
79	3.0	4.0	30.0	13.0	
64-68	4.0	5.0	28.0	6.0	
74-78	8.0	11.0	48.0	14.0	1.0
69-73	9.0	5.0	20.0	5.0	
53	2.0	7.0	15.0	4.0	0.4
52	1.0	3.0	30.0	15.0	
31	2.0	5.0	15.0	12.0	
85	210.0	40.0	79.0	9.0	2.0
96	2.0	8.0	25.0	15.0	
18	5.0	11.0	11.0	2.0	
92	12.0	5.0	21.0	13.0	
91	205.0	6.0	25.0	19.0	12.0
93	5.0	5.0	31.0	8.0	
38	10.0	10.0	7.0	9.0	
302	1.0	3.0	45.0	9.0	
424	4.0	12.0	46.0	22.0	
322	15.0	8.0	24.0	3.0	
328	5.0	10.0	26.0	17.0	
334	3.0	4.0	14.0	3.0	

Variable	TOTAL	MEAN	MAXIMUM	MINIMUM
Cu	793.0	11.2	210.0	1.0
Pb	596.0	8.4	40.0	1.0
Zn	2063.0	29.1	83.0	7.0
Fe	880.0	12.4	30.0	2.0

Variable	RANGE	VARIANCE	STD.DEV.
Cu	209.0	1170.8	34.2
Pb	39.0	41.3	6.4
Zn	76.0	222.0	14.9
Fe	28.0	41.8	6.5

TABLE 8 - ATOMIC ABSORPTION ANALYSIS OF LEUCORHYOLITE (Til)
(Cu, Pb, Zn, Mo content in PPM; Fe in PPT)

Sample Number	Cu	Pb	Zn	Fe	Mo
17	5.0	8.0	13.0	3.0	1.0
19	5.0	6.0	23.0	6.0	
323	4.0	7.0	7.0	4.0	

Variable	TOTAL	MEAN	MAXIMUM	MINIMUM
Cu	14.0	4.7	5.0	4.0
Pb	21.0	7.0	8.0	6.0
Zn	43.0	14.3	23.0	7.0
Fe	13.0	4.3	6.0	3.0

Variable	RANGE	VARIANCE	STD.DEV.
Cu	1.0	0.3	0.6
Pb	2.0	1.0	1.0
Zn	16.0	65.3	8.1
Fe	3.0	2.3	1.5

TABLE 9 - ATOMIC ABSORPTION ANALYSIS OF SYENODIORITE (Tis)
(Cu, Pb, Zn, Mo content in PPM; Fe in PPT)

Sample Number	Cu	Pb	Zn	Fe	Mo
10	5.0	25.0	44.0	22.0	1.0
11	7.0	24.0	25.0	16.0	
1	10.0	22.0	55.0	35.0	2.0
6	13.0	15.0	70.0	69.0	1.6
5	5.0	14.0	51.0	43.0	
3	13.0	12.0	36.0	38.0	1.0
7	28.0	12.0	60.0	58.0	
2	6.0	11.0	16.0	25.0	
4	2.0	10.0	49.0	36.0	
8	16.0	10.0	47.0	36.0	
337	15.0	8.0	29.0	23.0	
385	5.0	6.0	36.0	33.0	
94	6.0	5.0	15.0	28.0	
9	3.0	5.0	30.0	8.0	

TABLE 9 CONTINUED

Variable	TOTAL	MEAN	MAXIMUM	MINIMUM
Cu	134.0	9.6	28.0	2.0
Pb	179.0	12.9	25.0	5.0
Zn	563.0	40.2	70.0	15.0
Fe	470.0	33.6	69.0	8.0

Variable	RANGE	VARIANCE	STD.DEV.
Cu	26.0	48.4	7.0
Pb	20.0	44.3	6.7
Zn	55.0	267.0	16.3
Fe	61.0	252.9	15.9

TABLE 10- ATOMIC ABSORPTION ANALYSIS OF ORTHOCLASE ADAMELLITE (Tio)
(Cu, Pb, Zn, Mo content in PPM; Fe in PPT)

Sample Number	Cu	Pb	Zn	Fe	Mo
303	1.0	5.0	47.0	12.0	
444	52.0	99.0	120.0	22.0	2.0
215	2.0	5.0	23.0	14.0	
306	5.0	3.0	26.0	15.0	
362	3.0	5.0	47.0	27.0	
301	5.0	4.0	20.0	3.0	
114	7.0	3.0	17.0	4.0	
14	9.0	13.0	37.0	33.0	
13	35.0	36.0	65.0	24.0	2.0
16	2.0	5.0	21.0	9.0	
352	1.0	4.0	63.0	10.0	

Variable	TOTAL	MEAN	MAXIMUM	MINIMUM
Cu	122.0	11.1	52.0	1.0
Pb	182.0	16.6	99.0	3.0
Zn	486.0	44.2	120.0	17.0
Fe	173.0	15.7	33.0	3.0

Variable	RANGE	VARIANCE	STD.DEV.
Cu	51.0	277.5	16.7
Pb	96.0	840.5	29.0
Zn	103.0	924.4	30.4
Fe	30.0	92.8	9.6

TABLE 11- ATOMIC ABSORPTION ANALYSIS OF UNDIFFERENTIATED DIKES (Tid)
(Cu, Pb, Zn, Mo content in PPM; Fe in PPT)

Sample Number	Cu	Pb	Zn	Fe	Mo
324	111.0	7.0	26.0	11.0	0.1
348	37.0	4.0	30.0	40.0	
326	30.0	36.0	130.0	63.0	1.0
420	28.0	6.0	16.0	4.0	
421	21.0	6.0	72.0	20.0	
346	19.0	11.0	56.0	45.0	
115	8.0	23.0	58.0	22.0	
95	6.0	9.0	25.0	15.0	
411	5.0	11.0	17.0	6.0	
347	5.0	5.0	36.0	23.0	
380	3.0	5.0	20.0	4.0	
320	3.0	7.0	41.0	27.0	
384	2.0	5.0	19.0	2.0	
321	1.0	6.0	40.0	15.0	
344	1.0	9.0	42.0	45.0	
447	1.0	6.0	26.0	10.0	

Variable	TOTAL	MEAN	MAXIMUM	MINIMUM
Cu	281.0	17.6	111.0	1.0
Pb	156.0	9.8	36.0	4.0
Zn	664.0	41.5	130.0	16.0
Fe	352.0	22.0	63.0	2.0

Variable	RANGE	VARIANCE	STD.DEV.
Cu	110.0	761.1	27.6
Pb	32.0	69.4	8.3
Zn	114.0	832.8	28.9
Fe	61.0	317.3	17.8

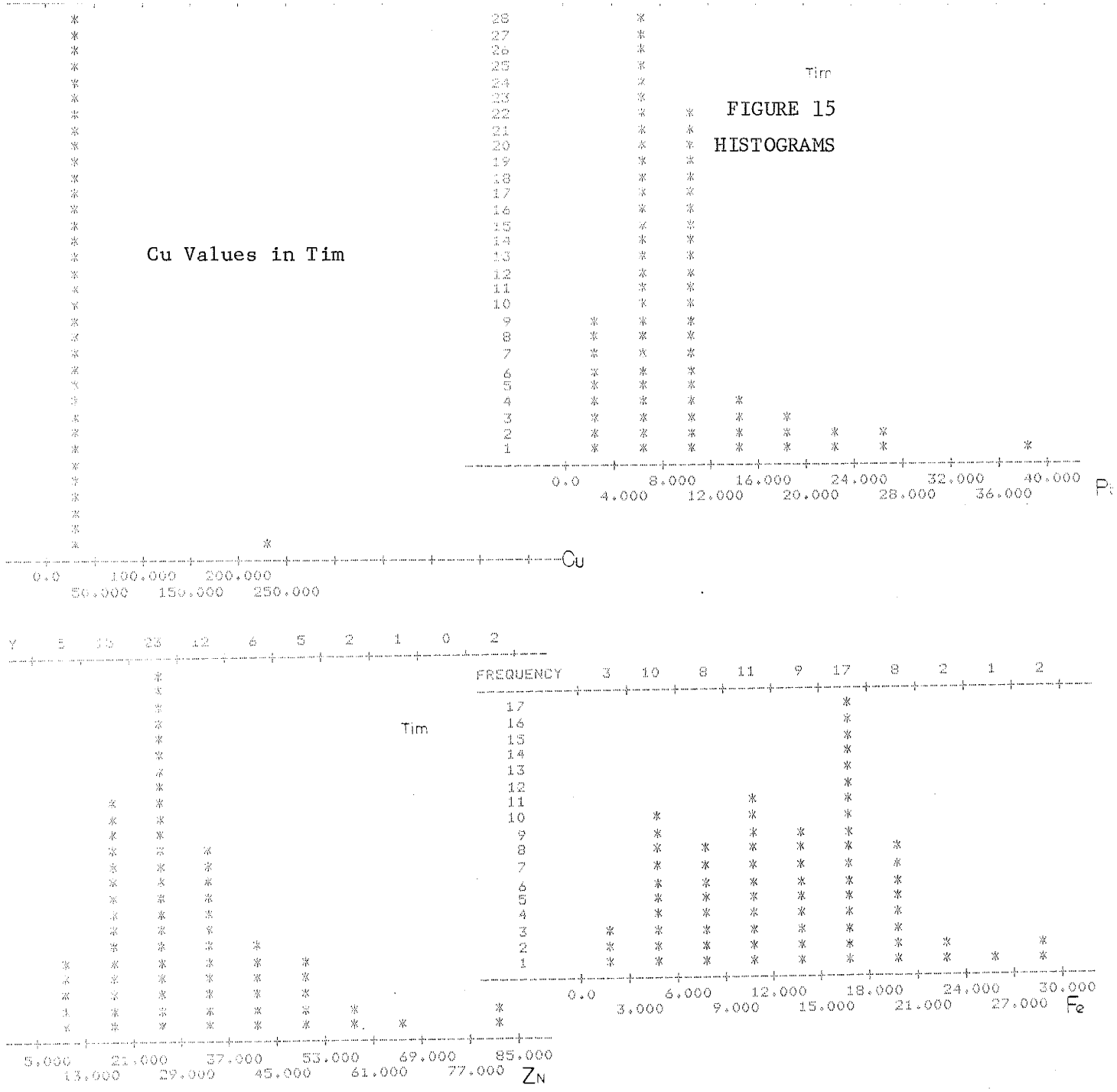

FIGURE 15

HISTOGRAMS

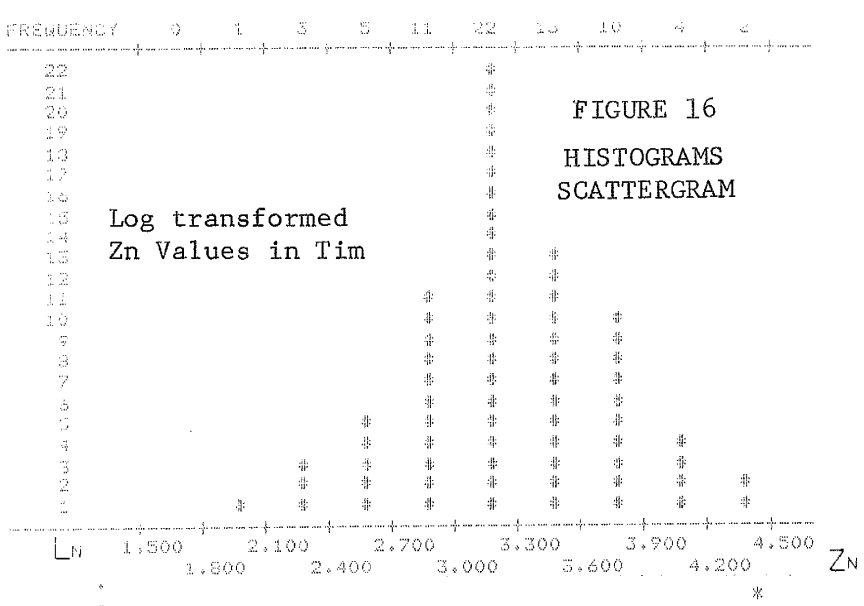

FIGURE 16

HISTOGRAMS
SCATTERGRAM

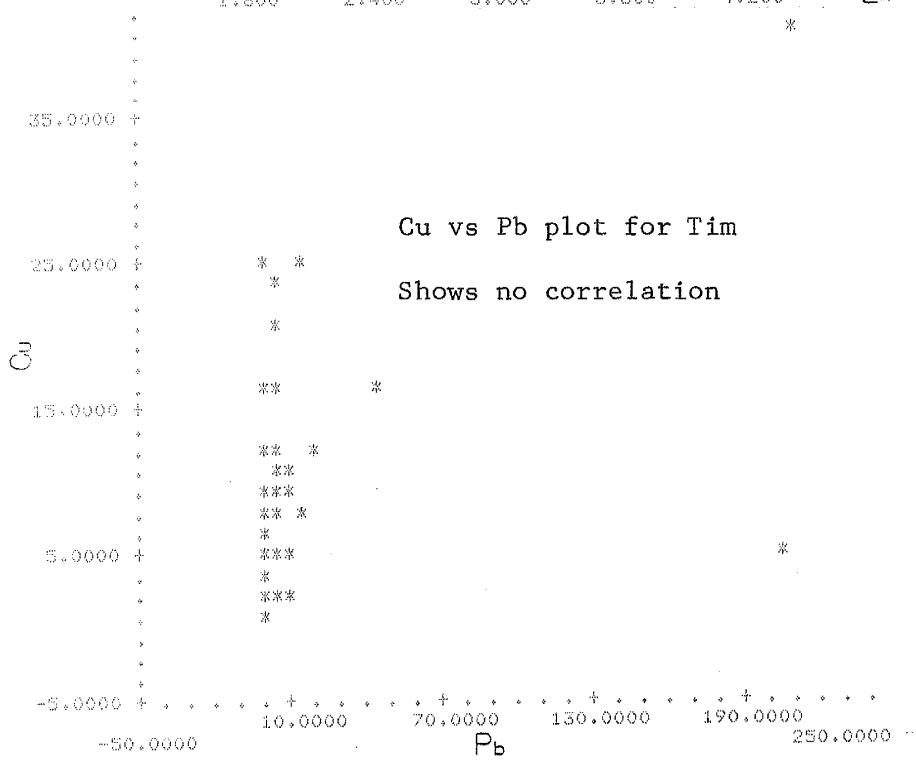

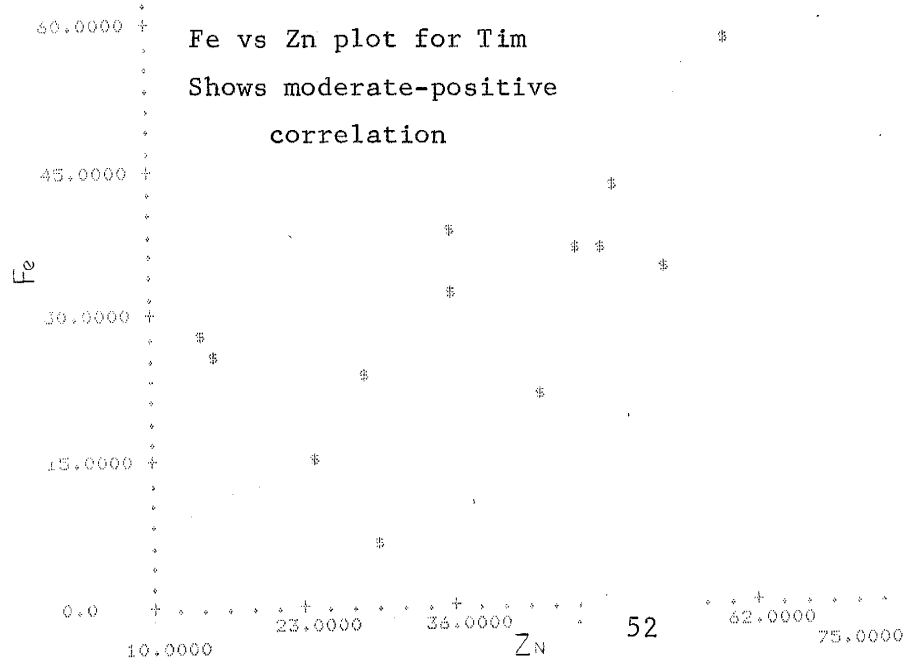

FIGURE 17: Distribution of Cu in Monzonite Adamellite (Tim)

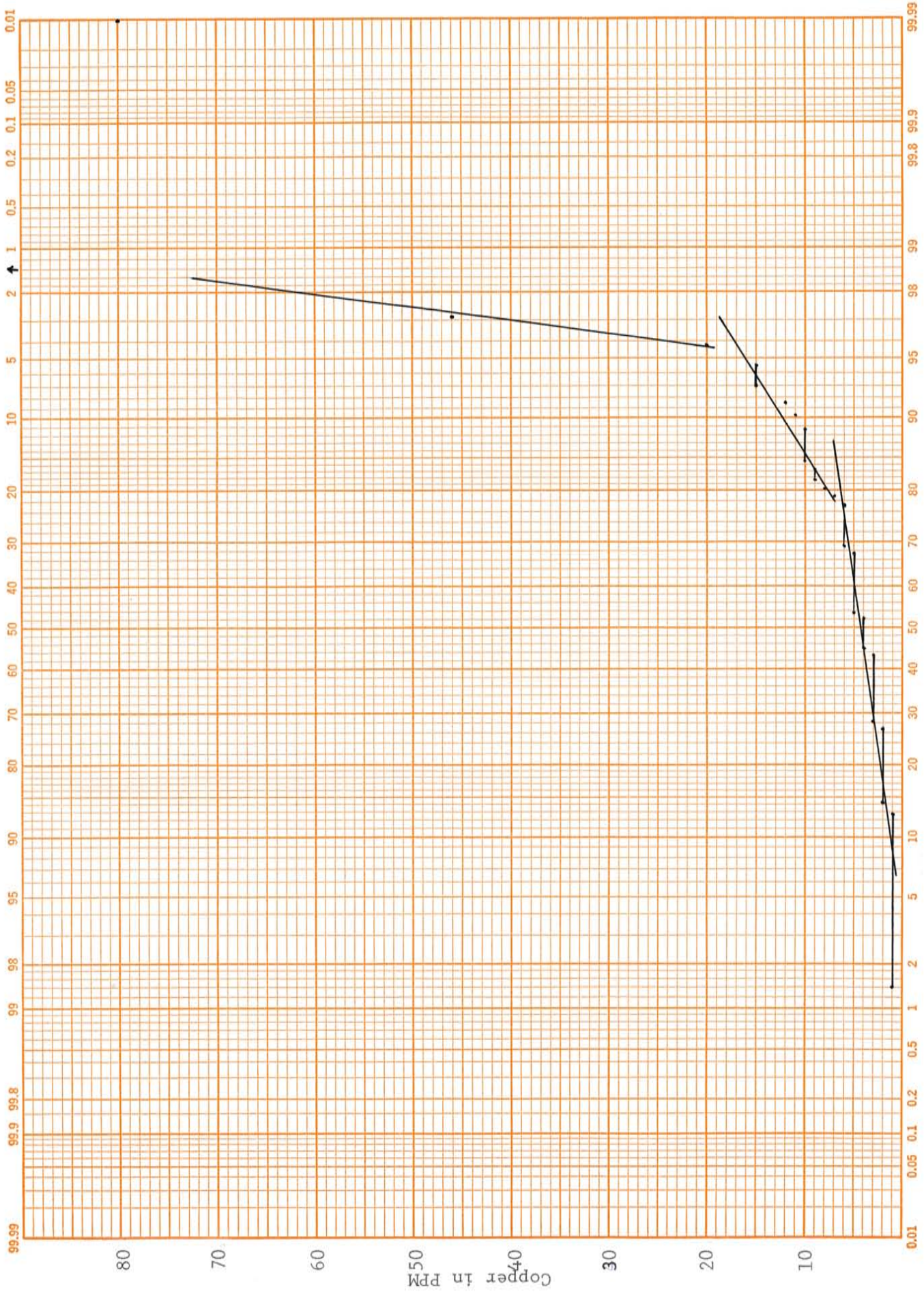

plotted on normal probability paper. The data clearly does not fall on a straight line and therefore is not normally distributed. Figure 18 is a normal probability plot of Cu in Tis, Tio and Tid. Although the number of samples "n" taken in these rock types are small the plots reveal a distinct non-normal distribution for copper. The three samples of leucorhyolite have not been plotted. The Cu values in Tim are next plotted on the logarithmic probability paper of Figure 19 . This plot shows a straight line for most of the data with a break occuring at the upper end for a few of the highest copper values. Ahrens (1965) reports that in igneous rocks copper and many other trace elements including zinc, lead and molybdenum are lognormally distributed while the major elements including iron are normally distributed. Based on the conclusions of Ahrens, Tennant and White and a number of other authors it will be assumed in this study that copper is lognormally distributed or more precisely that the Cu values can be transformed into a normal or near normal distribution by taking the log of the values. Having made this assumptions then the interpretation of Figure 19 is that copper is bi-modally distributed. The lower part of the curve represents the background values for Cu from 1 to about 15 ppm. This background distribution is presumably the result of magmatic differentiation and emplacement of the monzonite adamellite stock. The more steeply sloped curve represents a copper distribution added to the background by a subsequent process, probably hydrothermal mineralization. The samples making up this upper slope are #85 - 210 ppm, #91 - 205 ppm, #21 - 46 ppm, and possibly #15 - 20 ppm, #76 - 20 ppm and #69 - 24 ppm. These last two samples are part of two different five sample traverses that are

FIGURE 18: Distribution of Cu Biotite Syenodiorite (Tis)
" " " Undifferentiated Dikes (Tid)
" " " Orthoclase Adamellite (Tio)

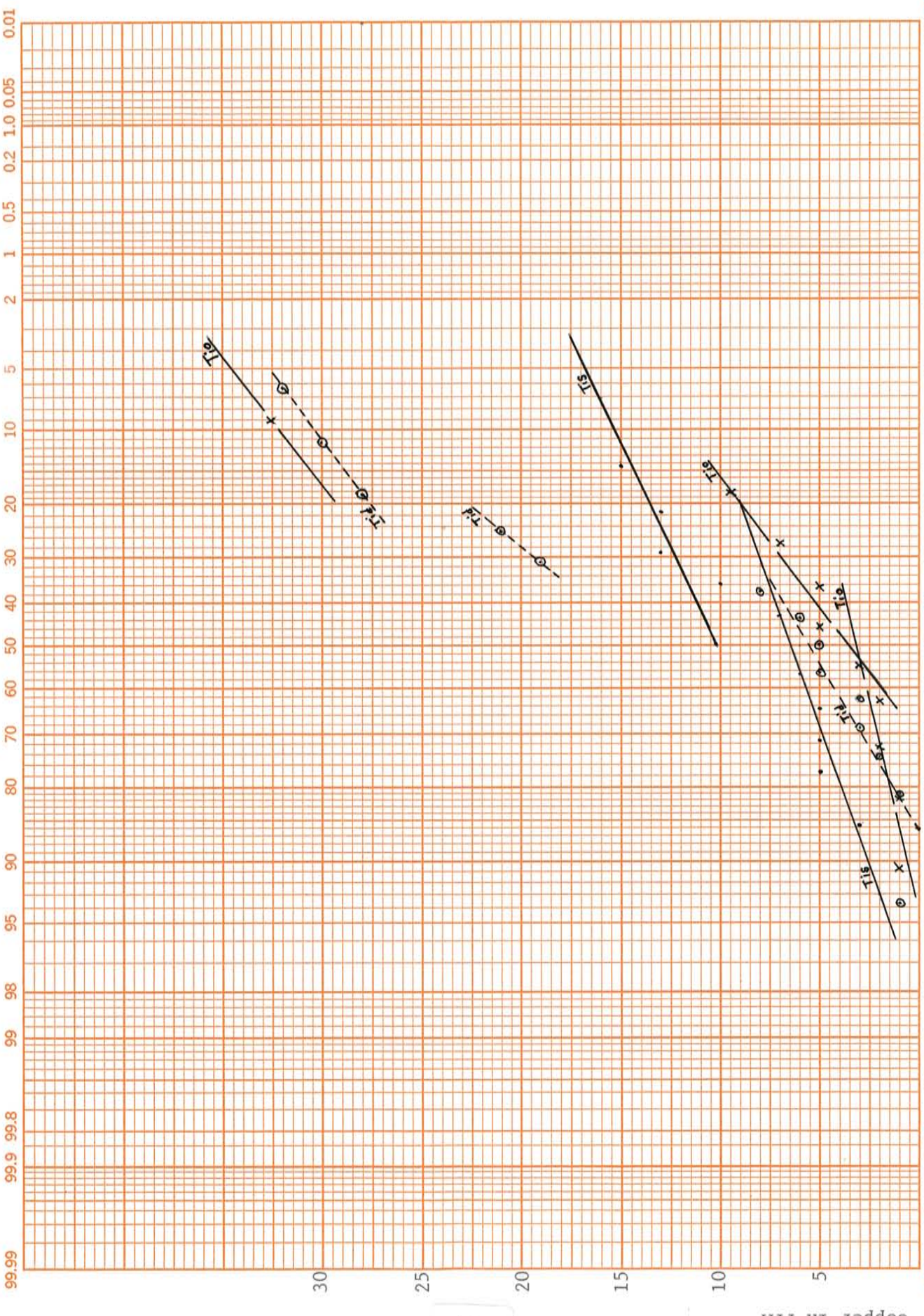

FIGURE 19: Distribution of Copper in Monzonite Adamellite (Tim)

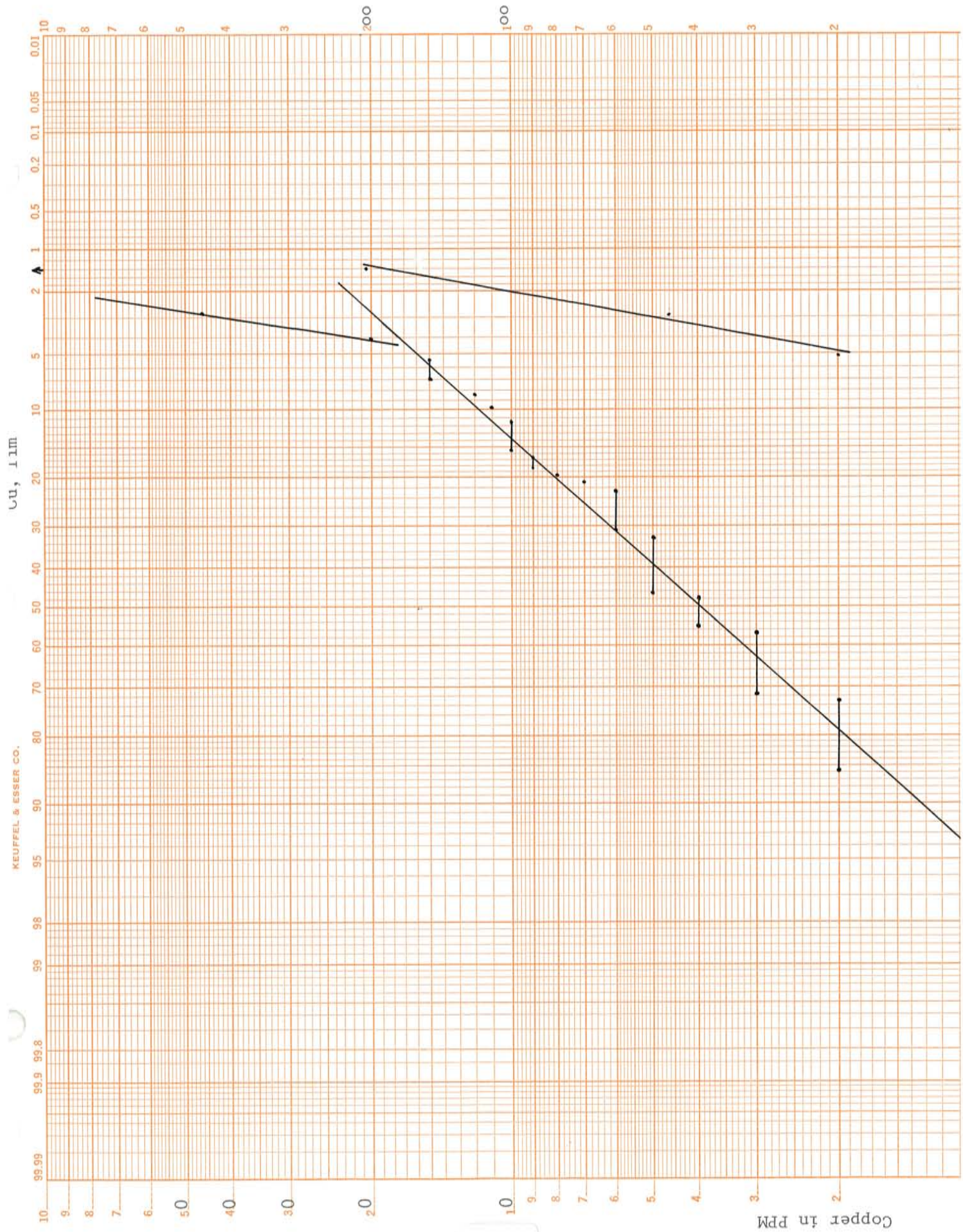

averaged in Table 7 and described in detail in Figure 20. A common rule of thumb for determining the lower limit of anomalous values or threshhold value is to add two times the standard deviation to the mean value. In this case, the Cu threshold would be 80 ppm if the raw data is used and 34 ppm if the log transformed data is used and graphically the mean plus two standard deviations occurs where 97.5% of the population is less than the value of 21 ppm. The probability plot technique gives a lower threshold value because the second distribution, representing mineralization has been removed from the analysis. In Figure 21, ppm copper in biotite syenodiorite (Tis) orthoclase adamellite (Tio) and undifferentiated dikes (Tid), is plotted on a log probability paper although the number of values determined for these rocks is actually too small for a rigorous analysis. The Cu values in Tis are log-normally distributed in one background population. Orthoclase adamellite appears to have two distributions, with samples #23 - 35 ppm and #444 - 52 ppm defining the upper line in the plot. The undifferentiated dikes present a special problem because they are not a homogenous population. The rock types range from basalt to granite (See Table 3 &14). The logarithmic probability plot shows two populations, which are probably due to different rock types and to mineralization. All the rock types indentifed generally as Tid are outlined in Table 12. Possible anomalous values of copper in the Tid are samples #326 - 30 ppm, #421 - 21 ppm, #324 - 111 ppm, #420 - 28 ppm. Table 12 summarizes the anomalous copper values.

Rosler and Lange (1972) report that copper decreases from about

FIGURE 20

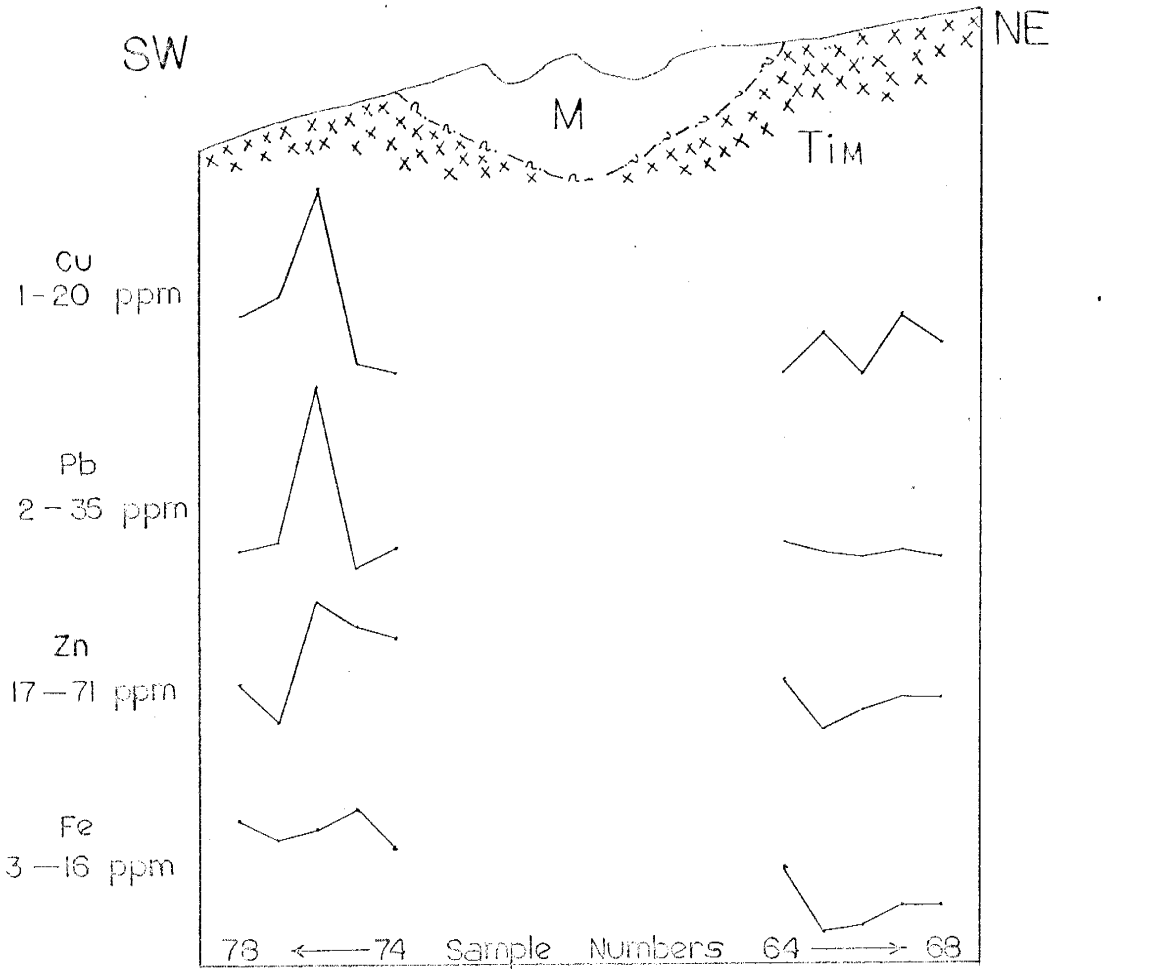
SW
NE
M
TIM
Cu
1-20 ppm
Pb
2-35 ppm
Zn
17-71 ppm
Fe
3-16 ppm
78 ←—74 Sample Numbers 64 —→ 68

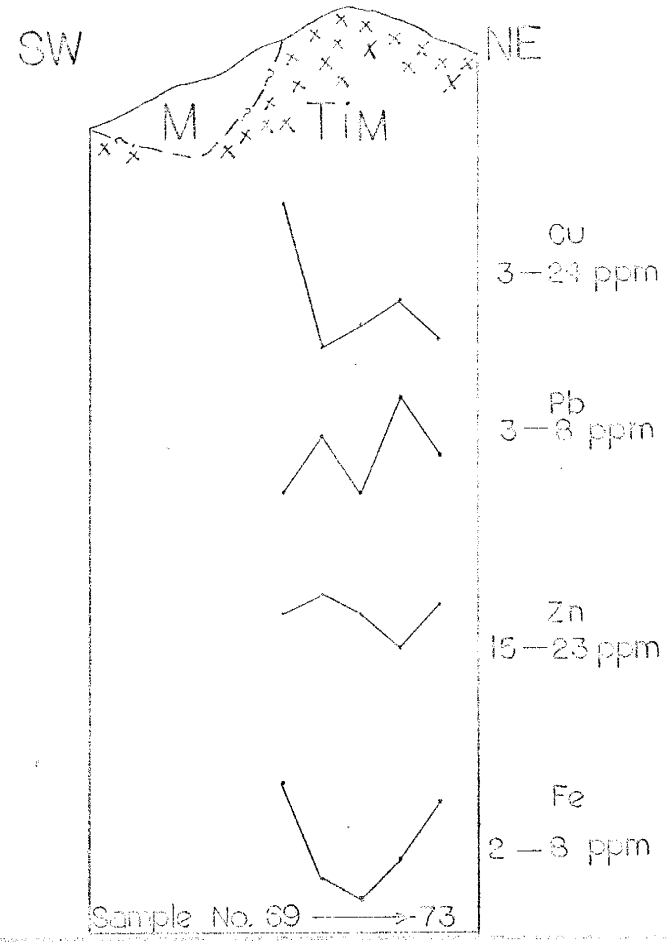
SW
NE
M
TIM
Cu
3-23 ppm
Pb
3-8 ppm
Zn
15-23 ppm
Fe
2-8 ppm
Sample No. 69 —→ 73

FIGURE 21: Distribution of Cu in Biotite Syenodiorite (Tis)
" " " " Orthoclase Adamellite (Tio)
" " " " Undifferentiated Dikes (Tid)

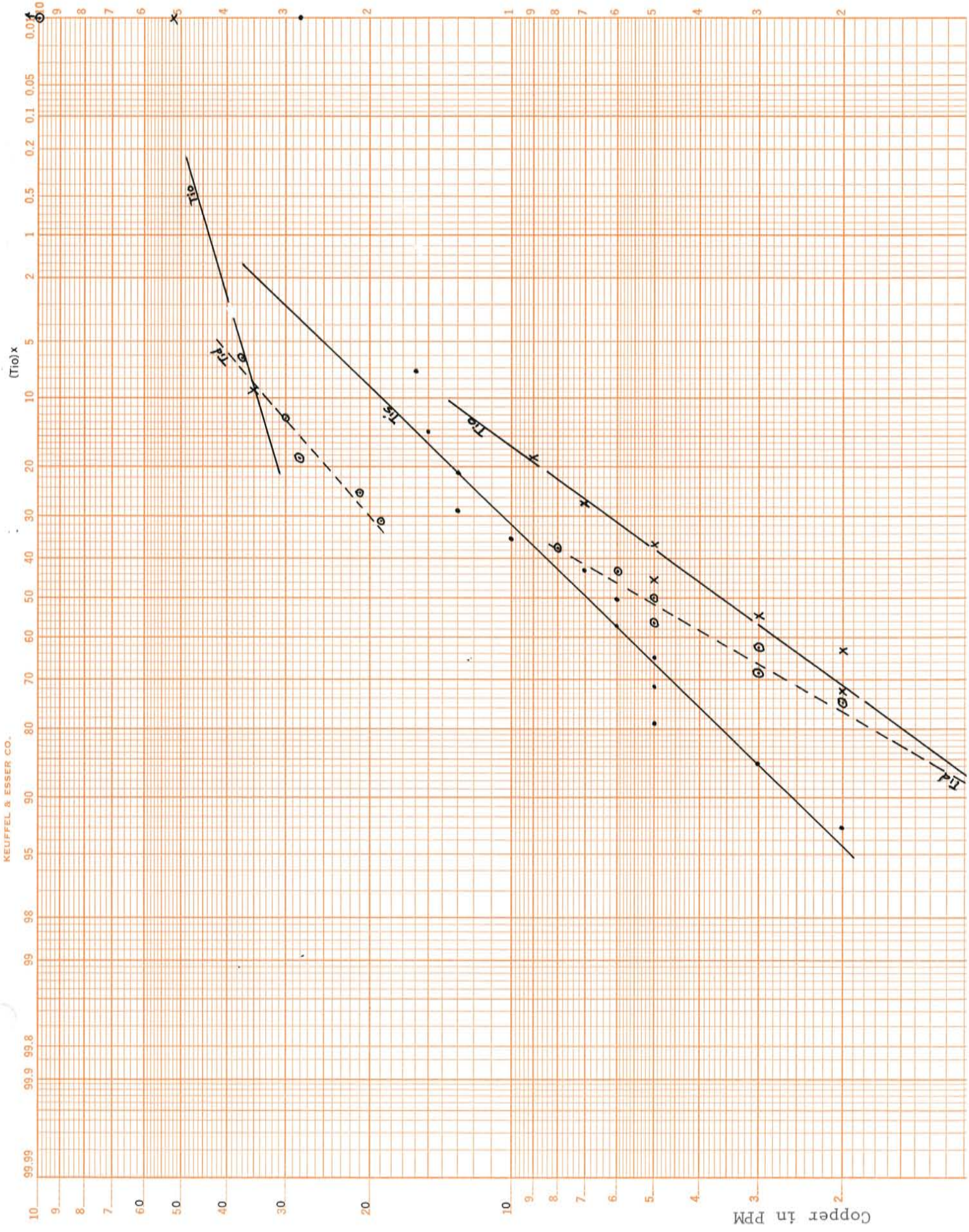

TABLE 12 ANOMALOUS COPPER CONCENTRATION IN PPM

Sample No.	Cu
85	210
91	205
21	46
15	20
76	20
69	24
444	52
13	35
324	111
326	30
420	28
421	21

TABLE 13 ANOMALOUS LEAD CONCENTRATION IN PPM

Sample No.	Pb
13	36
14	13
444	99
326	36
115	23

100 ppm in basic rocks to 30 ppm for intermediate to 10 ppm in acid rocks. Specifically they give average values of 5 ppm for Syenites, 35 ppm for Diorites and 20 ppm for Granites. Chaffee (1976) shows the copper content continously increasing at Kalamazoo from a minimum of 100 ppm up to the ore zone. The background in this area is indicated to be about 30 ppm. The spatial distribution of copper is shown on Figure 22.

LEAD DISTRIBUTION

Sample locations and lead concentrations are presented in Tables 7 through 11 (pages 48-50). The normal probability plot (Figure 23) of lead values in Tim does not fall on a straight line indicating that Pb is not normally distributed. The log normal probability plot of Pb concentration shown in Figure 24 indicates one population of log-normally distributed Pb values in the monzonite adamellite. Figure 25 shows normal probability plots of Pb concentration in biotite syenodiorite (Tis), orthoclase adamellite (Tio), and undifferentiated dikes (Tid); none of the distributions are normal. The lead values are next plotted on log-probability paper (Figure 26) and show that Pb in Tis has one distribution with no anomalous values while Tio and Tid have two distributions each and a few values that may indicate mineralization. In the orthoclase adamellite samples #13 - 36 ppm, #14 - 13 ppm, and #444 - 99 ppm form the second distribution. The two highest values of Pb in the dike rocks are samples #115 - 23 ppm and #326 - 36 ppm and they appear to form a distribution distinct from the background values. Lead values that may

FIGURE 22

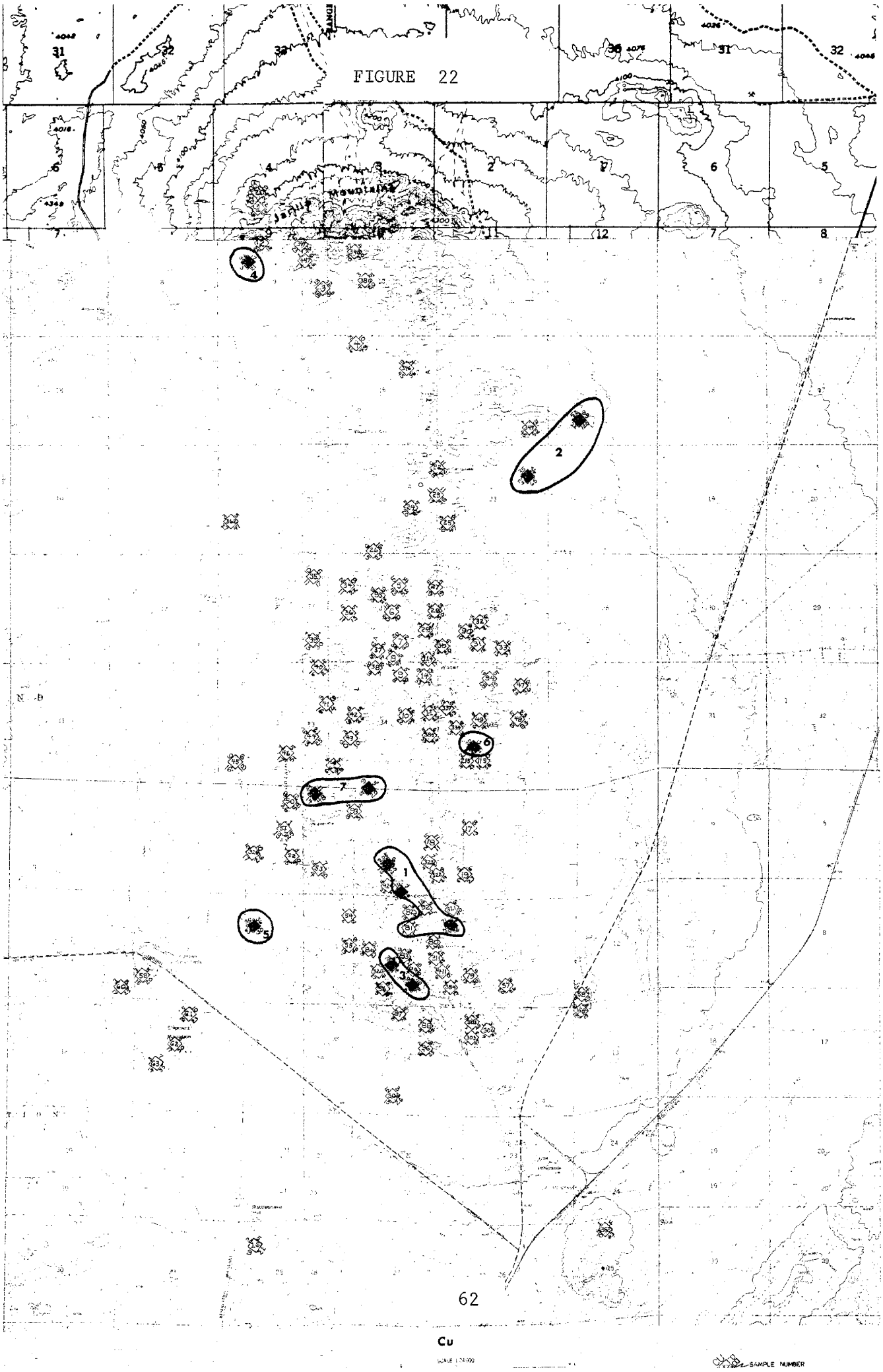

FIGURE 23: Distribution of Pb in Monzonite Adamellite (Tim)

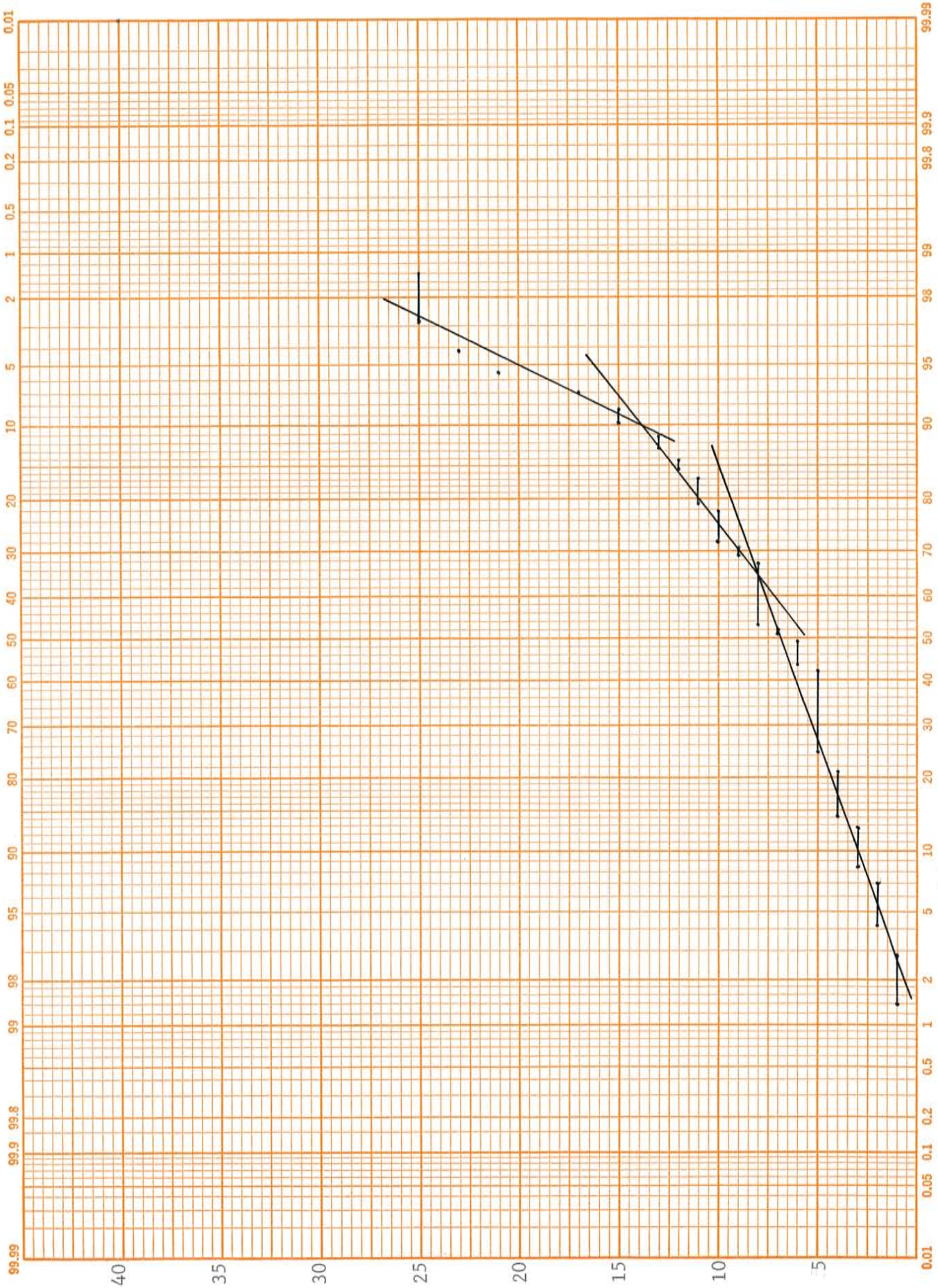

FIGURE 24: Distribution of Pb in Monzinite Adamellite (Tim)

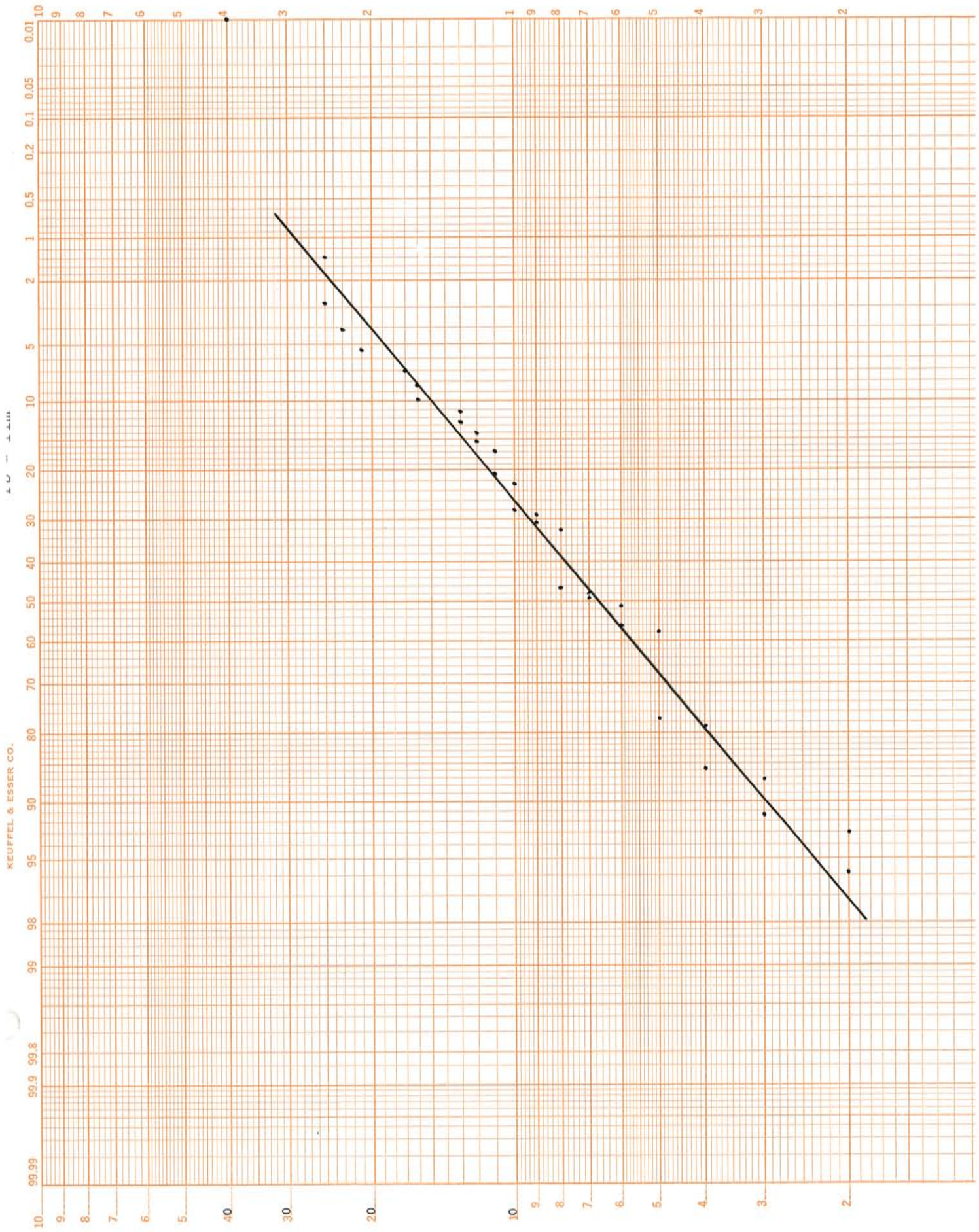

FIGURE 25: Distribution of Pb in Biotite Syenodiorite (Tis)
Orthoclase Adamellite (Tio)
Undifferentiated dikes (Tid)

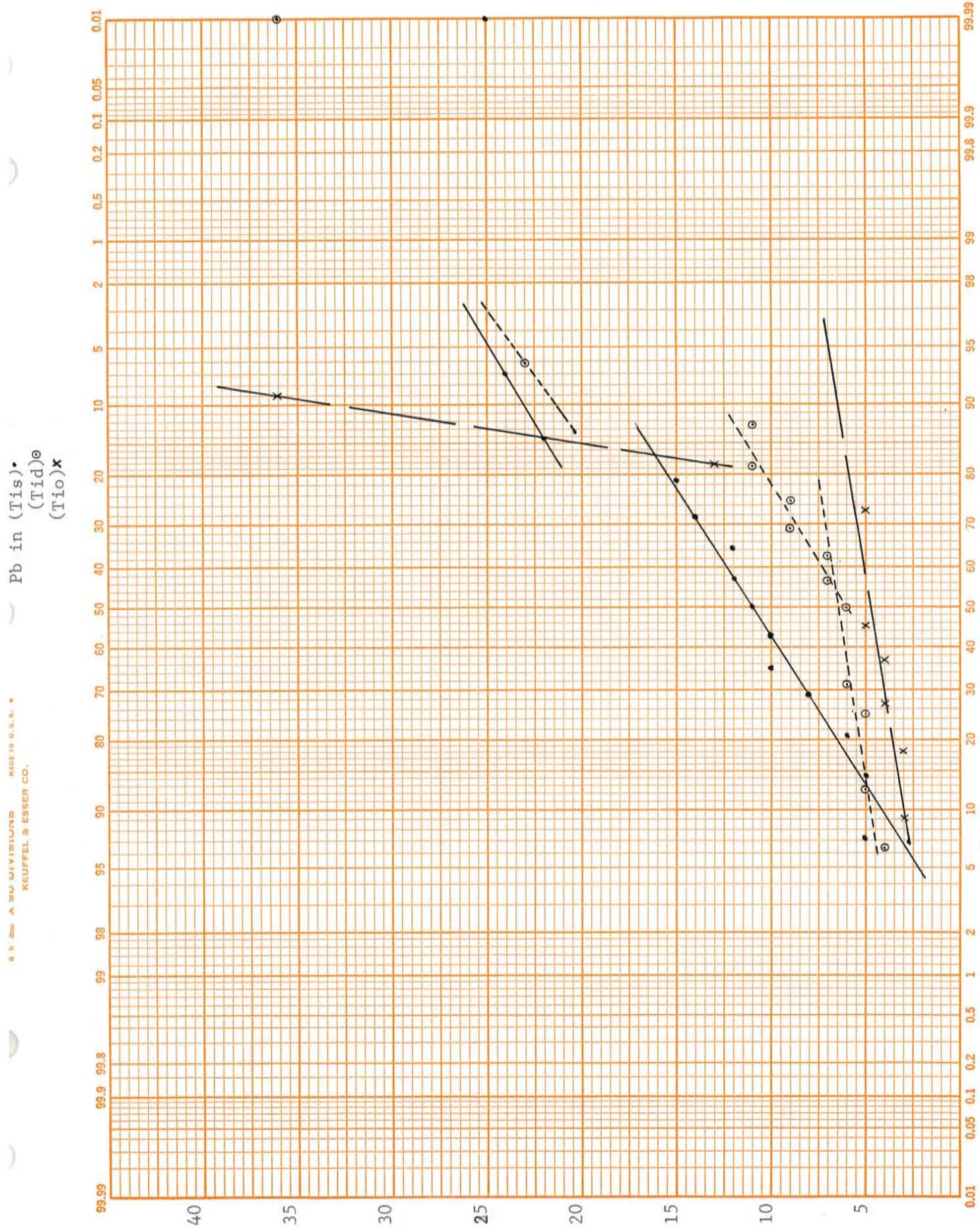

FIGURE 26: Distribution of Pb in Biotite Syenodiorite (Tis)
Orthoclase Adamellite (Tio)
Undifferentiated Dikes (Tid)

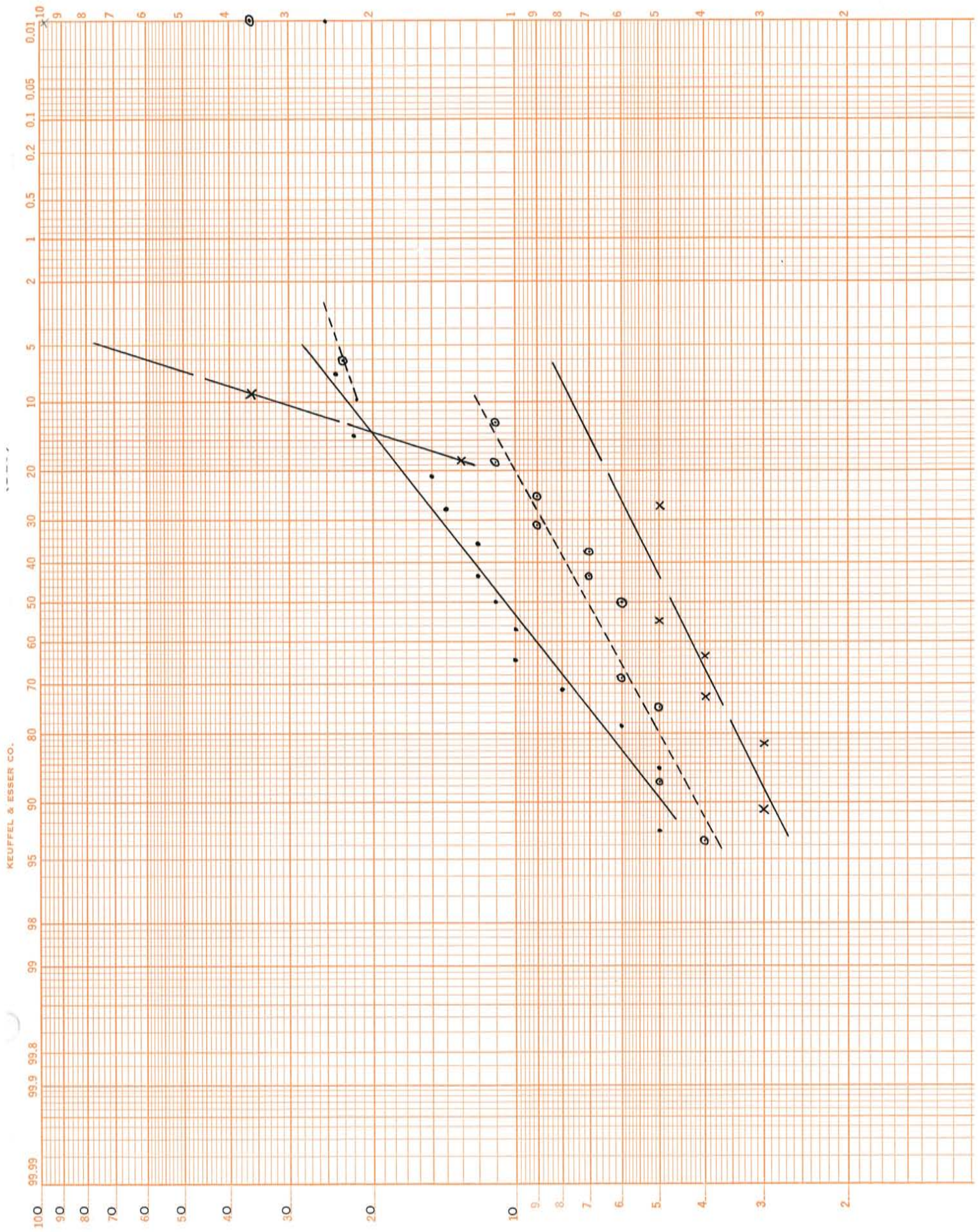

be associated with mineralization are summarized in Table 13.

The spatial distribution of Pb values are shown on Figure 27. Lead averages 8 ppm in basic rocks, 15 ppm in intermediate and 20 ppm in acid rocks (Rosler and Lange (1972)).

ZINC DISTRIBUTION

Sample locations and zinc concentrations are presented in Tables 7 through 11 (pages 48-50). The zinc distribution in monzonite adamellite is log-normal with one population as shown in Figures 28 and 29. The distribution of zinc in biotite syenodiorite is apparently normal with one population. The Zn values in Tis plot as a straight line on the normal probability plot (Figure 30) and display a distinct break in slope on the log-normal probability paper (Figure 31). Zinc may be normally distributed in this rock type because of the close assocation between zinc and iron as shown in the scatter diagram Figure 16. The zinc distribution in orthoclase adamellite and undifferentiated dikes is log-normal as shown in Figures 30 and 31. There is apparently only one zinc population in Tio and Tid rocks. Zinc is a very minor constituent of the ores found in the Jarilla Mountains and this fact is apparently reflected in the trace distribution of zinc in fresh igneous rocks of the range. The spatial distribution of Zn is shown in Figure 1 and Map 2. Chaffee (1975) reports a broad negative anomaly for zinc adjacent to the ore zone. Rosler and Lange (1972) indicate that zinc averages over 100 ppm in basic igneous rocks, about 80 ppm in intermediate types, and 60

FIGURE 27

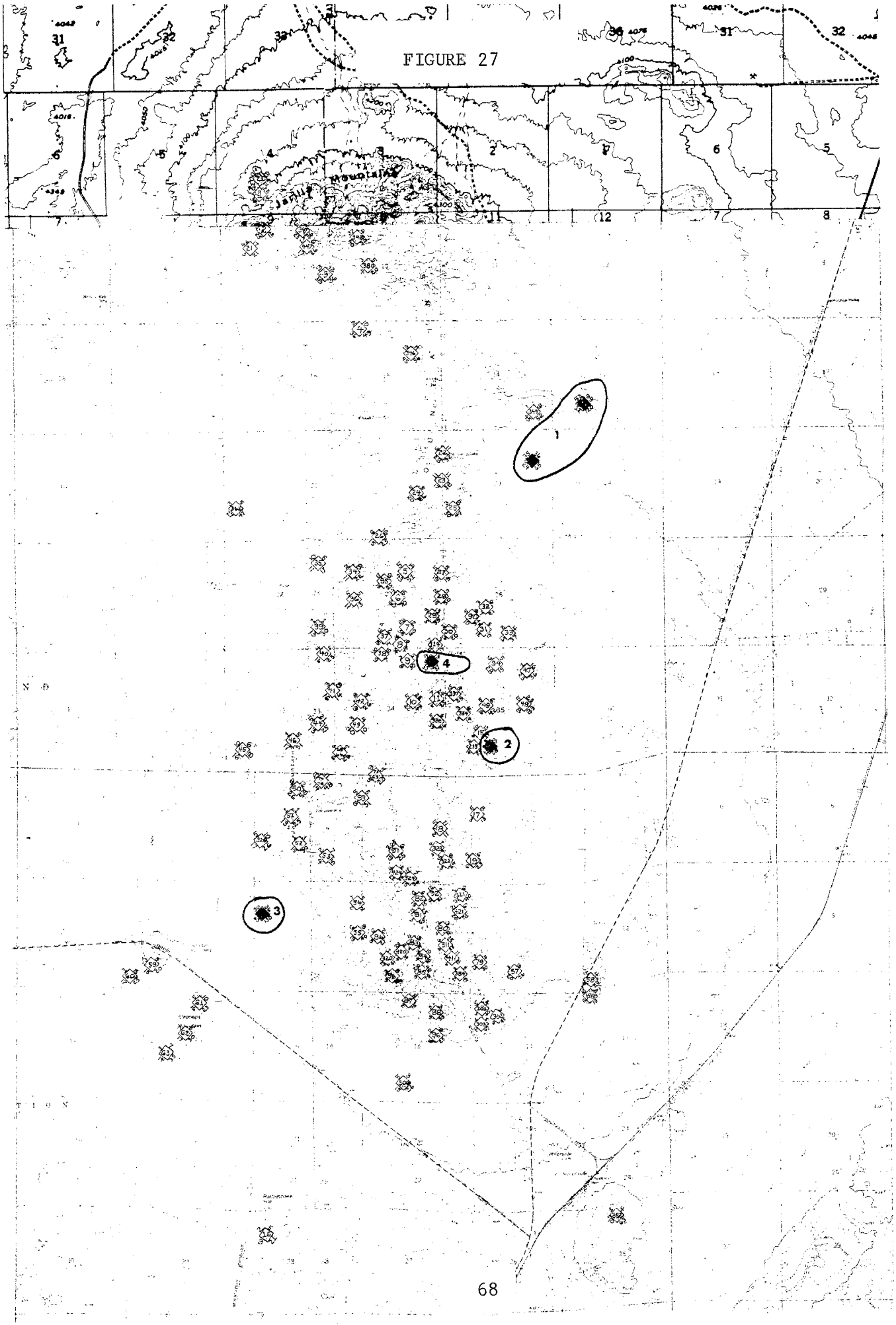

FIGURE 28: Distribution of Zn in Monzonite Adamellite (Tim)

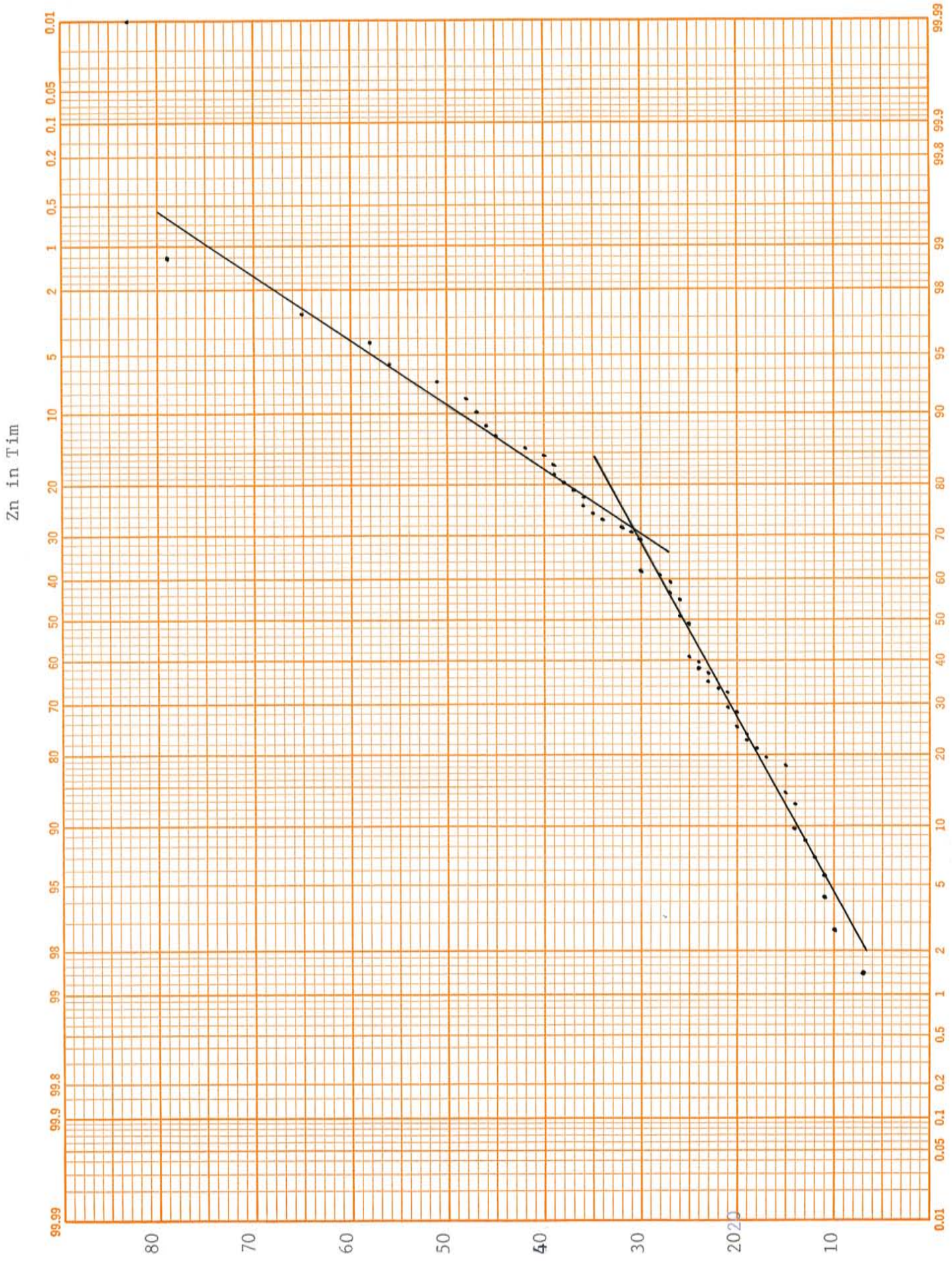

FIGURE 29: Distribution of Zn in Monzonite Adamellite

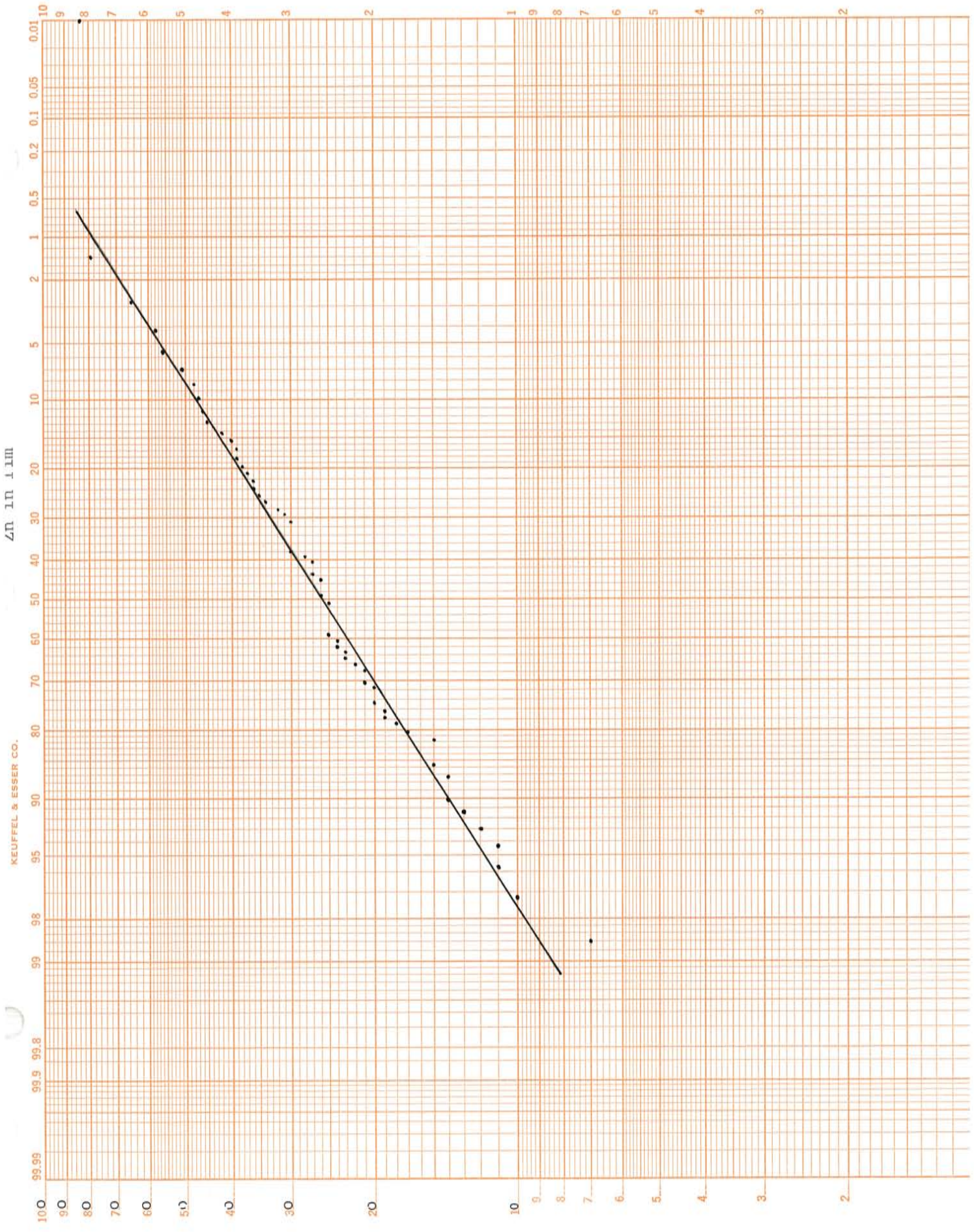

Figure 30: Distribution of Zn in Biotite Syenodiorite (Tis)
Orthoclase Adamellite (Tio)
Undifferentiated Dikes (Tid)

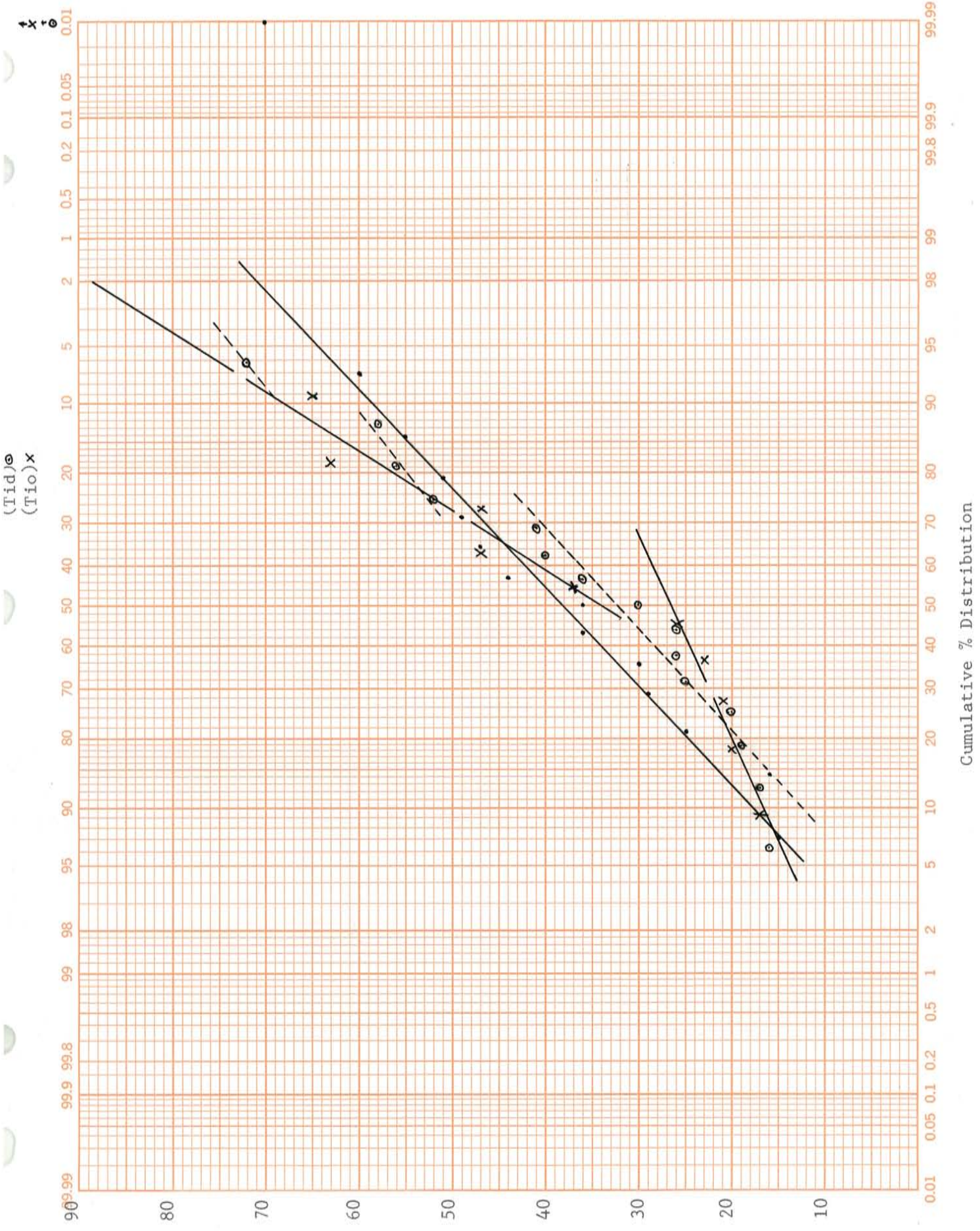

FIGURE 31: Distribution of Zn in Biotite Syenodiorite (Tis)
Orthoclase Adamellite (Tio)
Undifferentiated Dikes (Tid)

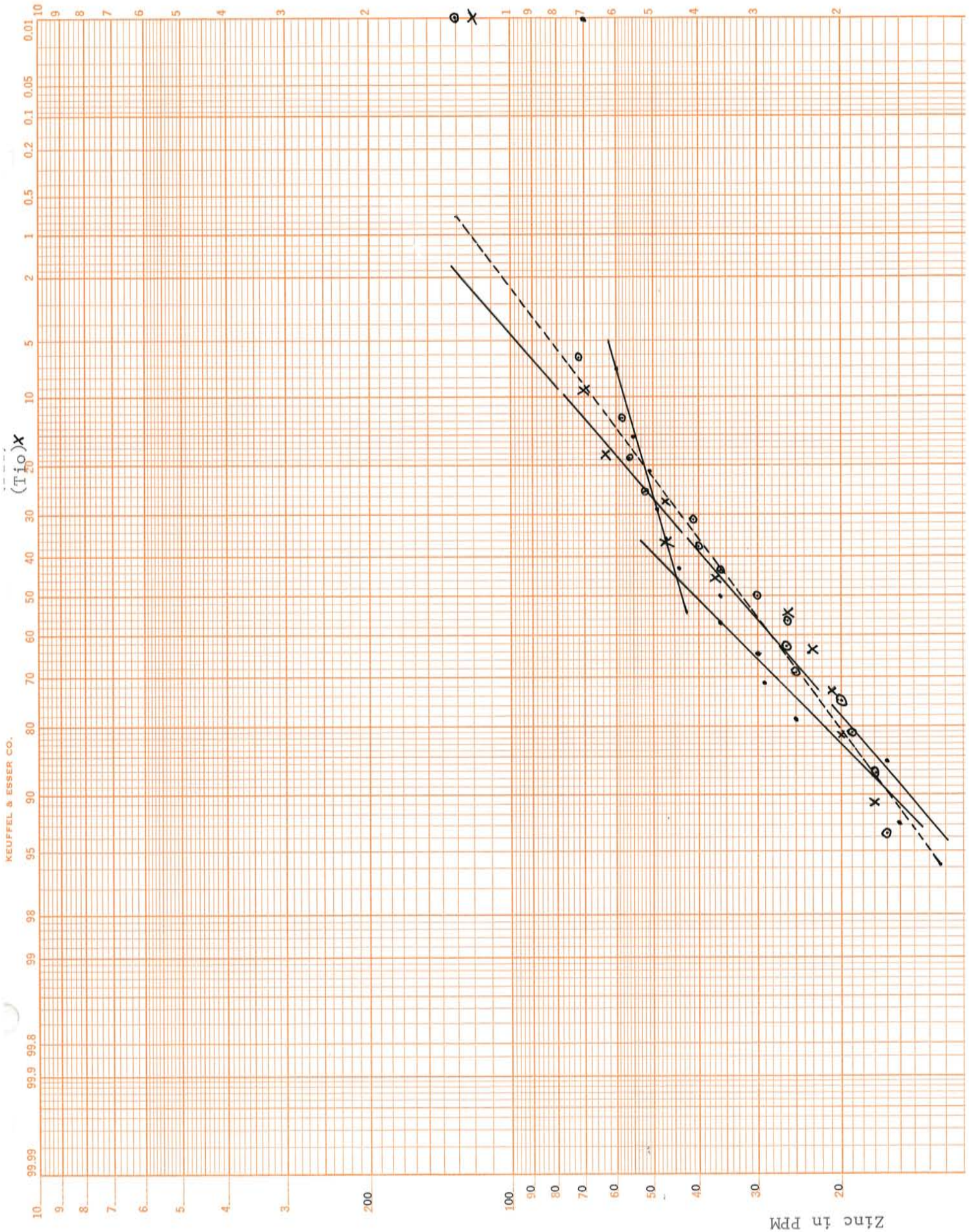

ppm in the acid end member.

IRON DISTRIBUTION

Iron, along with the other major rock forming minerals, is reported in the literature to have a normal distribution in igneous rocks. The Jarilla Mountains proved to be no exception to this rule as Fe was found to be normally distributed in all the igneous rock types. Figure 32 and 33 show the plots of Fe for the various rock types. The break in slope of the Tid plot is probably due to differences in rock type rather than a bimodal distribution. Tables 7 through 11 give the sample locations and iron concentrations for all the igneous rock types. The spatial distribution of iron in parts per thousand is given in Map 2 & Figure 1 . At Kalamazoo Chaffee reports a positive iron anomaly ranging between 20 and 30 ppt above the ore zone and notes that the iron distribution is related to lithologies. Rosler and Lange (1972) show that Fe content in igneous rocks decreases from 80 ppt in basic rocks to 60 ppt in intermediate to 20 ppt in acid rocks.

MOLYBDENUM DISTRIBUTION

The background values for Mo are approximately 1.1 ppm in monzonite adamellite, 1.4 ppm for biotite syenodiorite and 2.3 ppm in basalt which correspond quite well with the values given by Rosler and Lange (1972) of 2 ppm basic and 1 ppm in intermediate and acid rocks. At Kalamazoo Chaffee (1976) reports a Mo background of about 1.5 ppm and a Mo anomaly that extends above and below the ore zone with values over

FIGURE 32: Distribution of Fe in Monzonite Adamellite (Tim)

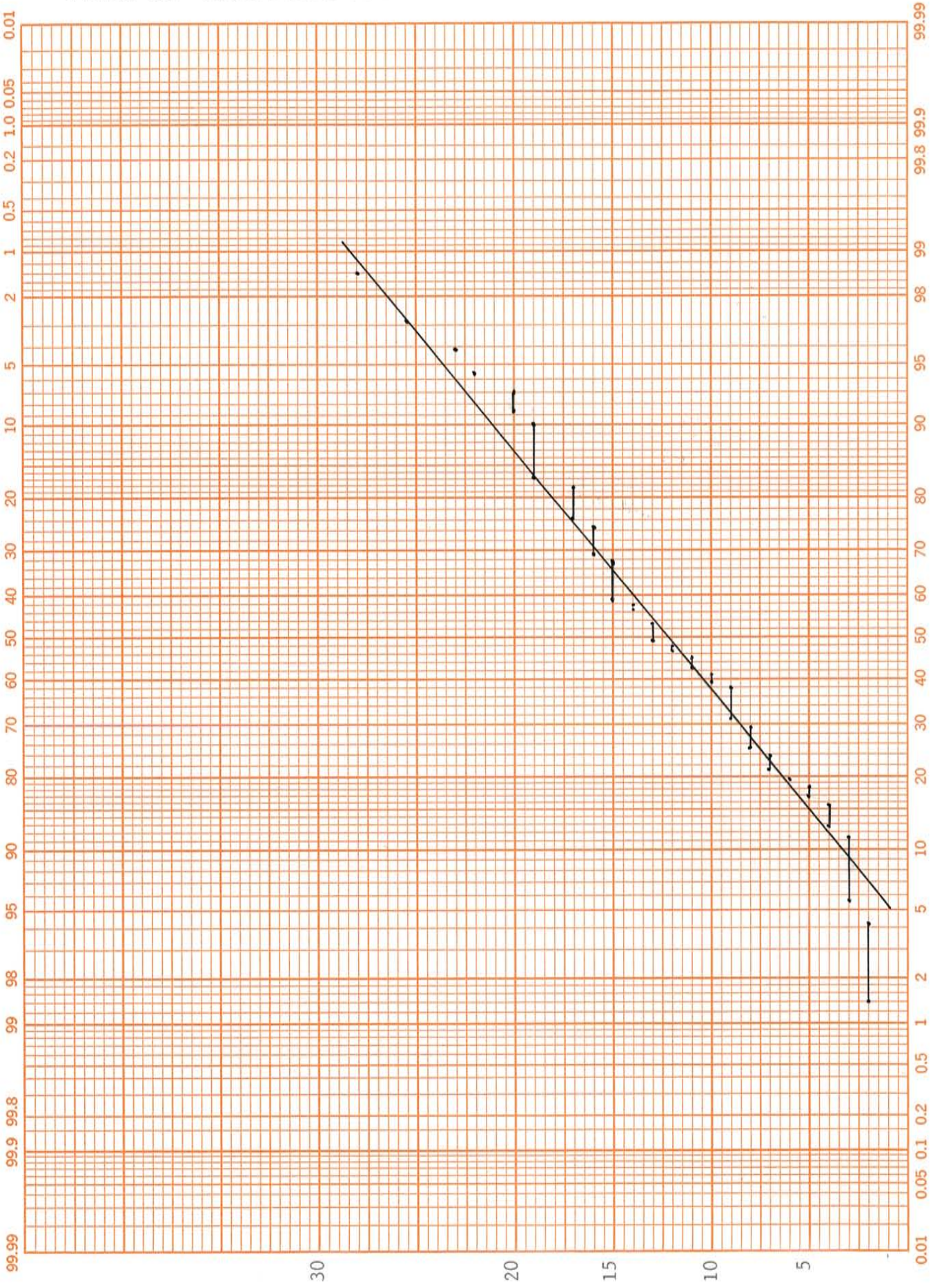

FIGURE 33: Distribution of Fe in Biotite Syenodiorite (Tis)
Orthoclase Adamellite (Tio)
Undifferentiated Dikes (Tid)

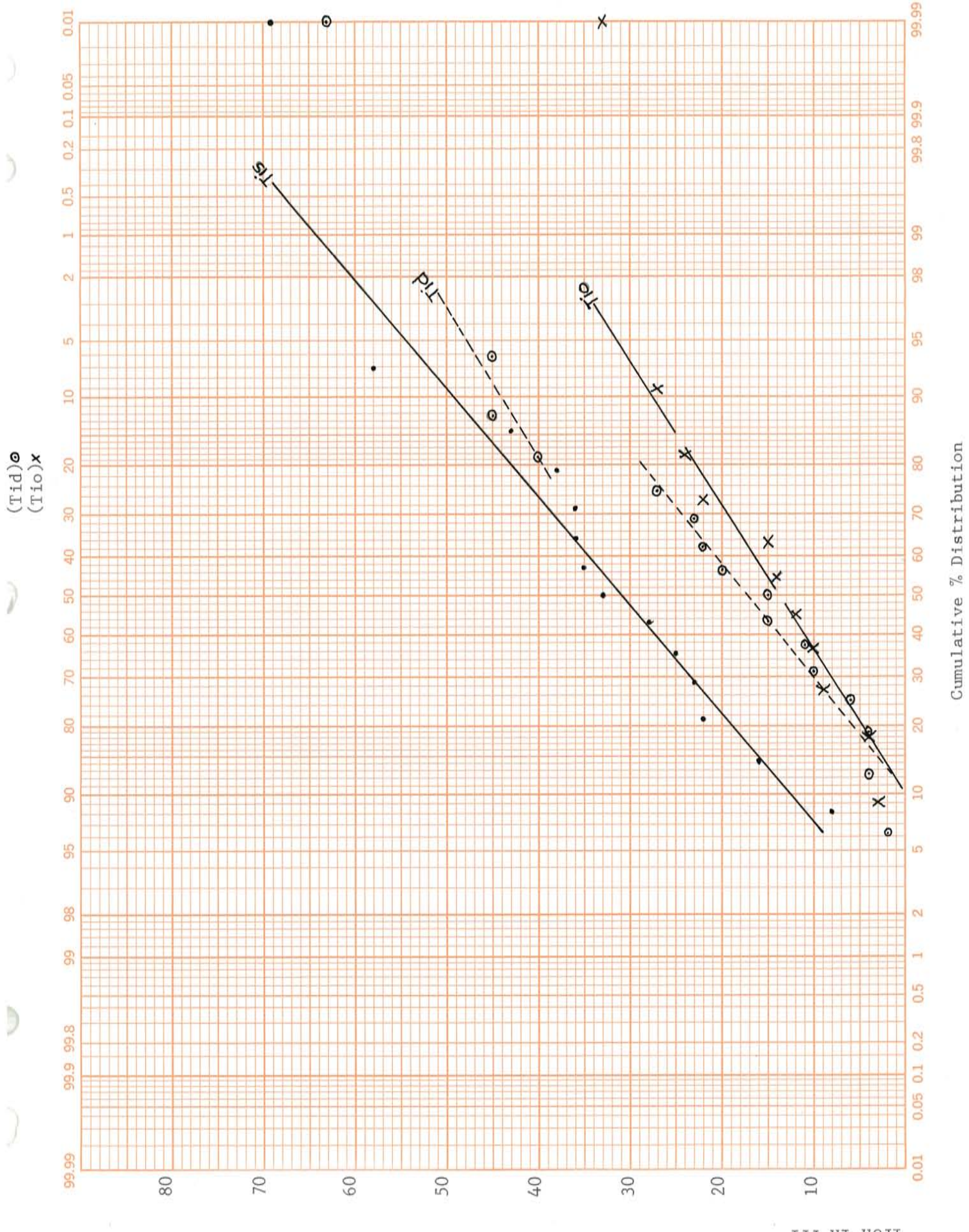

10 ppm confined to the ore zone. In this study one anomalous value of 12 ppm in sample #91 is associated with a Cu anomaly. The spatial distribution of molybdenum is given in Figure 34 .

CORRELATION OF JOINT PATTERN AND METAL DISTRIBUTION

With the exception of two weak anomalies in samples #15 - 20 ppm Cu in Tim and #115 - 23 ppm Pb in Tid all the anomalous metal values occur within the area of strong to moderate fracture intensity (Figure 35). The two strong copper anomalies in samples #85 - 210 ppm and #91 - 205 ppm are associated with strong fracture intensity. There may be a weak correlation between the N-60-W preferred fracture orientation in Tim (Figure 34) and the geochemical anomalies in samples #85 to #420 and samples #421 to #324 to #91. In general, the geochemical anomalies do not appear to have any prominent linear trend. The large eliptical area of moderate to intense fracturing in the southern end of the range contains copper anomalies 1, 3, 5, and 7 and lead anomaly 3. The "T" shaped area of fracturing in the central part of the range contains the copper anomaly 2 and the lead anomalies 1 and 4. Copper anomaly 4 and 6 and lead anomaly 2 are isolated cases not associated with the areas of wide spread fracturing. The copper anomaly 7 is associated with skarn mineralization (Figure 22). Rehrig and Heidrick (1972) state that "repeated activiation of this fracture system played an important role in mechanically preparing ground to allow porphyry copper mineralization to attain ore grade" and apparently, in the Jarillas, even geochemical anomalies in the hundreds of ppm range are

FIGURE 34

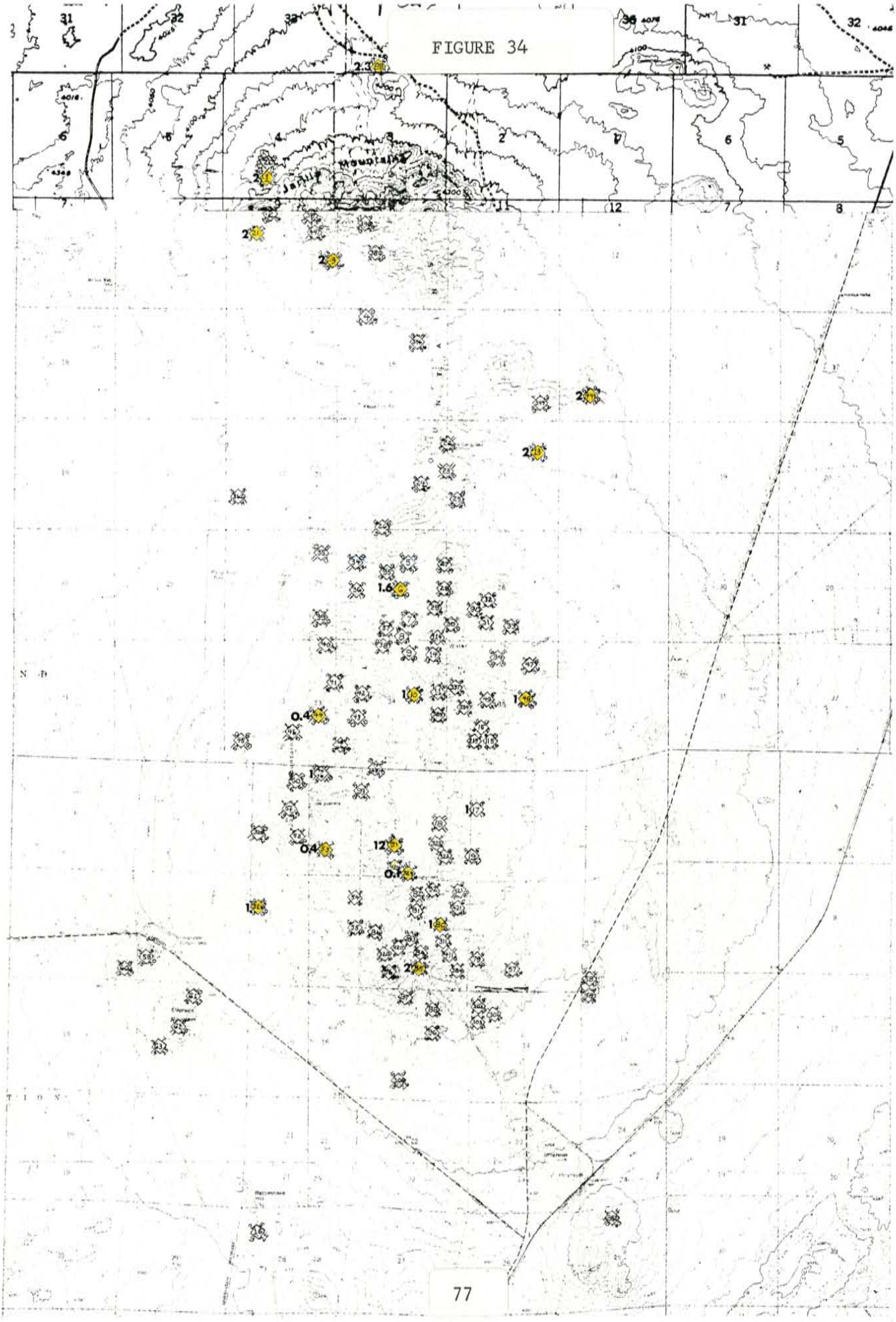

FIGURE 35

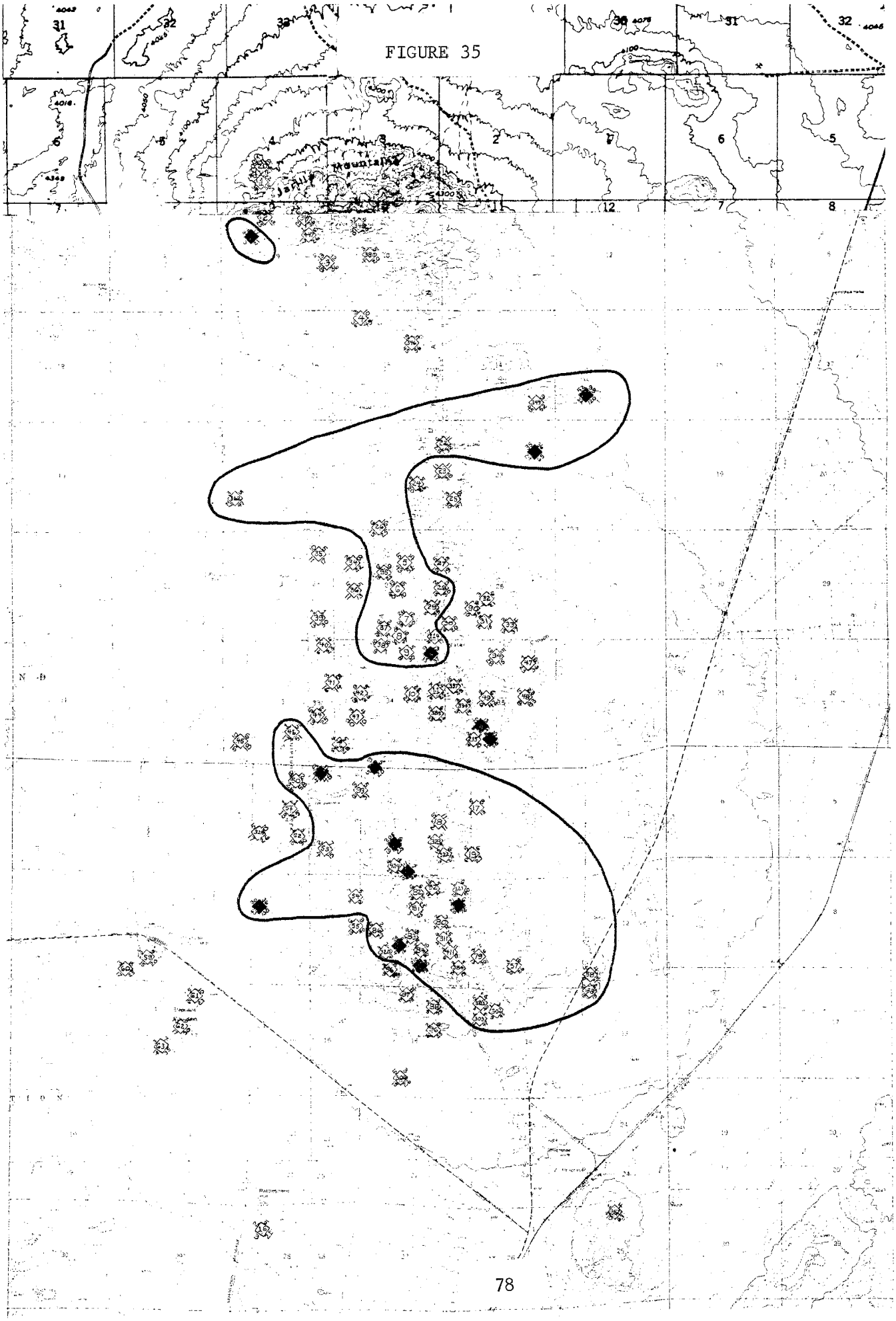

so controlled. Mackin's (1954) study of the Granite Mountains iron ore deposits revealed a joint pattern that provided travel routes for iron rich mineralizing fluids to escape from the center of laccolith and move into the limestones on the periphery. In addition to the systematic joint pattern the Granite Mountain igneous rocks are depleted of iron in the central part of the body. In the Jarilla Mountains there are extensive areas in the southern part of the range with lower than average iron content. Whether this represents depletion or not is open to debate. The probability plot for iron (Figure 32) does not allow part of the Fe population to be significantly depleted. If depletion were an important process that operated on part of the population a break in slope on the Fe probability plot would occur. If a constant amount of iron were removed from the entire population, an unimodal distribution would be maintained. Also the amount removed might be so small as to be obscured in the random fluctuations of the sample and analytic procedure. Based on the data accumulated in this report, it is my opinion that the iron deposited in the limestone replacement bodies was not obtained from the igneous rocks exposed at the surface of the Jarilla Mountains. Figure 20 shows three SW to NE sampling traverses made in igneous rocks adjacent to iron rich skarns. Five samples were collected in each traverse at 100 foot intervals starting a few feet from the skarn - monzonite adamellite contact. The metal concentrations graphed under the cross-sections may show an introduction of metal values on the southwest side of the skarn. If additional sampling confirmed this relationship a case could be made for mineralizing fluid flow and travel path.

The zonal distribution of selected elements above the Kalamazoo porphyry copper deposit provides a model with which the element distribution in the Jarilla Mountains can be compared (Chaffee, 1976). Below the ore zone at Kalamazoo boron, barium and potassium are enriched and zinc and possibly iron are depleted. In the Jarillas three samples containing detectable boron occur in the center of the range, barium is abundant throughout the range except for an area t the extreme southern end, and the potassium distribution is very similar to barium which probably substitutes for K in the crystal lattice of feldspar and mica. In the Jarilla Mountains zinc and iron average 25 ppm and 1.4% repsectively and three samples in the central and northern end of the range contain silver in amounts close to the 0.5 ppm detection limit, these values are comparable to ones reported below the ore zone at Kalamazoo. The generally low copper and molybdenum values in the Jarillas are not in agreement with some of the value reported at Kalamazoo for the area below the ore zone. Also, the general geology of the Jarilla Mountains argues against the outcroping igneous rocks being part of a root zone of an eroded porphyry system. Schmidt and Craddock (1964) and Seager (1961) indicate that the intrusive rocks in the southern end of the range form a complex roof area with xenoliths and roof pendants of sedimentary rocks.

The two drill holes from which Chaffee (1976) obtained his sample material were collared in propylitic and plhllic-argillic altered rock with a minimum copper concentration of over 100 ppm copper. If the Jarilla Mountains are part of a porphyry copper system, and the rocks now exposed are not

below a previously eroded ore zone, then they are above or adjacent to the ore zone and unfortunately if an ore zone does exist in the Jarillas it is significantly further away from the samples taken in this study than the ore zone at Kalamazoo is from the top of the core holes sampled in Chaffee's study. A more conclusive geochemical study of the Jarilla prospect will have to wait until additional orientations studies similar to but more extensive than the one at Kalamazoo are completed.

CONCLUSIONS

Preferred orientation of joints in the Jarilla Mountains is weak and obscured by local radial or random fractures. Geochemical anomalies do not form significant linear trends. Fracture intensity can be mapped and areas of strong to moderate fracturing outlined. Copper and lead geochemical anomalies are highly correlated to areas of strong to moderate fracturing. A comparison of the element distribution in the Jarilla Mountains with the distribution at the Kalamazoo porphyry copper deposit is inconclusive. Seager (1961) and Schmidt and Craddock (1964) both note that the igneous intrusives in the Jarilla Mountains were forcefully emplaced. Seager indicates that the entire intrusive, much of which is unexposed may be a laccolith and that much of the intrusive exposed in the range should be classified as a chonolith and not a stock which is a discordant steep-walled intrusive. M. R. Mudge (1968) studied the depth control of some concordant intrusives and concluded that a minimum of 3000 feet of overburden is required to contain a concordant pluton. If the thickness of cover is less than 3000 feet, the sedimen-

tary rocks behave in a brittle fashion allowing steam and magma to escape and a discordant intrusive is emplaced. Stringham (1959) and DeGeofroy and Wignall (1972) in studies concerned with criterian used to distinguish productive from barren intrusives list passive emplacement - cross cutting structive as either the most important or second most important characteristic of a productive stock. It may be then that the Jarilla intrusive was too deeply buried at the time of emplacement to form the steep-walled, discordant, passively emplaced body that results in ground preparation required for a porphyry ore system to form.

TABLE 14: CROSS-REFERENCE TABULATION WITH N.M.B.M. BULLETIN 82

SAMPLE NUMBER	SCHMIDT and CRADDOCK 1964-Specimen	ROCK TYPE	Cu in PPM	Pb in PPM	Zn in PPM	Fe in PPT
Tid						
421	M-21-B	Granite Porphyry	21	6	72	20
420	M-20-B	Adamellite Porphyry	28	6	16	4
321	M-21-A	Adamellite Porphyry	1	6	40	15
344	M-44-A	Latite Porphyry	1	9	52	45
411	M-11-B	Monzonite	5	11	17	6
447	M-47-B	Monzonite Porphyry	1	6	26	17
347	M-47-A	Calcimonzonite Porphyry	5	5	36	23
384	M-84	Rhyodocite Porphyry	2	5	19	2
326	M-26	Trachite Porphyry	30	36	130	63
324	M-24-A	Trachite Porphyry	111	7	26	10
320	M-20-A	Diorite Porphyry	3	7	41	27
380	M-80	Trachyondesite Porphyry	3	5	20	4
348	M-48	Syenogabbro Porphyry	37	4	30	40
346	M-46	Basalt Porphyry	19	11	56	45
Tim						
322	M-22	Monzonite Porphyry	15	8	24	3
328	M-28	Monzonite	5	10	26	17
424	M-24-B	Adamellite	4	12	46	22
302	M-2	Adamellite Porphyry	1	3	45	9
334	M-34	Adamellite Porphyry	3	4	14	3
311	M-11-A	Leucoadamellite Porphyry	4	25	25	4

TABLE 14: CONTINUED

SAMPLE NUMBER	SCHMIDT and CRADDOCK 1964-Specimen	ROCK TYPE	Cu in PPM	Pb in PPM	Zn in PPM	Fe in PPT
Tio						
352	M-52	Granite Porphyry	1	4	63	10
301	M-1	Monzonite Porphyry	5	4	20	3
362	M-62	Monzonite Porphyry	3	5	47	27
306	M-6	Adamellite Porphyry	5	3	26	15
444	M-44-B	Adamellite Porphyry	52	99	120	22
303	M-3	Adamellite Porphyry	1	5	47	12
Tis						
337	M-37	Melamonzonite	15	8	29	23
385	M-85	Syenodirotie	5	6	36	33
Til						
323	M-23	Leucorhyolite Porphyry	4	7	7	4
Rb						
89	V-2	Melabasalt	47	6	62	59

REFERENCES

Ahrens, L. H., 1965, Distribution of the Elements in Our Planet, McGraw Hill, New York.

Beane, R. E., Jaramillo, C. L. E., and Bloom, M. S., 1975, Geology and Base Metal Mineralization of the Southern Jarilla Mountains, Otero County, New Mexico, in New Mexico Geological Society Guidebook, 26th Field Conference, Las Cruces Country, p. 151-156.

Bloom, M. S., 1975, Mineral Paragenesis and Contact Metamorphism in the Jarilla Mountains, Orogrande, New Mexico: N.M. Thesis, New Mexico Institute of Mining and Technology, Socorro, New Mexico.

Chaffe, M. A., 1976, The Zonal Distribution of Selected Elements Above the Kalamazoo Porphyry Copper Deposit, San Manuel District, Pinal County, Arizona: J. Geochem. Explor., Vol. 5 No. 2: p. 145-165.

Coope, J. A., 1973, Geochemical Prospecting for Porphyry Copper-Type Mineralization - A Review: J. Geochem. Explor., Vol 2 No. 2: p. 81-102.

Darton, N. H., 1921, Geologic Structures of Parts of New Mexico: U. S. Geological Survey Bulletin 726: p. 173-276.

....., 1928, Geologic Map of the State of New Mexico, Scale 1: 500,000: U. S. Geological Survey.

DeGeoffray, J. and Wignall, T. K., 1972, A Statistical Study of Geologic Characteristics of Porphyry-Copper-Molybdenum Depsotis in the Cordilleran Belt - Application to the Rating of Porphyry Prospects: Econ. Geol., V67: p. 656-668.

Govett, G. J. S., 1972, Interpretation of a Rock Geochemical Exploration Survey in Cyprus - Statistical and Graphical Techniques: J. Geochem. Explor. Vol 1 No. 1: p. 77-102.

Griffitts, W. R., and Nakagawa, H. M., 1960, Variations in Base-Metal Contents of Monzonite Intrusives: U. S. Geological Survey Professional Paper 400-B: p. B93-B95.

Gutjahr, A. L., 1973, A Summary of Results in Robustness: Unpublished class notes, Math 485, New Mexico Institute of Mining and Technology, Socorro, New Mexico.

Hidden, W. E., 1893, Two New Localities for Turquoise: American Journal Science, V 46 No 3: p. 400-402.

Jaramillo, C. L. E., 1973, Alteration and Mineralization in the Jarilla Mountains, Otero County, New Mexico: Unpublished M. S. Report, New Mexico Institute of Mining and Technology, Socorro, New Mexico.

Kelley, V. C., 1949, Geology and Economics of New Mexico Iron-Ore Deposits: University of New Mexico Published in Geology No 2.

Koch, G. S., and Link, R. F., 1970, Statistical Analysis of Geological Data: John Wiley and Sons, Inc., New York.

Lasky, S. G., and Wooton, T. P., 1933, The Metal Resources of New Mexico and their Economic Features: New Mexico State Bureau of Mines and Mineral Resources, Bulletin 7.

Lindgren, Waldemar, Graton, L. C., and Gordon, C. H., 1910, The Ore Deposits of New Mexico, U. S. Geological Survey Professional Paper 68.

Mackin, J. H., 1954, Geology and Iron Ore Deposits of the Granite Mountain Area, Iron County, Utah: U. S. Geological Survey Mineral Investigations 14.

Mackin, J. H., and Ingerson, E., 1960, An Hypothesis for the Origin of Ore-Forming Fluid: U. S. Geological Survey Professional Paper 400-B: p. B1-B2.

Mantei, E., Bolter, E., and Al-Shaiebz, 1970, Distribution of Gold, Silver, Copper, Lead and Zinc in the Productive Marysville Stock, Montana; Mineral Mineral Deposits, (Berl.) V5: p. 184-190.

Meinzer, O. E., and Hare, R. F., 1915, Geology and Water Resources of Tularosa Basin, New Mexico and Adjacent Areas, U. S. Geological Survey, Water Supply Paper 343.

Mudge, M. R., 1968, Depth Control of Some Concordant Intrusions: Geological Society of America Bulletin V 79: p. 315-332.

Needham, C. E., 1937, Some New Mexico Fusulinidae: New Mexico Bureau of Mines and Mineral Resources, Bulletin 14.

Olade, M. A., 1977, Major Element Halos in Granitic Wall Rocky of Porphyry Copper Deposits, Guichon Creek Batholith, British Columbiz; J. Geochem. Explor., V 7 No 1: p. 59-71.

....., and Fletcher, W. K., 1976, Trace Element Geochemistry of the Highland Valley and Guichon Creek Batholith in Relation to Porphyry Copper Mineralization: Economic Geology, V 71: p. 733-748

Pawlowicz, R. M., 1974, Discrimination Among Depositional Environments Based on Element Abundances in Upper Cretaceous Rocks of Southern Alberta: Unpublished Ph. D. Disseration, New Mexico Institute of Mining and Technology, Socorro, New Mexico.

Proctor, P. D., and Doraibabu, P., 1973, Trace Base Metals, Petrography, and Alteration, Tres Hermanas Stock, Luna County, New Mexico: New Mexico State Bureau of Mines and Mineral Resources, Circular 132.

Putman, G. W., and Alfors, J. T., 1967, Frequency Distribution of Minor Metals in the Rocky Hill Stock, Tulare County, California: Geochemica et Cosmochimica Acta, V 31: p. 431-450.

Rehrig, W. A., and Heidrick, T. L., 1972, Regional Fracturing in Laramide Stocks of Arizona and its Relationship to Porphyry Copper Mineralization: Economic Geology V 67: P. 198-213.

Reynolds, C. B., and Craddock, C., 1959, Geology of the Jarilla Mountains: Guidebook to the Sacramento Mountains, Permian Basin Section, Society of Economic Paleontologists and Mineralogists and Roswell Geological Society: p 279-283.

Schmidt, P. G., 1962, The Geology of the Jarilla Mountains, Otero County, New Mexico: Unpublished M. S. Thesis, University of Minn., Minneapolis.

....., and Craddock, C., 1964, The Geology of the Jarilla Mountains, Otero County, New Mexico: New Mexico Bureau of Mines and Mineral Resources Bulletin 82.

Seager, W., 1961, Geology of the Jarilla Mountains, Tularosa Basin, New Mexico: Unpublished M. S. Thesis University of New Mexico, Albuquerque, New Mexico.

Sheraton, J. W., and Black, W. P., 1973, Geochemistry of Mineralized Granitic Rocks of Northeast Queensland: J. Geochem. Explor., V 2 No 4: p. 331-348.

Shrivastava, J. N., and Proctor, P. D., 1962, Trace Element Distribution in the Searchlight, Nevada, Quartz Monzonite Stock: Economic Geology V 57: p. 1062-1070.

Stringham, B., 1959, Differences Between Barren and Productive Intrusive Porphyry: Unpublished paper, University of Utah.

Tennant, C. B., and White, M. L., 1959, Study of the Distribution of Some Geochemical Data: Economic Geology V 54: p. 1281-1290.

Theobald, P. K., and Havens, R. G., 1960, Base Metals in Biotite, Magnetite, and their Alteration Products in Hydorthermally Altered Quartz Monzonite Porphyry Sill, Summit County, Colorado: (abs.) Geological Society of American Proc. Annual Meeting: p. 223.

Vistelius, A. B., 1966, Structural Diagrams, Translated by R. Barker: Pergamon Press, Oxford, New York.

Walpole, R. E., and Myers, R. H., 1972, Probability and Statistics for Engineers and Scientists: The Macmillan Company, New York.

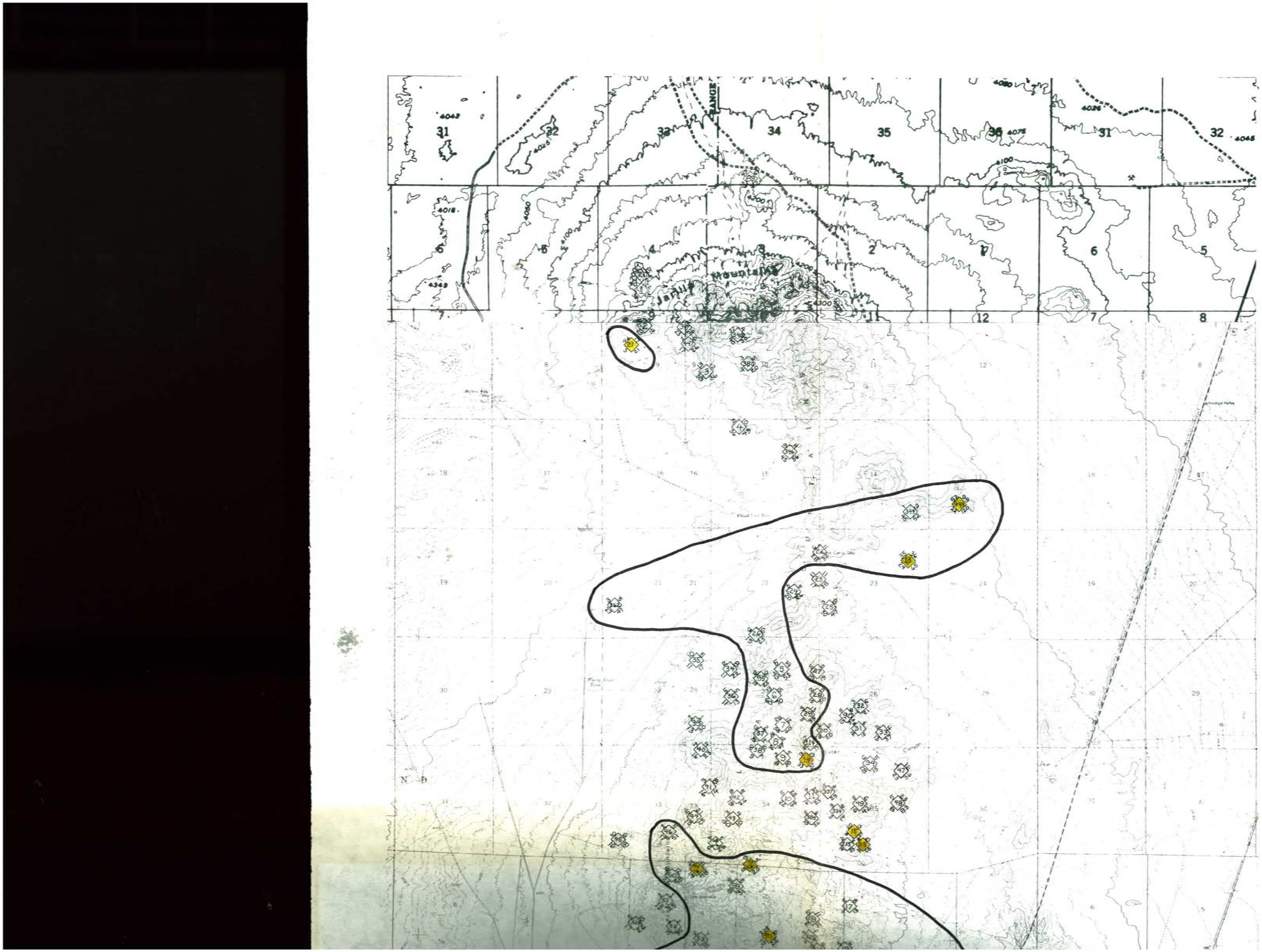
RANGE
Jarbidge Mountains
31
32
33
34
35
36
1
2
3
4
5
6
7
8
9
10
11
12
N

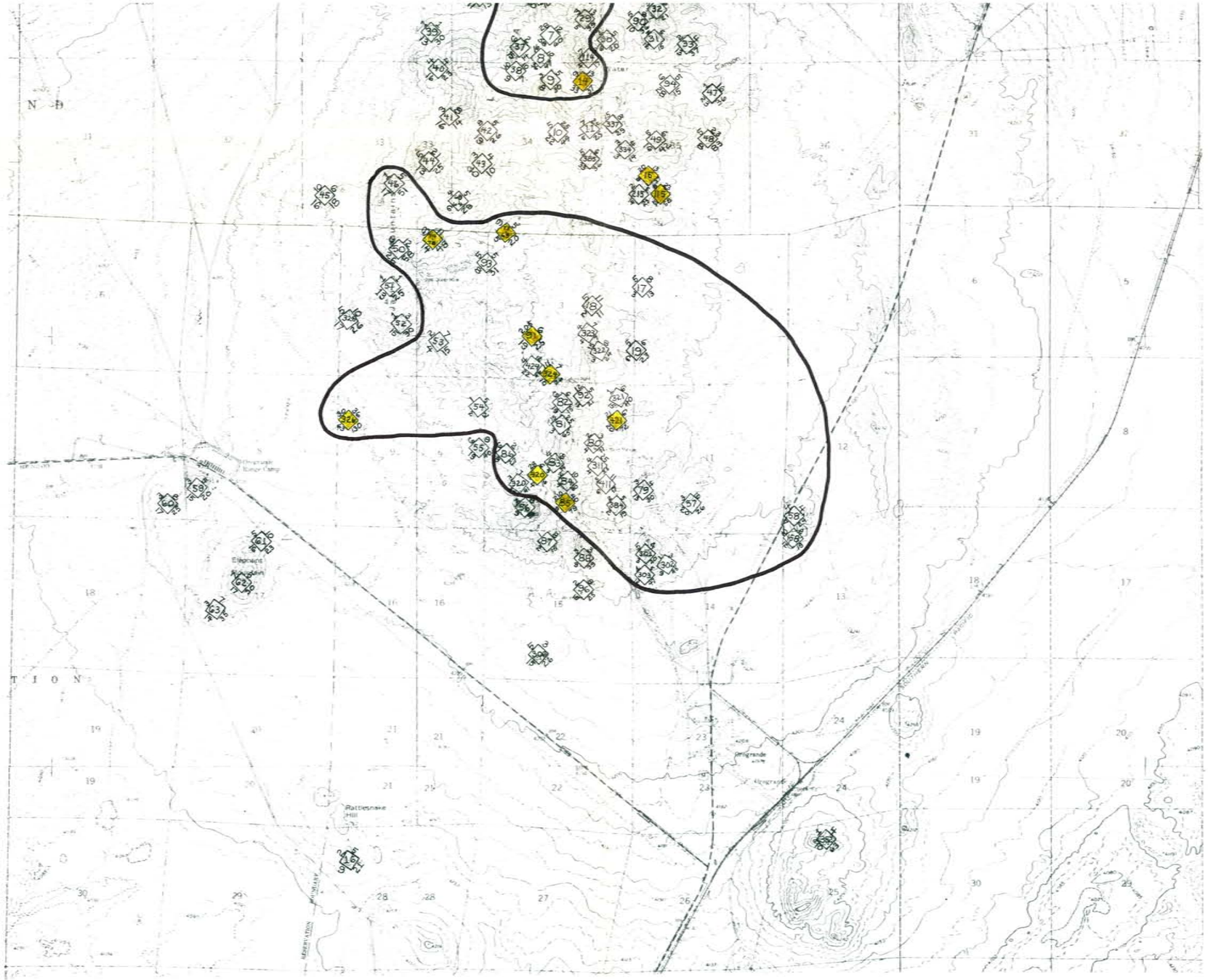
N
T I O N
Rattlesnake Hill
SCALE 1:24000
CONTOUR INTERVAL 20 FEET
SAMPLE NUMBER
TRUE NORTH
MAGNETIC NORTH
APPROXIMATE MEAN

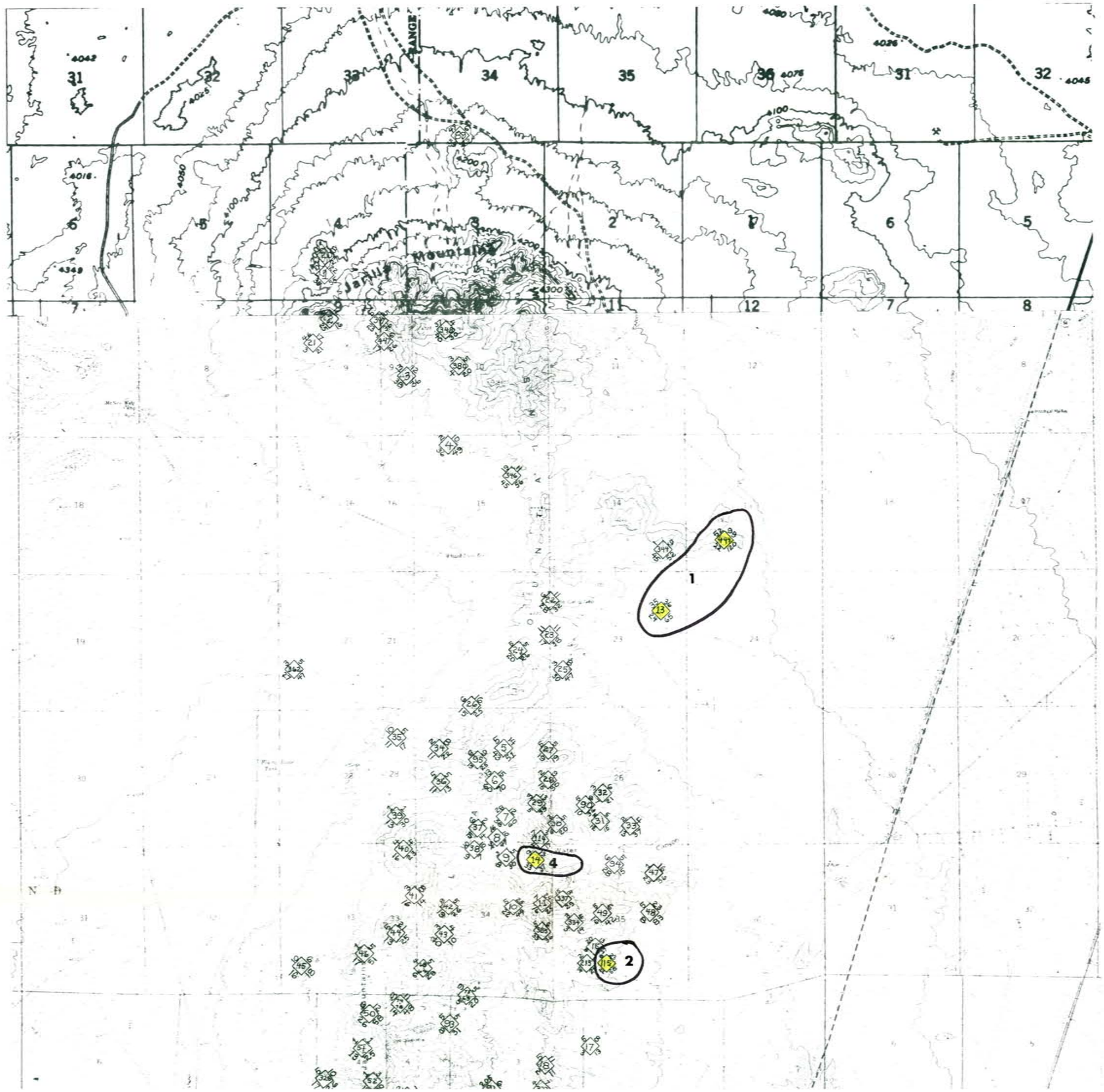
RANGE
Jarbidge Mountains
1
2
4

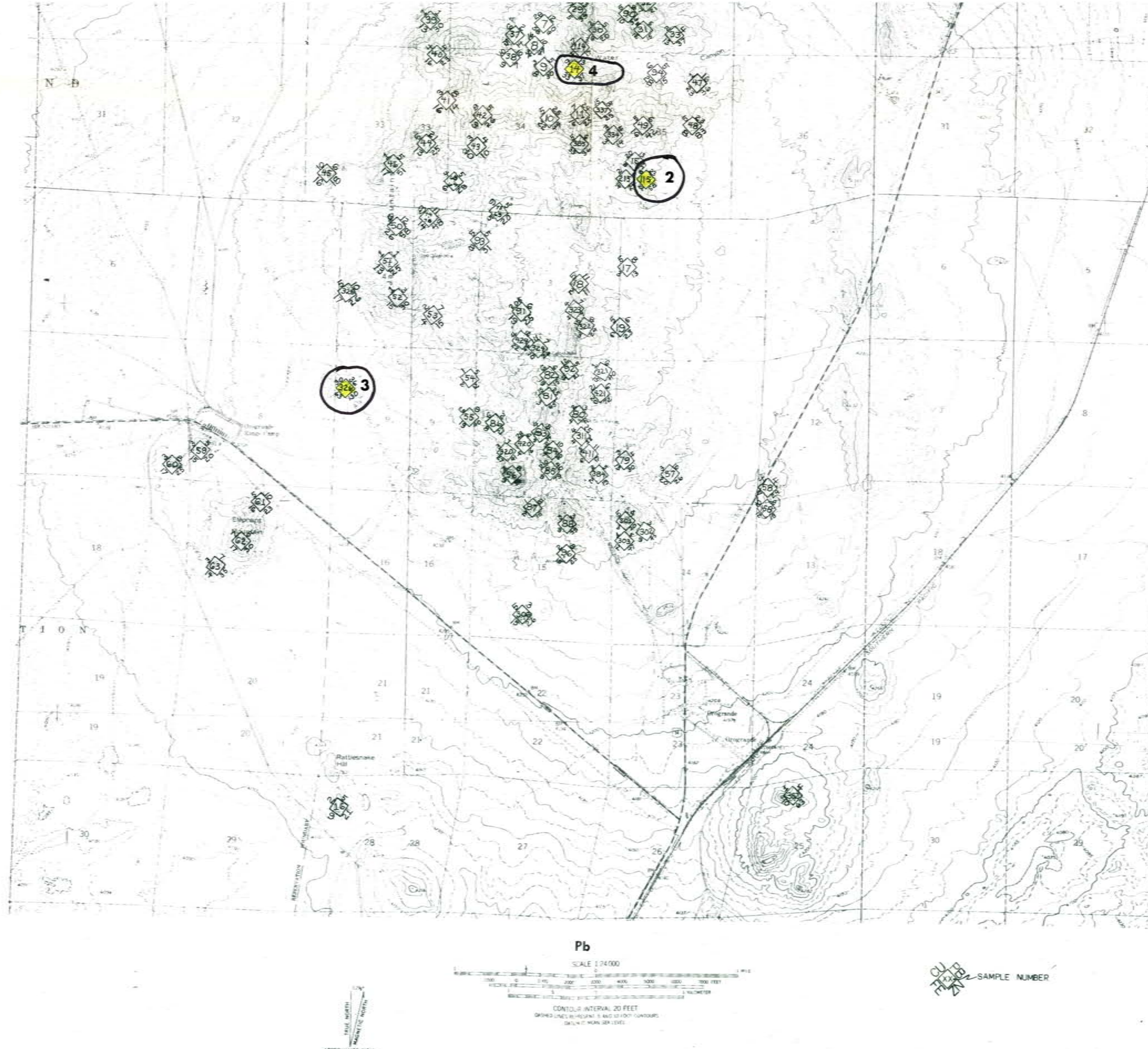

4
2
3
Rattlesnake Hill
Pb
SCALE 1:24000
CONTOUR INTERVAL 20 FEET
SAMPLE NUMBER
TRUE NORTH
MAGNETIC NORTH
APPROXIMATE MEAN

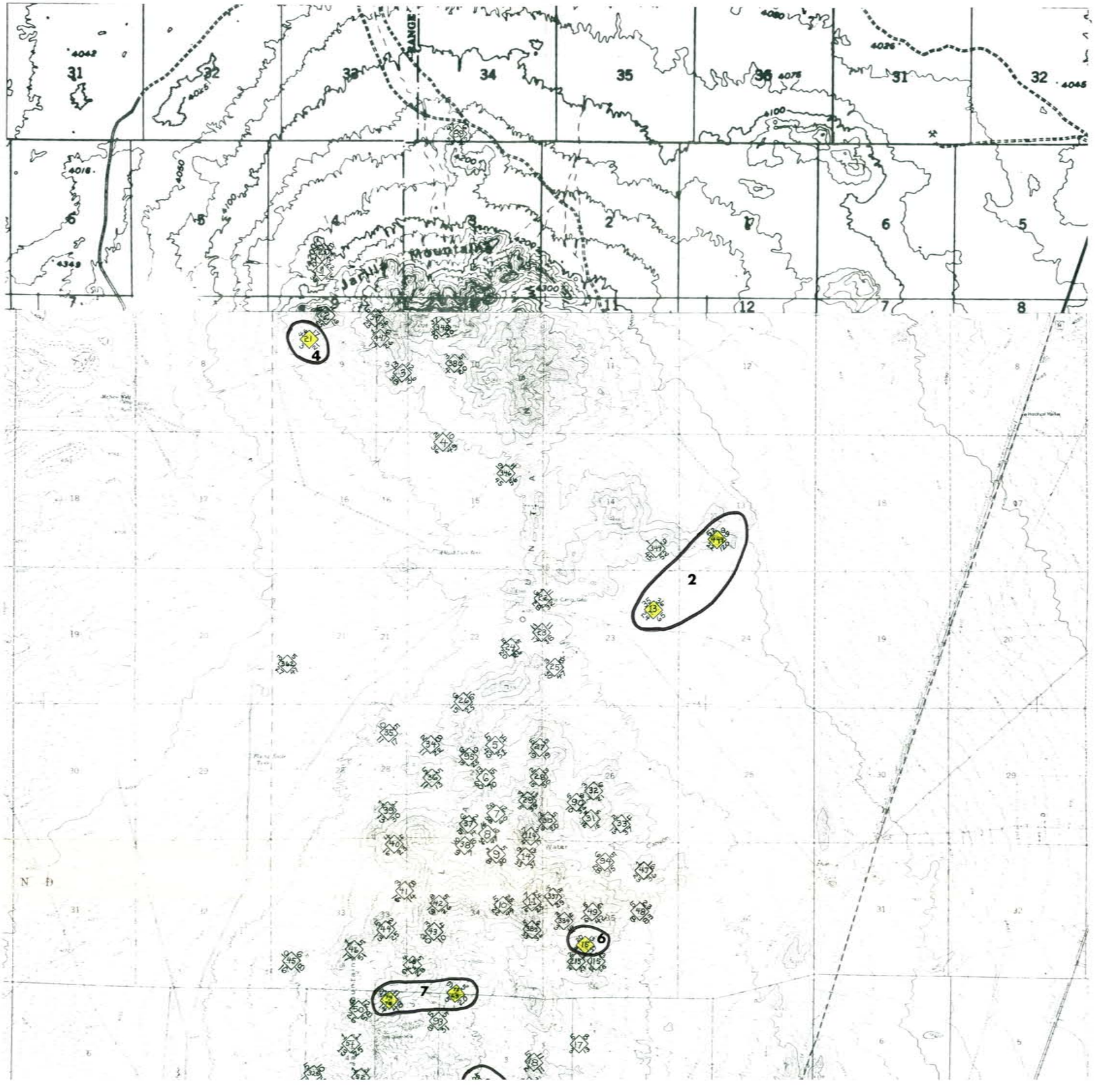
Jarbidge Mountains
CANYON
2
4
6
7

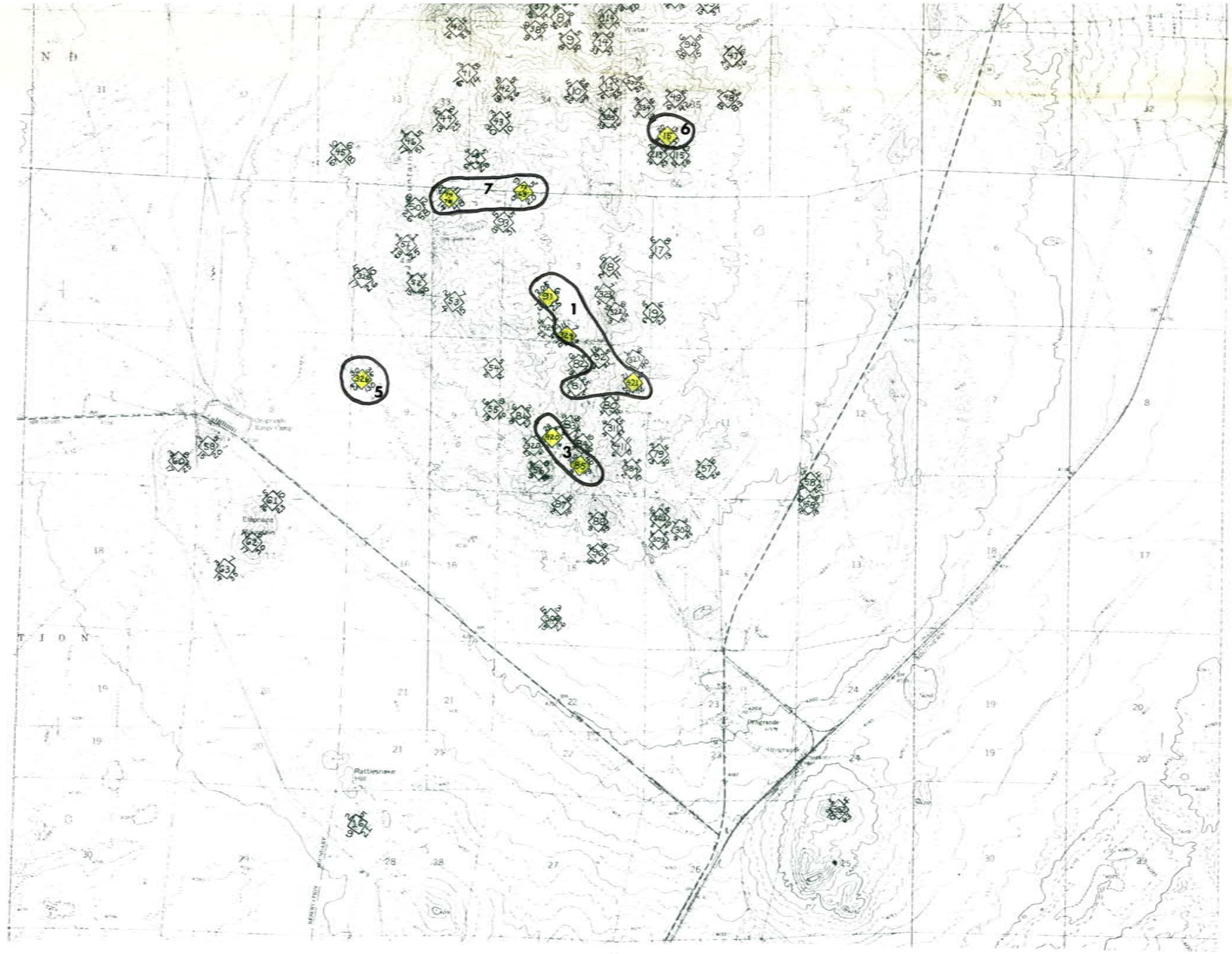
6
7
1
5
3
Rattlesnake Hill
Pilgrande
Cu
SCALE 1:24000
CONTOUR INTERVAL 20 FEET
SAMPLE NUMBER

R8E. R9E.

T21S.
T22S.

T.21S.
T.22S.

FRACTURE PATTERN IN THE IGNEOUS ROCKS
OF THE JARILLA MOUNTAINS

Tin –
Tis –
Tio –
Til –
Tid –

SCALE 1:24000

1 0 1 MILE

FRACTURE INTENSITY

STRONG
MODERATE
WEAK

MAP 1